



January 2018

Role Of Triazoles In Wood Protection: Developing Analytical Approaches And Examining Sorption, Distribution, And Environmental Fate Of Fungicides

Klara Kukowski

Follow this and additional works at: <https://commons.und.edu/theses>

Recommended Citation

Kukowski, Klara, "Role Of Triazoles In Wood Protection: Developing Analytical Approaches And Examining Sorption, Distribution, And Environmental Fate Of Fungicides" (2018). *Theses and Dissertations*. 2259.
<https://commons.und.edu/theses/2259>

This Dissertation is brought to you for free and open access by the Theses, Dissertations, and Senior Projects at UND Scholarly Commons. It has been accepted for inclusion in Theses and Dissertations by an authorized administrator of UND Scholarly Commons. For more information, please contact zeinebyousif@library.und.edu.

**ROLE OF TRIAZOLES IN WOOD PROTECTION: DEVELOPING
ANALYTICAL APPROACHES AND EXAMINING SORPTION,
DISTRIBUTION, AND ENVIRONMENTAL FATE OF FUNGICIDES**

by

Klara Kukowski

Bachelor of Science, University of Chemistry and Technology, Prague, 2013

A Dissertation

Submitted to the Graduate Faculty

of the

University of North Dakota

in partial fulfillment of the requirements

for the degree of

Doctor of Philosophy

Grand Forks, North Dakota

May

2018

Copyright 2018 Klara Kukowski

This dissertation, submitted by Klara Kukowski in partial fulfillment of the requirements of the Degree of Doctor of Philosophy from the University of North Dakota, has been read by the Faculty Advisory Committee under whom the work has been done and is hereby approved.



Dr. Alena Kubátová (Chairperson)



Dr. Evguenii I. Kozliak



Dr. David T. Pierce

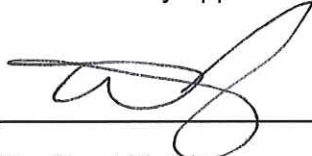


Dr. Julia Zhao



Dr. Frank Bowman

This dissertation is being submitted by the appointed advisory committee as having met all the requirements of the School of Graduate Studies at the University of North Dakota, and is hereby approved.



Dr. Grant McGimpsey

Dean of the School of Graduate Studies

April 12/18

Date

PERMISSION

Title Role of Triazoles in Wood Protection: Developing Analytical Approaches and Examining Sorption, Distribution, and Environmental Fate of Fungicides

Department Chemistry

Degree Doctor of Philosophy

In presenting this dissertation in partial fulfillment of the requirement for a graduate degree from the University of North Dakota, I agree that the library of this University shall make it freely available for inspection. I further agree that permission for extensive copying for scholarly purposes may be granted by the professor who supervised my dissertation work or, in her absence, by the chairperson of the department or the dean of the graduate school. It is understood that any copying or publication or other use of this dissertation or part thereof for financial gain shall not be allowed without my written permission. It is also understood that due recognition shall be given to me and the University of North Dakota in any scholarly use which may be made of any material in my dissertation.

Klara Kukowski

Table of Content

LIST OF TABLES	viii
LIST OF FIGURES.....	x
LIST OF ABBREVIATIONS	xv
ACKNOWLEDGEMENTS	xvi
ABSTRACT	xviii
I. CHAPTER: CHALLENGES TO WOOD PRESERVATION: UNDERSTANDING SORPTION, DISTRIBUTION, ENVIRONMENTAL FATE, AND CHARACTERIZATION OF TRIAZOLES	1
I.1 DIFFUSION OF TRIAZOLE FORMULATIONS INTO WOOD	4
I.2 ENVIRONMENTAL FATE OF TRIAZOLES	5
I.2.1 Leaching	5
I.2.2 Evaporation	7
I.2.3 Biodegradation & Biotransformation	8
I.3 FUNGICIDE DETERMINATION IN WOOD LEACHATE	9
I.4 STATEMENT OF PURPOSE.....	11
II. CHAPTER: DIFFUSION OF TEBUCONAZOLE INTO SOFTWOOD UNDER AMBIENT CONDITIONS AND ITS DISTRIBUTION IN FRESHLY TREATED AND AGED WOOD	14
II.1 MATERIALS AND METHODS.....	14
II.1.1 Chemicals and Reagents	14
II.1.2 Experimental Procedures.....	15
II.1.3 Extraction Procedure.....	19
II.1.4 Liquid Scintillation Counting	20
II.1.5 Diffusion Coefficient Determination.....	20
II.1.6 Mass Balance Closure	23

II.1.7 Numerical Simulation	24
II.2 RESULTS AND DISCUSSION	24
II.2.1 Woodlife Absorption	24
II.2.2 TAZ Absorption.....	27
II.2.3 Mass Balance	33
II.2.4 Data Evaluation	34
II.3 CONCLUSIONS.....	42
III. CHAPTER: FATE OF TRIAZOLES IN SOFTWOOD UPON ENVIRONMENTAL EXPOSURE	44
III.1. MATERIALS AND METHODS.....	44
III.1.1 Chemicals and Reagents	44
III.1.2 Outdoor Exposure Study.....	45
III.1.3 Controlled-Environment Study	48
III.1.4 Wood Leaching Experiments	51
III.1.5 Wood Cutting & Extraction	52
III.1.6 Analysis & Instrumentation.....	52
III.1.7 Statistical Data Processing	54
III.2 RESULTS AND DISCUSSION	55
III.2.1 Loosely and Strongly Bound TAZ	55
III.2.2 TAZ Loss upon Environmental Exposure	56
III.2.3 Evaluation of Triazole Degradation.....	59
III.2.4 Environmental Factors Contributing to Triazole Loss.....	64
III.2.5 Triazole Leaching	66
III.3 CONCLUSIONS.....	68
IV. CHAPTER: THE EXTENT OF TEBUCONAZOLE LEACHING FROM UNPAINTED AND PAINTED SOFTWOOD	70
IV.1 MATERIALS AND METHODS	70
IV.1.1 Chemicals	70
IV.1.2 Wood Treatment	71
IV.1.3 Wood Exposure.....	71
IV.1.4 Extraction & Analysis	73
IV.1.5 Estimate of Maximum Leachable TAZ	74
IV.1.6 Data Analysis	75
IV.2. RESULTS AND DISCUSSION.....	76

IV.2.1 ¹⁴ C-TAZ Distribution and Recoveries from Wood End Grain and Middle Sections	77
IV.2.2 ¹⁴ C-TAZ Leaching Kinetics	80
IV.2.3 TAZ Depletion from Wood Exposed to the Outdoor Environment	83
IV.2.4 Impact of TAZ Loss on Wood Protection.....	85
IV.3 CONCLUSIONS	86
V. CHAPTER: METHOD DEVELOPMENT FOR TRIAZOLE AND IPBC QUANTIFICATION IN WOOD LEACHATE USING SPE FOLLOWED BY LC-ESI-TOFMS DETECTION	88
V.1 MATERIALS AND METHODS	88
V.1.1 Chemicals and Reagents.....	88
V.1.2 Wood Matrix Extract for SPE Validation.....	88
V.1.3 Industrial Wood Leachate Samples.....	89
V.1.4 SPE-HLB.....	90
V.1.5 ESI-TOFMS Optimization	91
V.1.6 Instrumentation	94
V.1.7 Data Processing.....	95
V.2 RESULTS AND DISCUSSION.....	97
V.2.1 SPE-HLB Recoveries and Purification	97
V.2.2 Screening of the Solvent System and Electrolyte	99
V.2.3 Detailed ESI-TOFMS Optimization.....	101
V.2.4 Matrix-Affected LOD and LOQ.....	104
V.2.5 Method Application to Industrial Wood Leachate.....	106
V.3 CONCLUSIONS	108
APPENDICES	109
APPENDIX A.....	109
APPENDIX B.....	115
APPENDIX B.1	116
APPENDIX B.2	122
APPENDIX C.....	130
APPENDIX D.....	134
REFERENCES.....	143

LIST OF TABLES

Table 1. Determination of extraction and liquid scintillation counting efficiencies.	19
Table 2. Effective diffusion coefficients for three phases of Woodlife solution penetration into untreated ponderosa pine wood.....	27
Table 3. Effective diffusion coefficients for TAZ longitudinal penetration calculated for wood slices at various distances.	30
Table 4. Mass balance closure for TAZ and the solvent performed on wood blocks (15.2 cm x 3.8 cm x 3.8 cm).	34
Table 5. Experimental layout for outdoor study.	46
Table 6. The experimental layout proposed by the Taguchi design evaluating the impact of temperature, RH, UV light and time, on the fate of fungicides in wood. Saturated salt solutions were used to ensure the required humidity levels.	49
Table 7. Application of two-sample t-test for comparison of TAZ amounts recovered from various wood slices and quantified by GC-MS and scintillation counting. The two data sets were not found to be statistically different ($p > 0.05$).	61
Table 8. Application of Taguchi design for the evaluation of four factors on fungicide removal from wood. The highlighted factors were of a significance ($p \leq 0.05$).....	65
Table 9. Experimental layout including the exposure types with corresponding chamber conditions. For all experiments, conditioned ponderosa pine wood was dip-treated with Woodlife containing ^{14}C -TAZ.....	72
Table 10. The SPE-HLB protocol developed for retention of fungicides present in wood leachate.	90
Table 11. Electrolytes and their concentrations evaluated in both MeOH-water and ACN-water solvent systems as part of the screening of ESI-TOFMS conditions.	92

Table 12. Factors and levels used for the optimization of ESI-TOFMS conditions using DOE response surface design. Ammonium acetate was chosen as the electrolyte based on the screening experiments.	93
Table 13. Protonated molecular ions used for the analyte LC-MS quantitation.	95
Table 14. Fungicide recoveries using SPE-HLB protocol.	97
Table 15. ESI-TOFMS conditions yielding the highest fungicide response based on the response surface optimization.	103
Table 16. Instrumental and matrix-affected LODs and LOQs for triazoles and IPBC expressed as amounts injected into LC-ESI-TOFMS.....	105
Table 17. Intra- and inter-day repeatability of triazole determination in industrial wood leachate samples.	107
Table B.1. 1. GC-MS LOD and LOQ values for TAZ, PAZ, and IPBC calculated from calibration curves.	117
Table B.2. 1. LC-MS LOD and LOQ values for TAZ, PAZ, and IPBC calculated from calibration curves.	123
Table B.2. 2. TAZ and PAZ concentrations in wood leachate. The experimental setup is shown in Figure B.2. 5.....	128
Table D. 1. Response surface experimental design.	135
Table D. 2. DOE response surface design including integrated peak areas of TAZ, PAZ, and IPBC molecular ions.	136

LIST OF FIGURES

- Figure 1.** Chemical structures of triazoles used in wood industry and a common additive, IPBC. 3
- Figure 2.** Wood cutting scheme. Selected 2-mm wide slices (1–6) were further cut so the outer 5-mm wide layer (reflecting the surface absorption) could be analyzed separately from the inner part (reflecting the longitudinal diffusion). Overall, 12 wood samples (6 slides) were analyzed with a liquid scintillation counter. 18
- Figure 3.** Mass uptake of Woodlife into wood blocks (15.2 cm x 3.8 cm x 3.8 cm) as described in section II.1.2.1. 25
- Figure 4.** The distribution profile of TAZ in freshly contaminated wood (Figure 2) for the outer parts of wood slices (**A**) and the inner parts (**B**), thus reflecting the surface absorption (**A**) and longitudinal diffusion (**B**). White and grey bars represent 0.5 and 3.0 min immersion time, respectively. 29
- Figure 5.** The TAZ distribution profile in freshly treated and aged wood after 3.0 min immersion time for the outer (**A**) and inner (**B**) parts of wood slices, thus reflecting the surface absorption (**A**) and longitudinal diffusion (**B**). Grey, white, and striped bars represent the distribution of TAZ in freshly treated wood, aged wood for 1 months, and aged wood for six months, respectively. 32
- Figure 6.** Boundary conditions associated with the user-defined scalars (UDS) during the numerical simulation of the solvent mass uptake (**A**); the logarithmic variation in the effective diffusion coefficient (longitudinal direction) as a function of time employed in the numerical simulations (**B**)..... 37
- Figure 7.** Normalized solvent concentration within the wood after 10,000 seconds of solvent mass uptake (**A**); measurements and numerical predictions of the normalized solvent mass uptake (**B**). 39
- Figure 8.** User-defined scalars (UDS) boundary conditions employed to simulate the complete immersion process (**A**); normalized TAZ concentrations across the different sections of the wood after 0.5 min of immersion time (**B**); normalized TAZ concentrations across the different sections of wood after 3.0 min of immersion time (**C**). 40

Figure 9. Numerically estimated (using CFD code ANSYS FLUENT) distribution profiles of TAZ in the longitudinal (**A, C**) and transversal directions (**B, D**) across the different sections compared against their corresponding measured values. 42

Figure 10. Wood corner section (41.2 cm x 3.6 cm x 3.6 cm, when assembled together) cutting scheme. Each “T” shaped wood block was cut into 2-mm wide wood slices (#1–11, 12, 14, 16) that were subjected to analysis by either liquid scintillation counting or GC-MS. 46

Figure 11. The glass chamber (23 cm ID x 35 cm H) design used for the desorption experiments..... 50

Figure 12. The TAZ amount recovered from slice #12 for sun-exposed and control wood employing a three-step extraction protocol. Individual extracts were analyzed and quantified using GC-MS. 56

Figure 13. The spatial distribution of loosely bound TAZ (recovered through two consecutive sonications) in a “T” shaped wood block after various environmental exposures..... 57

Figure 14. Recoveries of loosely bound TAZ from a "T" shaped wood block after varying environmental exposures for six months. 59

Figure 15. Comparison of the loosely bound TAZ amounts (results from first and second sonication) recovered in selected wood slices after freezing (**A**) or direct-sun (**B**) exposure quantified by either liquid scintillation counting or GC-MS. Their difference was found to be statistically insignificant. 61

Figure 16. Comparison of TAZ and PAZ amounts found in control (**A**) and sun-exposed (**B**) wood. Amounts recovered from various slices were quantified by GC-MS. 63

Figure 17. Leaching of TAZ and PAZ from wood corner sections with respect to the amount of water applied. 67

Figure 18. Experimental design of TAZ-treated wood exposure to simulated rain. 73

Figure 19. Percent ¹⁴C-TAZ recoveries from end grains of painted and unpainted treated wood exposed to various humidity and simulated rain conditions, complemented by ¹⁴C-TAZ recoveries from the run-off water. The error bars represent one standard deviation and RH denotes relative humidity. 77

Figure 20. Distribution of ¹⁴C-TAZ recovered from the exposed wood. 79

Figure 21. ¹⁴C-TAZ recovered in the collected run-off water from unpainted and painted wood exposed to simulated continuous and intermittent rain. 81

Figure 22. Determination of the highest ¹⁴ C-TAZ amount that can be leached using the results obtained from wood exposure to continuous rain.	84
Figure 23. LC-ESI-TOFMS total ion current (TIC) chromatograms of unpurified wood matrix extract containing fungicides (grey) and an SPE-HLB purified sample (black), followed by EIC chromatograms for IPBC, AZA, TAZ, HAZ, and PAZ in the purified sample.	98
Figure 24. Impact of electrolyte type and its concentration in ACN-water system (50:50, v/v) on TAZ (A) and IPBC (B) MS response.	100
Figure 25. Surface plots for TAZ (A), PAZ (B), and IPBC (C) constructed using the two most influential factors. The highest points of the surface plots illustrate the ESI-TOFMS experimental conditions yielding the largest fungicide peak areas.	102
Figure 26. Optimal ESI-TOFMS conditions predicted by DOE response optimizer to maximize TAZ, PAZ, and IPBC responses.	104
Figure 27. LC-ESI-TOFMS TIC chromatograms of week 2 industrial wood leachate containing TAZ and PAZ (grey) and an SPE-HLB pre-concentrated sample (black), followed by EIC chromatograms for TAZ, HAZ, and PAZ in the pre-concentrated sample.	106
Figure A. 1. Setup of racks for automatic counting analysis on a Beckman Coulter LS6500.	110
Figure A. 2 Scintillation method used to detect ¹⁴ C-TAZ in wood extracts.	111
Figure A. 3. Smaller wood slices (0.2 cm x 3.8 cm x 3.8 cm) cut using a Craftsman 9" band saw.	112
Figure A. 4. Protective hood enclosure to eliminate ¹⁴ C-wood dust contamination. The enclosure contained two chambers separated by a plastic sheet. Entrance to the first chamber is shown on the left, while the second chamber attached to the hood is shown on the right.	113
Figure A. 5. Glass tubes containing smaller wood pieces (cut with a blade) and 3.5 mL of acetone.	114
Figure B. 1. Cutting of "T" wood sections with a band saw into 2-mm wide wood slices (#1–12, 14, and 16).	115
Figure B.1. 1. A: GC-MS chromatogram of acetone wood extract displayed as TIC, B: extracted m/z 125 corresponding to TAZ, C: extracted m/z 173 corresponding to PAZ, and D: TIC of a calibration sample.	118
Figure B.1. 2. High and low calibration curves for TAZ and PAZ.	119

Figure B.1. 3. High and low calibration curves for IPBC.	120
Figure B.1. 4. Comparison of the unbound IPBC amounts recovered in selected wood slices from sun-exposed and control wood. The IPBC amounts were quantified in extracts from first and second sonication using GC-MS.	121
Figure B.2. 1. LC-MS calibration of fungicides in the full concentration range (0.02–100 ppm) accompanied by overlaid chromatograms of the same calibration standard ran five times throughout the analysis demonstrating good repeatability.	124
Figure B.2. 2. TAZ and PAZ LC-MS calibration curves plotted using standards in the concentration range of 0.02–7 ppm. The full calibration curve is displayed on the top and an expanded view is located below demonstrating the fit of low ppm standards.	125
Figure B.2. 3. IPBC LC-MS calibration curve plotted using standards in the concentration range of 0.02–7 ppm. The full calibration curve is displayed on the top and an expanded view is located below demonstrating the fit of low ppm standards.	126
Figure B.2. 4. TIC chromatogram of Week 1, Bin 2 sample (dark green) with extracted molecular ions corresponding to TAZ (light green) and PAZ (blue). IPBC was not found in any of the wood leachate samples.....	127
Figure B.2. 5. Assembled wood sections placed on a raised platform in Rubbermaid roughneck totes (18-gallon volume) under a flowing, recirculating water irrigation system. The sections were laid horizontally on the platform and water was sprayed in a 90° angle (exposing the radial and tangential wood surface).....	129
Figure C. 1. Ponderosa pine wood samples (5.0 × 2.5 × 1.5 cm ³) dipped in the radiolabeled Woodlife solution and placed on wooden skewers to dry for 24 hours.	130
Figure C. 2. Drying of primed and painted ponderosa pine wood samples.	131
Figure C. 3. Experimental setup of wood exposure to low and high humidity..	132
Figure C. 4. Experimental setup of wood exposure to continuous and intermittent rain.	133
Figure D. 1. FIA LC-ESI-MS chromatogram illustrating the TIC and EIC for TAZ, PAZ, and IPBC. The TIC is shown as a green line, while the EIC for fungicide molecular ions are shown in orange (TAZ), magenta (PAZ), and blue (IPBC).	134
Figure D. 2. Impact of electrolyte type and its concentration in MeOH-water system (50:50) on TAZ and IPBC MS response.	137

Figure D. 3. Data analysis of TAZ MS response using Minitab.	138
Figure D. 4. Data analysis of PAZ MS response using Minitab.	139
Figure D. 5. Data analysis of IPBC MS response using Minitab.....	140
Figure D. 6. Results from Minitab response optimizer.....	141
Figure D. 7. Overlaid contour plots for fungicide ESI-MS response. The factors included electrolyte concentrations, capillary voltage and fragmentor voltage. The optimal working range yielding the highest fungicide MS responses is colored white.....	142

LIST OF ABBREVIATIONS

ACN	Acetonitrile
AZA	Azaconazole
CFD	Computational fluid dynamics
DOE	Design of experiments
EIC	Extracted ion current
ESI	Electrospray
EWC	Extracted wavelength chromatogram
FIA	Flow injection analysis
GC	Gas chromatography
GC-MS	Gas chromatography - mass spectrometry
HAZ	Hexaconazole
IPBC	3-Iodo-2-propynyl butylcarbamate
IS	Internal standard
LC	Liquid chromatography
LC-ESI-TOFMS	Liquid chromatography - electrospray - Time-of-flight mass spectrometry
LC-MS	Liquid chromatography - mass spectrometry
LOD	Limit of detection
LOQ	Limit of quantification
MeOH	Methanol
MS	Mass spectrometry
MS/MS	Tandem mass spectrometry
PAZ	Propiconazole
RH	Relative humidity
SPE	Solid phase extraction
TAZ	Tebuconazole
TIC	Total ion current
TOFMS	Time-of-flight mass spectrometry
TWC	Total wavelength chromatogram
UDS	User-defined scalars

ACKNOWLEDGEMENTS

I would like to express my genuine appreciation to my advisors, Dr. Alena Kubátová and Dr. Evguenii Kozliak, for their unwavering support, guidance, motivation and mentoring throughout my doctoral studies. I would like to thank Dr. Gautham Krishnamoorthy for his thorough help with diffusion modelling and with revising my manuscript. I also appreciate the support of my other committee members Dr. David Pierce, Dr. Julia Zhao, and Dr. Frank Bowman.

I am very grateful to Ben Wallace and Steven Fisher from Marvin Windows and Doors for their financial support of all four projects, but also for providing me with technical guidance, advice, and insights into industrial wood treatment.

Big thanks go to Veronika Martinská for her work on tebuconazole diffusion and its environmental fate (Chapter II and III), to Josh Hatton for his help with the tebuconazole leaching study (Chapter IV), and to Brianna Gysberg for her work on wood purification using solid-phase extraction (Chapter V). I would also like to thank Rich Cochran and Jana Rousová for help training and troubleshooting various instruments.

I would like to thank the University of North Dakota, the UND Chemistry Department, and the UND Graduate School for financially supporting my studies and my travel to state and national conferences.

Finally, I would like to thank my husband, Jonathan Kukowski for his unconditional love, support, understanding, encouragement, and help editing my manuscripts.

To my babčulka Jana Balková,
who inspired me to pursue doctorate studies in science.

ABSTRACT

Triazoles are commonly used wood preservatives active against a wide range of fungi and bacteria. A full understanding of their diffusion and distribution in wood is essential for the development of enhanced treatment protocols ensuring long-term stability of wood products. Moreover, determining the fate of sorbed triazoles is critical to minimize their losses, but also to assess the environmental impact of the treated wood product. Herein, the diffusion, distribution and environmental fate of triazoles was studied using a radiolabeled tracer, ^{14}C -uniformly-labeled tebuconazole. The wood-treatment technique was representative of industrial practices for the manufacturing of above-ground products such as windows and doors; specifically, ponderosa pine wood was dip-treated with a solvent-based, metal-free formulation. A three-step extraction protocol was developed for triazole isolation from wood along with sensitive analytical techniques for fungicide quantification including liquid scintillation counting and solid phase extraction followed by liquid chromatography - Time-of-flight mass spectrometry (LC-TOFMS).

In order to assess the effectiveness of commercially used wood preservative treatments, the penetration of tebuconazole (TAZ) into softwood was measured

and then modeled using a double-logarithmic model. The longitudinal and surface penetration of TAZ dissolved in a naphtha-based solvent was investigated at ambient pressure and temperature. Solvent and TAZ time-dependent diffusion coefficients were estimated using solvent mass uptake data spanning six months and complete TAZ immersion data spanning three minutes. Results obtained from computational methods matched those calculated from experimental data for short treatment times, suggesting that the bulk of the TAZ diffused together with the solvent. TAZ redistribution was not observed in treated wood samples upon laboratory aging for six months with the exception of subsurface evaporative losses.

The fate of triazole fungicides in ponderosa pine wood was investigated in outdoor and controlled-environment experiments using TAZ, which was accompanied by propiconazole (PAZ) in selected experiments. To investigate TAZ fate in detail, loosely and strongly bound fractions were differentiated using a multi-step extraction. The loosely bound TAZ fraction, extracted through two sonications, accounted for $85 \pm 5\%$ of the total TAZ, while the strongly bound TAZ was extracted only with an exhaustive Soxhlet extraction and corresponded to the remaining $15 \pm 5\%$. A significant fraction ($\sim 80\%$) of the original TAZ remained in the wood despite a six-month exposure to harsh environmental conditions, maintaining wood preservation and assuring minimal environmental impact. Depletion of loosely bound TAZ was observed from cross-sectional surfaces when exposed to rain, high humidity and sunlight. Water leaching was the major route

leading to triazole losses from wood. The leaching rate was found to be slightly higher for TAZ than for PAZ. The contribution of bio-, photo- and thermal degradation of triazoles was negligible as both PAZ and TAZ sorbed in wood remained intact. Triazole evaporation was minor at the moderate temperature (20–25 °C) recorded throughout the outdoor study.

A detailed investigation of TAZ leaching was executed over a period of two months using various aqueous settings including high air humidity and simulated continuous or intermittent rain. Along with the exposure type, the effect of aqueous surface paint and end-grain sealing on TAZ loss was explored. Despite the exposure of treated wood to laboratory-simulated harsh environmental conditions, more than 75% of the originally sorbed TAZ remained in the wood under all scenarios. While high air humidity did not lead to TAZ depletion, simulated continuous rain led to a TAZ leaching mainly from the end grain. TAZ leaching was found to be higher for unpainted wood, where up to 40% of the originally sorbed TAZ was prone to depletion from an end grain. End-grain sealing with water-based primer and paint led to a substantial two-fold reduction of TAZ leaching.

Finally, a LC-TOFMS method was developed and optimized for simultaneous quantification of triazoles and IPBC in aqueous wood extracts, specifically wood leachate. Analyte concentration and wood matrix clean-up was achieved using a solid phase extraction prior to LC-TOFMS analysis, exhibiting > 94% fungicide recoveries. Optimization of electrospray ionization and MS conditions (e.g., solvent system, electrolyte type, electrolyte concentration, capillary and fragmentor

voltages) was accomplished using an initial screening followed by an in-depth optimization via design of experiments. The optimal conditions employed an acetonitrile-water solvent system with 1.7 mM ammonium acetate, capillary voltage of 4350 V, and fragmentor voltage of 115 V. Matrix-affected limits of detection were 13–20 ng·L⁻¹ for triazoles, and 63 ng·L⁻¹ for IPBC. The developed method was applied to industrial wood leachate samples.

I. CHAPTER: CHALLENGES TO WOOD PRESERVATION: UNDERSTANDING SORPTION, DISTRIBUTION, ENVIRONMENTAL FATE, AND CHARACTERIZATION OF TRIAZOLES

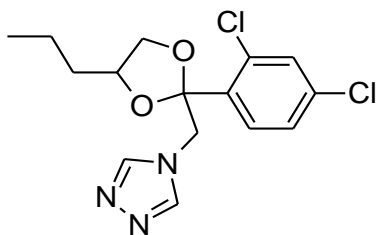
Wood matrix is known to be susceptible to biological attacks from microorganisms, such as fungi and bacteria. The resulting gradual wood decay contributes to natural recycling but also leads to deterioration of wood products while still in service.¹ As a result, wood is commonly treated with various biocides to enhance its durability. Inorganic preservatives had been widely used for wood treatment in the last century, however metal leaching²⁻⁴ and problematic combustion of the treated wood⁵ triggered health and environmental concerns⁶. As an alternative, organic biocides (metal-free or copper containing) have been introduced exhibiting lower mammalian toxicity and possessing lesser harm to the environment.⁷

The main classes of metal-free organic fungicides used for wood protection include carbamates, creosotes, isothiazolones, quaternary ammonium compounds, sulfamides, and triazoles.⁸ Many of these preservatives are effective against a specific class of microorganism, nonetheless, synergistic effects were reported for a group of triazole fungicides, helping to overcome this selectivity.⁹⁻¹⁰ Aside from formulations containing mixtures of triazoles, they are often enriched with 3-iodo-2-propynyl butylcarbamate (IPBC) to further enhance the efficacy and broaden the

spectrum of activity. Furthermore, triazoles have an added advantage of exhibiting high antifungal activity in both solvent- and water-based formulations.¹¹

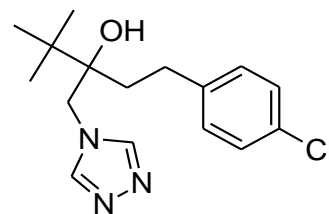
Triazoles were first introduced to the market after the 1980s,¹²⁻¹⁴ and they are now among the most commonly used fungicides in the wood industry.¹⁵⁻¹⁷ Frequently used examples include tebuconazole (TAZ), propiconazole (PAZ), azaconazole (AZA), and hexaconazole (HAZ) (Figure 1). Globally, TAZ accounts for the largest share of triazole demand across all industries with 16,000 tons consumed per year and a market of \$600 million in 2015.¹⁸

Propiconazole (PAZ)



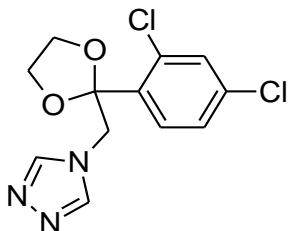
Molecular Formula = $C_{15}H_{17}Cl_2N_3O_2$
Formula Weight = 342.22038
Monoisotopic Mass = 341.069782 Da

Tebuconazole (TAZ)



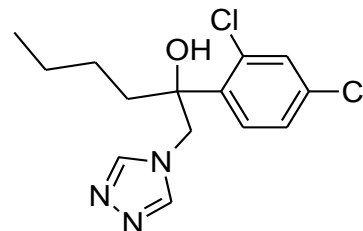
Molecular Formula = $C_{16}H_{22}ClN_3O$
Formula Weight = 307.81838
Monoisotopic Mass = 307.14514 Da

Azaconazole (AZA)



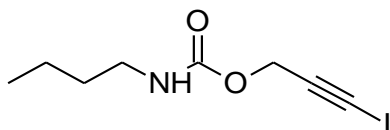
Molecular Formula = $C_{12}H_{11}Cl_2N_3O_2$
Formula Weight = 300.14064
Monoisotopic Mass = 299.022832 Da

Hexaconazole (HAZ)



Molecular Formula = $C_{14}H_{17}Cl_2N_3O$
Formula Weight = 314.21028
Monoisotopic Mass = 313.074868 Da

3-Iodo-2-propynyl butylcarbamate (IPBC)



Molecular Formula = $C_8H_{12}INO_2$
Formula Weight = 281.09085
Monoisotopic Mass = 280.991264 Da

Figure 1. Chemical structures of triazoles used in wood industry and a common additive, IPBC.

I.1 DIFFUSION OF TRIAZOLE FORMULATIONS INTO WOOD

Studying the penetration of individual components present in wood treatment solution is critical for the design and development of successful impregnation protocols due to differences in physical properties of active fungicides and the solvent. Although much effort has been devoted to understanding water sorption¹⁹⁻²⁴ and moisture transport in wood,²⁵⁻²⁸ less information is available on the absorption of organic solvents, which are frequently used for wood treatment with triazoles. Furthermore, most of the previous studies on non-aqueous liquid absorption were conducted using supercritical fluid treatment,²⁹⁻³¹ which limits their applicability, as many current wood treatment application protocols assume ambient conditions. Moghaddam et al. compared the wettability and liquid sorption of water and *n*-octane into pine wood.³² The overall *n*-octane uptake was smaller than for water. The *n*-octane sorption kinetics consisted of two phases, i.e., initial fast sorption (30 s) followed by a slower absorption phase.³² Popova et al. studied the penetration of *n*-hexadecane, naphthalene and 2,4-dinitrotoluene into small southern yellow pine samples at ambient conditions.³³ In this study, the effective point-source diffusivities increased with increased solvent volatility. Haloui et al. examined the diffusion of methanol in *Picea* wood.³⁴ Just as for water, the longitudinal penetration was found to occur significantly faster than those in the transverse directions. It is important to note that typical softwoods such as *Picea* have longitudinal tracheids representing 93% of the void volume whereas longitudinal resin canals and transversal wood rays account for merely 1% and 6%, respectively.³⁵ Since the rays and resin canals form only a small fraction of

the pore volume, the primary transport occurs through the longitudinal tracheids and as a result, longitudinal effective diffusion coefficients are several times greater than those in the transverse directions.³⁶⁻³⁷

A couple of studies have focused on the diffusion and distribution of carbon-based preservatives within wood structures. Volkmer et al. studied the penetration of water-based IPBC solutions into coniferous wood along with the resulting IPBC distribution.³⁸ The distribution of PAZ and IPBC in thermally modified wood was later reported by Sheikh.³⁹ Yet, this study may not be applicable to the distribution of preservatives within raw wood structures as thermal modification is expected to cause structural changes in wood. Thus, the diffusion and distribution of organic preservatives in wood treated with solvent-based formulations at ambient conditions has not been examined. This gap will be addressed in Chapter II.

I.2 ENVIRONMENTAL FATE OF TRIAZOLES

I.2.1 Leaching

When used as a building material, wood is regularly exposed to water in the form of high air humidity and rain, which can mobilize sorbed triazoles and lead to their leaching. Understanding the kinetic of this process is essential to prevent wood deterioration.⁴⁰ While the leaching behavior of inorganic preservatives has been extensively studied,^{3, 41-42} leaching of organic preservatives has been investigated to a lesser extent, and was limited to pressure-treated wood using mainly metal-containing formulations.⁴³⁻⁴⁸ Since triazoles are among the most frequently used

organic wood preservatives,^{15-17, 49-50} determination of their leaching potential under various conditions is warranted.

The leaching potential of preservatives was shown to depend on various parameters, such as affinity to wood in terms of sorption and fixation.⁵¹⁻⁵³ In general, the leaching process is characterized by preservative partitioning between the wood and the aqueous phase (mobilization), followed by its diffusion through the wood porous matrix.⁴³ Studies performed by Lupsea *et al.* using a copper-borate-azole formulation showed that TAZ fixation within wood was pH dependent and thus suggested hydrogen bonding of TAZ with the carboxyl and phenolic groups of wood.⁴⁴⁻⁴⁵ TAZ leaching likely occurred through its molecular association and co-elution with wood extractives, such as carboxylic acids, alcohols, phenols, and ketones.^{43, 45} TAZ was also found to be physically dislodged from pressure-treated wood by rain as opposed to its dissolution in water.^{45, 54}

Previous studies focusing on TAZ leaching mainly used wood co-treated with copper and other metals;⁴³⁻⁴⁸ however many wooden products, such as windows, are treated with formulations that do not contain metals. Since complexation with a metal has been shown to reduce TAZ leaching rates,⁵⁵⁻⁵⁷ the published results cannot be used to describe metal-free systems. For instance, the natural depletion of TAZ from pine decks co-treated with copper during a ten-month exposure to rain was found to be between 0.8–1.4% of the original amount present in decks.⁵⁸ In contrast, a year-long leaching study on treated spruce using a formulation without metals showed the percentages of leached TAZ to be 21.0–25.5% in the first 7 months and 22.5–30.3% in 12 months.⁵⁴

In addition to using metals as part of the formulation, the majority of studies were performed on pressure-treated wood that was fully immersed into water.^{44, 47-48, 51} Pressure treatment of wood (e.g., wood impregnation with preservatives under pressure) is commonly used for ground contact wood (e.g., decks) to increase the penetration depth and active loading.⁵⁸ However, in North America, nearly all of the wood used to produce windows and door frames is dip-treated,¹⁷ which is cost-effective and ensures sufficient concentration of preservatives near the wood surface. Moreover, full immersion of treated wood into water is not a real-world scenario descriptive of window exposure to rain, where only the surface is exposed to water droplets. Schoknecht *et al.* have confirmed this assertion by comparing PAZ leaching from treated materials via full immersion into water to water spraying onto the surface (simulated rain) and found that the initial preservative emissions were much higher for the immersion experiments than those obtained with simulated rain.⁵¹

I.2.2 Evaporation

In addition to leaching, evaporation may also decrease the amount of fungicide in wood and thus affect the product's service life. Even though vaporization of triazoles is not expected, as the corresponding Henry's constants suggest their non-volatility (e.g., TAZ has a Henry's constant of $1 \times 10^{-5} \text{ Pa m}^3 \cdot \text{mol}^{-1}$), low yet detectable emission rates were reported in several studies.⁵⁹⁻⁶² A two-year indoor cabin study on treated timber (using a water-based formulation containing TAZ, PAZ, and other preservatives) showed the concentration of airborne triazoles

between 3–10 ng·m⁻³.⁶² Horn et al. also reported low TAZ emission rates of 0.5 µg m⁻²·h⁻¹ for wood treated with an organic solvent.⁶⁰

I.2.3 Biodegradation & Biotransformation

Past studies also described both biotransformation and biodegradation of TAZ and PAZ by the surrounding microbial species (fungi, bacteria) in liquid media,⁶³⁻⁶⁵ soil,⁶⁶⁻⁶⁷ and wood matrix⁶⁸. Cleavage of the triazole ring is one of the major pathways for TAZ degradation by bacteria, mold, and soft and brown rot fungi.⁶⁴⁻⁶⁵ Once theazole ring is cleaved, TAZ loses its fungicidal activity. Another common detoxification path is TAZ oxidation leading to hydroxy-substituted products.⁶⁴ The hydroxyl group can be further acetylated or oxidized to form an ester or carboxyl group. Acetylation causes the deactivation of TAZ by decreasing its hydrophilicity. Aside from triazole ring cleavage and alkyl chain oxidation, PAZ was also found to undergo degradation of the dioxolane ring⁶⁹ and yield breakdown products such as 1,2,4-triazole, 2,4-dichlorobenzoic acid, and 1-chlorobenzene⁷⁰.

Even though previous studies identified the presence of triazoles in leachate water and indoor air, they only focused on one of the depletion scenarios as opposed to their combination. Also, metals were often added to the treatment solution, and majority of leaching studies were performed on pressure treated wood by full immersion into water. Therefore, these studies cannot be used to assess triazole environmental fate in wood dip-treated with formulations without metal additives. This gap will be addressed in Chapter III and IV.

I.3 FUNGICIDE DETERMINATION IN WOOD LEACHATE

As triazoles and IPBC are prone to leaching, their amounts in wood leachate should be regularly monitored to assess the losses from treated products and to determine the potential for environmental contamination. The American Wood Preservers Association (AWPA) method for triazole determination in waterborne solutions utilizes liquid chromatography coupled to ultraviolet detection (LC-UV) with no prior sample manipulation resulting in higher limits of detection than those achievable by mass spectrometers (MS), or by employing sample pretreatment.⁷¹ Even though sensitive LC-MS methods for determination of fungicides in aqueous samples were developed, to our knowledge, they did not simultaneously target triazoles and IPBC, or were not optimized for wood leachate matrix.

Wood leachate is a highly variable chemical matrix changing with respect to wood age, location, and environmental conditions.⁷² The complexity and the difference in polarity and structure of the components complicate the direct and simultaneous analysis of preservatives in wood leachate. Therefore, a sample purification step prior to LC-MS analysis is required to achieve good accuracy, repeatability, low limits of detection, but also to extend column lifespan. Solid phase extraction (SPE) has been the most commonly applied purification method for triazole determination in various matrixes, such as water,⁷³⁻⁷⁷ beverages,⁷⁸⁻⁷⁹ food and soil,⁸⁰⁻⁸⁶ wood,⁸⁷⁻⁸⁸ and animal tissue⁸⁹. However, SPE techniques targeting only triazoles may not be applicable to IPBC isolation as its chemical nature greatly differs from that of triazoles (Figure 1). Only a couple of SPE methods were developed targeting both

triazoles and IPBC,^{88, 90-91} and often employed an HLB cartridge. Since HLB is a reversed-phase sorbent composed of two monomers, hydrophilic N-vinylpyrrolidone and lipophilic divinylbenzene, it is suitable for the retention of a wider range of analyte polarities. Also, SPE prior to LC-MS aids the preconcentration of analytes on the cartridge, since their amounts in industrial wood leachate, although significant, may be near the method's limits of detection.

For quantification of triazoles in aqueous samples, LC is generally preferred over GC,⁷¹ which typically requires implementation of a drying step. The majority of published LC studies used either MS^{75, 86, 89-90, 92-99} or UV detection^{87, 100-102}. Specifically, quantification of triazoles and/or IPBC in aqueous samples was largely accomplished using electrospray tandem mass spectrometers (ESI-MS/MS) to achieve limits of quantification in the sub-ppb levels, however, none of these methods were developed for wood leachate matrix.^{75, 86, 89-90, 92, 94-99} As part of these studies, ESI-MS/MS parameters were typically optimized (e.g., ion transitions, capillary and collision voltages), but the solvent and electrolyte system did not appear to be evaluated, or were not reported. Nonetheless, the composition of LC mobile phase and the choice of electrolyte and its concentrations has a significant impact on ESI ionization efficiency, and hence the limits of detection.¹⁰³ Finally, only a couple of triazole quantification methods for aqueous samples were developed on a non-tandem MS, such as time-of-flight MS (TOFMS), but did not target IPBC.¹⁰⁴⁻¹⁰⁵ Therefore, a simultaneous determination of triazoles and IPBC from wood leachate using TOFMS will be addressed in Chapter V.

I.4 STATEMENT OF PURPOSE

To ensure efficient wood protection yielding long-term product durability, the diffusion, distribution, and fate of triazoles has to be well understood to optimize the following key areas:

1. Wood impregnation (commonly referred to as treatment)
2. Wood surface coatings
3. Quality control

The steps taken in this dissertation to address these challenges have been explained below and are focused specifically on optimizing wooden windows and door manufacturing practices.

Due to the nonhomogeneous nature of wood, diffusion of triazoles is a complex, multifactorial process. An understanding of this process (i.e., rate of triazole diffusion and their subsequent distribution within wood) is essential for the development and optimization of **wood treatment** protocols ensuring sufficient amounts in desired locations. Chapter II focuses on the penetration of a hydrocarbon solvent containing triazole fungicides into ponderosa pine wood under ambient temperature and pressure. The sorption of a commercially available solution of Woodlife formulation was measured using gravimetry, while the distribution of triazoles was studied by liquid scintillation counting with ^{14}C -uniformly-labeled TAZ (^{14}C -TAZ). For both TAZ and the solvent, the effective diffusion coefficients were calculated to reveal the details of fungicide penetration

and distribution in wood. The TAZ distribution was also determined for treated wood after six months to find out whether the preservative continued to move when the treatment ended. The experimental data lead to the development of a simple numerical model that accurately predicts the extent of solvent and TAZ sorption and can be utilized in industry.

Under harsh environmental conditions, sorbed triazole fungicides can undergo biological, thermal and photo-degradation or be lost through vaporization and water leaching. Therefore, studying the long-term fate of triazoles is critical to further adjust the treatment length to account for these losses, or to design **wood surface coatings** that aid in stabilizing triazoles and reducing their mobility. Knowing the outdoor fate of triazoles also helps the industry to evaluate the environmental impact of their products. Therefore, in Chapter III, a three-part study investigating the environmental fate of triazole fungicides in ponderosa pine corner pieces (representing window frame corners) is presented. Leaching, vaporization and degradation of triazoles were examined to determine their potential removal paths. First, the impact of environmental exposure on wood treated with a representative triazole, TAZ, was studied upon harsh outdoor conditions. Then, smaller-scale indoor experiments enabled an assessment of the effects of light, humidity, temperature, and time on TAZ and PAZ behavior in wood. Finally, the contribution of leaching to triazole depletion from wood was evaluated by determining TAZ and PAZ water leaching rates in laboratory settings. Throughout this study, both ¹⁴C-labeled and non-labeled TAZ were employed with the goal of achieving quantitative measurements using a radiolabeled tracer along with a

detailed characterization of potential degradation products using the non-labeled fungicide. Chapter IV builds on the findings of Chapter III by specifically targeting conditions such as high humidity and simulated rain in laboratory settings to close mass balance on triazole leaching, which is shown to be the main triazole depletion path. It also investigates the impact of aqueous surface paint and end-grain sealing on ^{14}C -TAZ mobility to provide recommendations to the industry on **wood coating** usage. Throughout the study, both the exposed wood and run-off water are analyzed using liquid scintillation counting.

Finally, a simple analytical method to quantify triazoles and IPBC in wood leachate is presented in Chapter V. Wood leachate purification is accomplished using an SPE prior to LC-MS, capable of retaining both triazoles and IPBC. Also, main factors affecting the fungicide MS response (e.g., solvent system, electrolyte type, electrolyte concentration, capillary and fragmentor voltages) are optimized using design of experiments (DOE) methodology. This method may be adapted by industry and used as a **quality control** measure or for environmental monitoring.

II. CHAPTER: DIFFUSION OF TEBUCONAZOLE INTO SOFTWOOD UNDER AMBIENT CONDITIONS AND ITS DISTRIBUTION IN FRESHLY TREATED AND AGED WOOD

II.1 MATERIALS AND METHODS

II.1.1 Chemicals and Reagents

Untreated ponderosa pine wood blocks (15.2 cm x 3.8 cm x 3.8 cm) were stored under standard conditions in an air-conditioned building (22 ± 2 °C, ambient pressure and ca. 45% relative humidity) for one month prior to experiments. Smaller wood slices (0.2 cm x 3.8 cm x 3.8 cm, shown in Figure A. 3) were cut using a Craftsman 9" band saw purchased from Sears Brands Management Corporation (Hoffman Estates, IL, USA) in a ventilated laminar hood. The saw blade was a Powertec brand (62" x 3/8", 10 teeth per inch). The hood was further protected by a plastic enclosure illustrated in Figure A. 4 to eliminate ¹⁴C-wood dust contamination.

Woodlife 111 RTU from Kop-Coat, Inc. (Pittsburgh, PA, USA) was used as a model nonpolar solvent with 0.22% of dissolved fungicides (TAZ, PAZ, IPBC). LC grade acetone was obtained from Fisher Scientific (Pittsburg, PA, USA). Betamax from MP Biomedicals, LLC (Solon, OH, USA) was used as a scintillation cocktail.

For the analysis of fungicide distribution, ^{14}C -TAZ obtained from Commerce Institute of Isotopes Co., Ltd. (Budapest, Hungary) with a radioactivity of $7.4 \text{ MBq}\cdot\text{mL}^{-1}$ was spiked as a labeled tracer to Woodlife. The amount of ^{14}C -TAZ obtained was diluted in 500 mL of Woodlife, the radioactivity of the resulting stock solution was $7.4 \text{ MBq}\cdot\text{L}^{-1}$. For specific experiments, $100 \mu\text{L}$ of the labeled stock solution was further diluted in 1.0 mL of non-labeled Woodlife, resulting in a radioactivity of $0.74 \text{ MBq}\cdot\text{L}^{-1}$.

II.1.2 Experimental Procedures

Wood blocks were subjected to a common commercial pretreatment for the allotted time periods. The determination of diffusion rates was based on the following experimental series: (1) gravimetric monitoring of the solvent penetration (mass uptake of Woodlife) over a period of 2 months; (2) determination of the saturation point of wood with Woodlife enabling the calculation of effective diffusion coefficients for the solvent; (3) distribution analysis of ^{14}C -TAZ in freshly contaminated wood enabling the calculation of TAZ effective diffusion coefficients at various sorption times; (4) distribution analysis of ^{14}C -TAZ in aged wood (three and six months) to determine whether the TAZ distribution changed with time.

II.1.2.1 Mass Uptake of Woodlife

To determine the mass uptake of Woodlife in wood, standard size wood blocks were placed vertically in glass containers along with the solvent covering ca. 1 cm of the wood samples. The height of the solvent was maintained at the same level throughout the entire experiment by periodic refilling. Gravimetric measurements

were conducted in quadruplicate at suitable time intervals based on the expected rate of absorption. At the allotted times, the wood blocks were taken out, gently wiped with a lint-free tissue to remove sorbent droplets from the sample's surface, weighed, then placed back into the glass container and sealed with a lid.

II.1.2.2 Wood Saturation with Woodlife

To determine the mass uptake equilibrium (i.e., final) values, smaller size wood slices (0.2 cm x 3.8 cm x 3.8 cm) were submerged into the solvent in quadruplicate. The purpose of the full submersion setup and the reduced size of the wood samples was to reach the mass uptake equilibrium faster. Once a week the wood slices were taken out, gently wiped with a lint-free tissue, weighed, and then placed back into the glass container and sealed with a lid. Three readings with a constant weight value were considered a sign of reaching equilibrium (approx. 1.5 months).

II.1.2.3 Processing of Freshly Contaminated Wood Samples

Wood blocks were submerged into a radiolabeled Woodlife solution in quadruplicate for two allotted times, 0.5 and 3.0 min. These treatment times were selected based on the solvent mass uptake in order to obtain sufficient amounts of ^{14}C -TAZ in wood and also to mimic industrial treatment. Wet wood was transferred into a glass container with several skewers placed on the bottom to limit the surface contact of the treated wood. To prevent possible cross-contamination of wood slices during the subsequent wood block cutting, wood blocks were dried for 24 hours and then cut into slices of 2-mm thickness. Selected slices were further cut as shown in Figure 2 so the outer 5-mm wide layer

(reflecting the surface absorption) could be analyzed separately from the inner part (reflecting the longitudinal diffusion). The width of the outer layer was selected based on preliminary experiments validating the full recovery of transversally penetrating chemicals.

Potential cross-contamination during the cutting was ruled out as there was no carryover from slices with higher radioactivity to those with lower radioactivity. In an experiment where one half of a wood block was cut from the outside end towards the inside (i.e., decreasing radioactivity) and the second half was cut in the opposite direction (thus increasing radioactivity), no statistically significant difference was found in the amounts of ^{14}C -TAZ recovered.

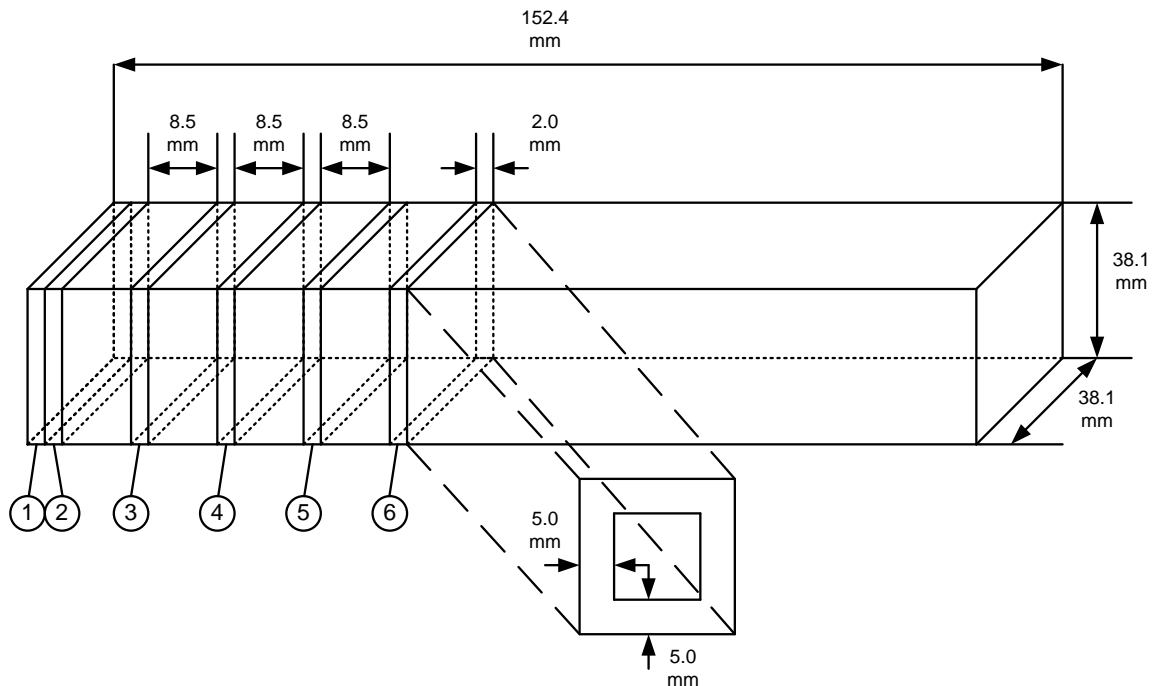


Figure 2. Wood cutting scheme. Selected 2-mm wide slices (1–6) were further cut so the outer 5-mm wide layer (reflecting the surface absorption) could be analyzed separately from the inner part (reflecting the longitudinal diffusion). Overall, 12 wood samples (6 slides) were analyzed with a liquid scintillation counter.

II.1.2.4 Processing of Wood Samples Aged for Six Months

Wood blocks were submerged into the radiolabeled Woodlife solution in quadruplicate for 3.0 min and dried on skewers as described in the previous section. After one day of drying, the wood blocks were transferred into a ventilated laminar hood, placed on a sheet of craft paper and left to age for either one or six months. Aged wood blocks were then cut according to the cutting scheme shown in Figure 2.

II.1.3 Extraction Procedure

To enhance the extraction of ^{14}C -TAZ from the wood matrix, wood slices were cut into smaller pieces using a blade. Smaller wood pieces were transferred into glass tubes and extracted with 3.5 mL of acetone (the volume was adjusted to cover all wood slices as shown in Figure A. 5) for one hour in an ultrasound bath.

In order to determine the extraction efficiency and wood matrix effect on scintillation counting, the specific set of experiments shown in Table 1 was performed in triplicate. A known amount of Woodlife radioactive solution (RS) was either analyzed directly or spiked (1) into acetone; (2) into acetone wood extract (wood sonicated in acetone for 1 hour); (3) onto smaller wood slices, which were then sonicated in acetone for 1 hour. The contribution of the wood matrix had a statistically significant impact reducing the recovery to $92 \pm 7\%$, which is similar to the values reported by others.^{88, 106} For laboratory-aged wood samples (six months), the overall recovery was found to be comparable to the non-aged wood recovery reported above.

Table 1. Determination of extraction and liquid scintillation counting efficiencies.

Sample	Recovery %	SD	RSD %
50 μL of RS ^a	99	3	3

Table 1 cont.

Sample	Recovery %	SD	RSD %
50 µL of RS + 400 µL of acetone	104	2	2
50 µL RS + 400 µL acetone wood extract ^b	101	3	3
50 µL of RS spiked onto wood & extracted with acetone	92	7	8

^aRS - radiolabeled Woodlife solution of a known ¹⁴C-TAZ concentration

^bnon-radiolabeled extract

II.1.4 Liquid Scintillation Counting

For the analysis, 1.0 mL of an extract was vortexed with 4.0 mL of the scintillation cocktail and analyzed after an overnight equilibration in a scintillation counter, Beckman Coulter LS 6500 purchased from Beckman Coulter, Inc. (Fullerton, CA, USA). The analysis was run for 3.0 min in a DPM calculation mode (disintegrations per minute, which is directly proportional to the tracer's concentration). Detailed information on the method and analysis procedure is provided in Appendix A (Figure A. 1 and Figure A. 2).

II.1.5 Diffusion Coefficient Determination

The general diffusion equation for one-dimensional analysis under non-steady state condition is defined by Fick's second law (Eq.1).

$$\frac{\partial C}{\partial t} = D \frac{\partial^2 C}{\partial x^2} \quad \text{Eq. 1}$$

This equation reflects the rate of change with time of the concentration between parallel planes at points x and $(x + dx)$. Fick's second law is valid for the conditions assumed, i.e., linear one-dimensional diffusion.¹⁰⁷ The solutions of Fick's second law are based on the given set of boundary conditions.

II.1.5.1 Diffusion of Woodlife into Wood

In terms of mass uptake in a medium bounded by two parallel planes, such as $y = 0$ and $y = L$ where the diffusion through the edges is negligible, Eq. 1 can be solved as

$$\frac{W_t - W_0}{W_\infty - W_0} = 1 - \frac{8}{\pi} \sum_{n=0}^{\infty} \frac{1}{(2n+1)^2} e^{-D(2n+1)^2 \pi^2 t / L^2} \quad \text{Eq. 2}$$

where W_t and W_0 are the wood block weights [g] at times t [s] and $t_0 = 0$, L is the length [m] of the wood block and D is the diffusion coefficient [$\text{m}^2 \cdot \text{s}^{-1}$].³⁶ The maximum possible mass of absorbed liquid in wood at an infinite time, W_∞ , was measured with smaller wood slices fully submerged into Woodlife.

For short times, Eq. 2 can be further simplified as Eq. 3.

$$\frac{W_t - W_0}{W_\infty - W_0} = \frac{4}{L\sqrt{\pi}} \sqrt{Dt} \quad \text{Eq. 3}$$

For rectangular shaped wood blocks, Eq. 3 can be re-written as Eq. 4¹⁰⁸ where A is the surface area [m^2] of a wood block in contact with the liquid and V is the volume [m^3] of a wood block.

$$\frac{W_t - W_0}{W_\infty - W_0} = \frac{2}{\sqrt{\pi}} \left(\frac{A}{V} \right) \sqrt{Dt} \quad \text{Eq. 4}$$

If h , w and l are the height [m], width [m] and length [m] of a wood block, respectively, and d is the depth [m] at which the wood block was immersed in the liquid, then $A = lw + 2dl + 2dw$ and $V = hwl$.

II.1.5.2 Diffusion of TAZ into Wood

The effective diffusion coefficient for fungicide penetration into wood can be estimated by determining the concentration as a function of position and time. The solution of Eq. 1 for $C_0 < C$ upon using the boundary conditions given below yields the normalized concentration expression (Eq. 5),¹⁰⁹

$$\frac{C}{C_0} = \operatorname{erfc} \frac{z}{2\sqrt{Dt}}; \quad \text{Eq. 5}$$

$$C = \begin{cases} C = C & \text{at } y > 0 \\ C = C_0 & \text{at } y = 0 \end{cases}$$

where z [cm] and t [s] are the penetration distance and time, respectively; D is the effective diffusivity [$\text{cm}^2 \cdot \text{s}^{-1}$], C is the concentration of the target chemical at certain z and t , C_0 is the total concentration, and erfc is the complementary error function. The diffusion coefficients were calculated for each separate slice using the solver function in Microsoft Excel.

As shown in Eq. 5, if a wood block at time t is cut into slices with a height of z , the successive slices would represent the penetration distances z , $2z$, $3z$, etc. The value of effective diffusivity obtained this way, by measuring (C/C_0) in each slice at a given t , would fully describe the fungicide distribution in wood at the allotted time.

II.1.6 Mass Balance Closure

The mass balance closures of both the solvent and total TAZ uptake were conducted for two immersion times, 0.5 and 3.0 min. The calculations were based on the set concentrations of ^{14}C -labeled and non-labeled TAZ in the solvent, 1.5×10^{-5} and 2.2×10^{-1} wt. %, respectively.

For the solvent, the measured uptake was obtained directly from gravimetry whereas the calculated uptake was estimated based on the amount of radioactivity (i.e., ^{14}C -TAZ) recovered after extraction of all pertinent wood cuts. The amount of tracer found in the inner part of a wood block (Figure 2) was included up to the distance where the tracer amount was zero (3–4 cm from the end of the block). The amount of tracer found in the outer part of a wood block was counted only up to the distance of 1 cm from the end and only on one side of the wood block, just as the wood samples were dipped into the solvent in the experiments involving gravimetric measurements. Overall, 1.8×10^{-7} and 2.7×10^{-7} grams of ^{14}C -TAZ were recovered for the immersion times of 0.5 and 3.0 min, respectively.

For TAZ, the amount of ^{14}C -tracer recovered in wood was measured directly by scintillation counting and recalculated to the total amount of TAZ. The calculated TAZ uptake was obtained by multiplying the measured solvent uptake from gravimetry by the total TAZ concentration in the solvent (both ^{14}C -labeled and non-labeled).

II.1.7 Numerical Simulation

To obtain order-of-magnitude estimates of the effective diffusion coefficients, Eq. 1 was solved numerically using the commercial Computational Fluid Dynamics (CFD) code ANSYS FLUENT¹¹⁰ by modeling the solvent as well as TAZ as user-defined scalars (UDS). The wood block was discretized into 16,000 hexahedral computational cells and the QUICK scheme¹¹¹ was employed for the spatial discretization of the diffusion term (RHS in Eq. 1). For TAZ penetration, time dependent variations in the longitudinal and surface diffusion coefficients were implemented through user-defined functions in ANSYS FLUENT.

II.2 RESULTS AND DISCUSSION

II.2.1 Woodlife Absorption

II.2.1.1 Solvent Mass Uptake

The mass uptake of Woodlife into untreated wood blocks was found to be nearly proportional to the immersion time within several different absorption phases (Figure 3). After 1 minute of treatment (Phase 1), the absorption rate decreased indicating the transition to the next sorption phase (Phase 2). As sorption continued, the absorbed liquid content continued to increase in time, but with a slower effective absorption rate ultimately leading to the third diffusion phase, Phase 3, which proceeded until complete wood saturation occurred.

To ascribe these sorption phases to specific physical processes, effective diffusion coefficients were calculated for each phase as described in the next section.

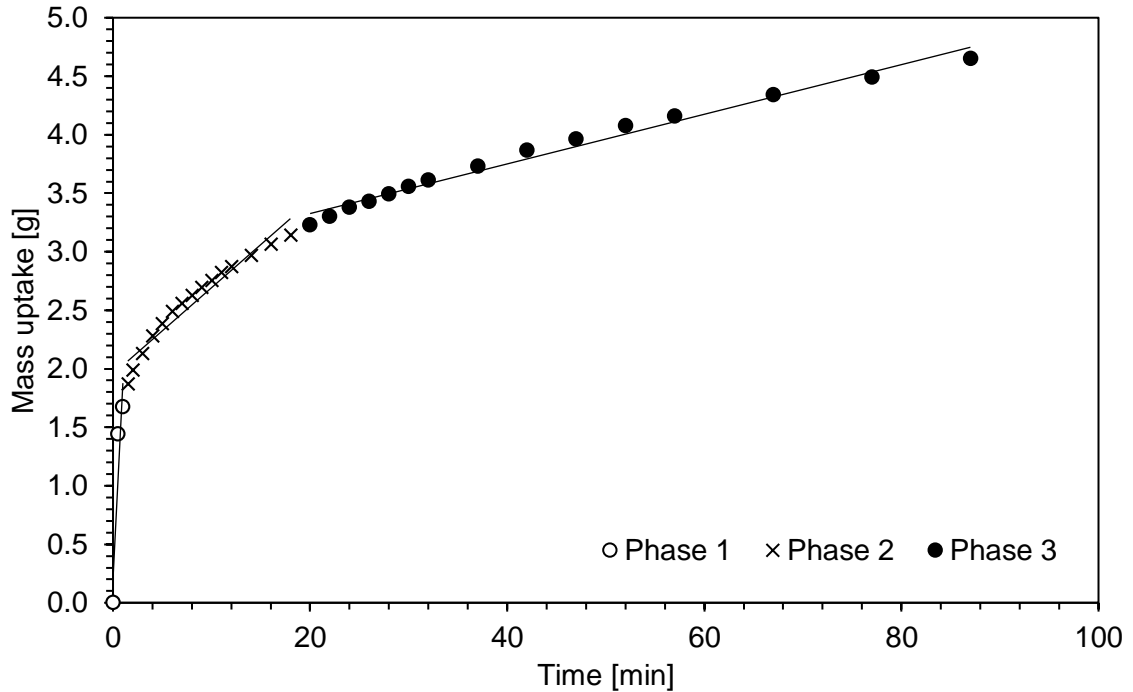


Figure 3. Mass uptake of Woodlife into wood blocks (15.2 cm x 3.8 cm x 3.8 cm) as described in section II.1.2.1.

II.2.1.2 Effective Solvent Diffusion Coefficients

To represent the transient variations in the effective diffusion coefficients in a more succinct manner, their values were estimated using Eq. 4 and summarized in Table 2. As seen from Eq. 4, mass uptake is proportional to the square root of the effective diffusion coefficient. The maximum possible mass of absorbed liquid in wood at an infinite time, W_{∞} , was calculated to be $1.8W_0$ in the equilibration

experiments using smaller wood slices fully submerged into the solvent (see section II.1.2.2). The calculation of diffusion coefficients for each of Woodlife's absorption phases included the effective values of W_0 and W_∞ for the pertinent phase. Values of W_∞ for the first and second sorption phases were pseudo equilibrium values, selected arbitrarily by inspecting the sorption curves at the times when the slope changes were observed. The measured W_∞ value was used only for the estimation of Phase 3 diffusion coefficients. Values of W_0 were also pseudo equilibrium values for both Phase 2 and Phase 3, whereas in Phase 1 the measured weight at zero time was used.

Phase 1, the initial rapid solvent uptake, appears to be due to the pore-filling on the wood surface and multilayered absorption. The sorption rate with the penetration time less than 1 min yielded an effective diffusion coefficient being one order of magnitude greater than that in Phase 2, which lasted ca. 20 min. During Phase 2, relatively large tracheids interconnected by smaller diameter pits near the surface appear to be filled. As can be seen in Figure 3, Phase 2 could be differentiated into two subphases differing in the extent of pore filling, but this level of detail was deemed to be unnecessary. Phase 3, an extremely slow final step of sorption, can be attributed to molecular diffusion by which a fluid migrates and spreads through capillaries and wood pores. As most of the air already escaped and all the surface voids were filled in the two initial phases, the liquid movement was restricted to the bulk of the matrix only. The effective diffusion coefficient in the final phase was yet another two orders of magnitudes lower.

Table 2. Effective diffusion coefficients for three phases of Woodlife solution penetration into untreated ponderosa pine wood.

Penetrating Liquid	Phase 1	Phase 2	Phase 3
	Diffusion Coefficient, D_1 [$\text{m}^2 \cdot \text{s}^{-1}$]	Diffusion Coefficient, D_2 [$\text{m}^2 \cdot \text{s}^{-1}$]	Diffusion Coefficient, D_3 [$\text{m}^2 \cdot \text{s}^{-1}$]
Woodlife	$(6.1 \pm 0.6) \times 10^{-5}$	$(6.1 \pm 0.5) \times 10^{-6}$	$(6.5 \pm 1.2) \times 10^{-8}$

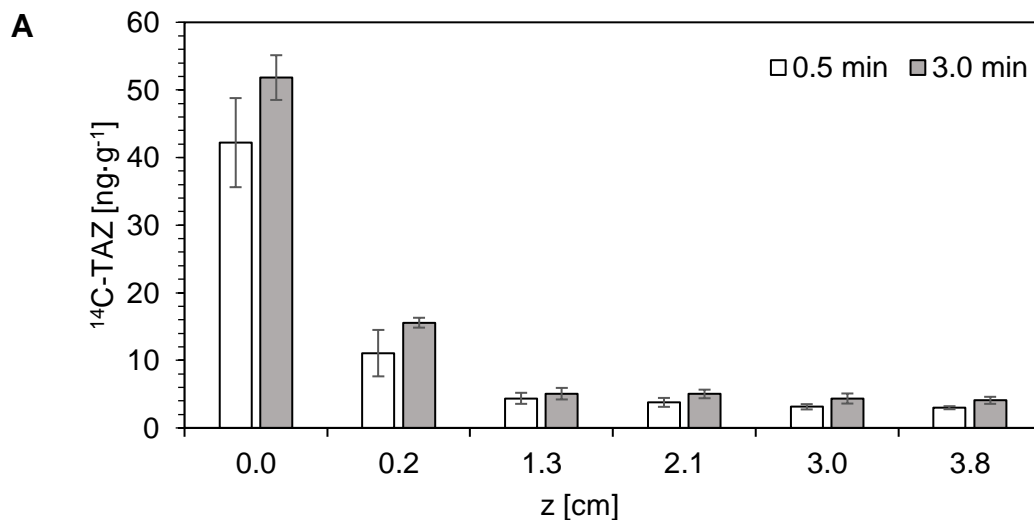
II.2.2 TAZ Absorption

II.2.2.1 TAZ Distribution in Freshly Contaminated Wood

The concentration profiles of ^{14}C -TAZ in wood after 0.5 and 3.0 min immersion times are shown in Figure 4. The TAZ amount recovered in the outer layer of a wood slice represented mainly the TAZ transversal diffusion. Since the movement across the grain is rather slow and limited to a small subsurface area, we will refer to it henceforth as surface absorption. As shown in Figure 4A, the first two surface slices contained a higher amount of TAZ, due to a partial contribution of longitudinal diffusion through near-surface tracheids at the corner of wood blocks. By contrast, all of the distant slices from the end-grain wood surface showed a constant TAZ amount (approx. 4 ng) absorbed near the wood surface. With increasing immersion time, the TAZ amount increased only slightly, so the effect of immersion time on TAZ surface absorption may be deemed insignificant.

Using only the inner cuts, the separation of longitudinal movement from the surface absorption was obtained (Figure 4B). The amount of TAZ in the inner parts of wood slices decreased exponentially as distance increased from the end-grain wood surface facing the solution. The maximum penetration distance was approx. 3 and 4 cm with immersion times of 0.5 and 3.0 min, respectively. The difference between the two immersion times was mostly reflected by the TAZ amount in the first slice, where the increased immersion time caused a 50% increase in the TAZ content.

Overall, with increasing distance of a wood slice from the wood surface, the TAZ uptake decreased, thus the bulk of TAZ remained adsorbed near the end-grain surface. This finding is consistent with other studies.^{39, 112} The increase in immersion time did not affect qualitatively the TAZ distribution profile in wood. It increased the amount of TAZ absorbed within the first surface slice, but not as significantly as would be expected given the large difference in immersion times.



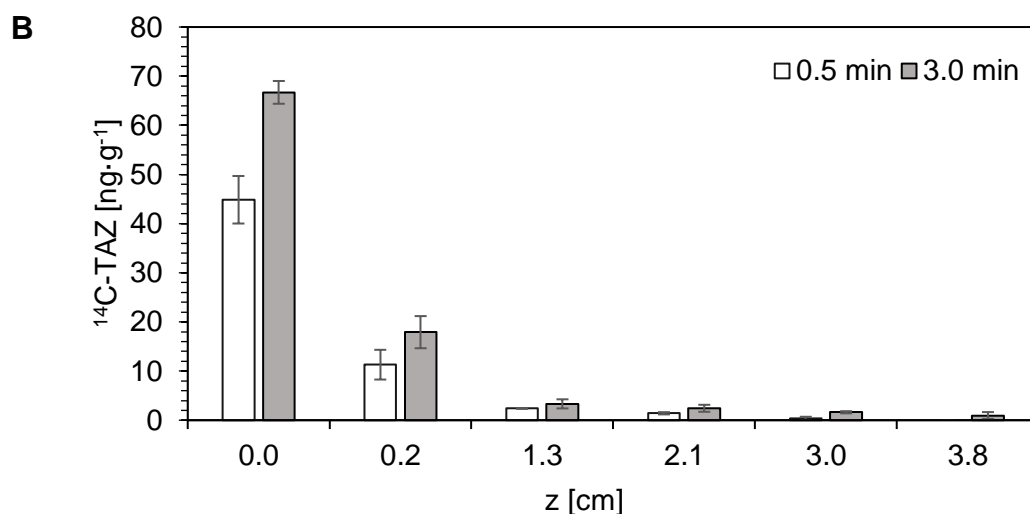


Figure 4. The distribution profile of TAZ in freshly contaminated wood (Figure 2) for the outer parts of wood slices (**A**) and the inner parts (**B**), thus reflecting the surface absorption (**A**) and longitudinal diffusion (**B**). White and grey bars represent 0.5 and 3.0 min immersion time, respectively.

II.2.2.2. TAZ Effective Diffusion Coefficients

The TAZ effective diffusion coefficients were calculated for each slice based on its distribution as a result of longitudinal penetration (Figure 4B). The numerical values increased gradually over five orders of magnitude for more distant slices (Table 3).

The connection between the numerical values of solute (¹⁴C-TAZ) and solvent (Woodlife) diffusivities may be obtained by assuming that the distance from the end-grain wood surface reflects the time when the solution enters the wood, i.e.,

sorption phases described in the section on solvent absorption. For example, the solute recovered in the most distant slices, with z being almost as high as 3 cm at an immersion time of 0.5 s, was absorbed within the first instants of the solution's contact with wood, i.e., in sorption Phase 1. Similarly, effective diffusion rates for TAZ in less distant slices ($z = 2\text{--}3$ cm) were comparable to those of the solvent in Phase 2, where the diffusion rate decreased by one order of magnitude. Finally, Phase 3 of solvent diffusion reflected the effective diffusion rates for TAZ found in the near-surface slices. The minimum penetration distance of 0.01 cm for the first slice was used instead of 0.00 cm since the calculation requires a non-zero distance value.

Table 3. Effective diffusion coefficients for TAZ longitudinal penetration calculated for wood slices at various distances.

Penetrating Chemical	Matrix	Effective Diffusion Coefficient, D [m ² ·s ⁻¹]		
		z [cm]	0.5 min	3.0 min
¹⁴ C-TAZ	Ponderosa pine	0.01	$(3.1 \pm 0.6) \times 10^{-10}$	$(5.1 \pm 1.0) \times 10^{-11}$
		0.20	$(4.4 \pm 0.4) \times 10^{-8}$	$(7.6 \pm 0.6) \times 10^{-9}$
		1.25	$(1.4 \pm 0.0) \times 10^{-6}$	$(2.3 \pm 0.5) \times 10^{-7}$
		2.10	$(3.8 \pm 0.0) \times 10^{-6}$	$(6.4 \pm 0.0) \times 10^{-7}$
		2.95	$(7.4 \pm 0.1) \times 10^{-6}$	$(1.2 \pm 0.0) \times 10^{-6}$
		3.80	$(1.2 \pm 0.0) \times 10^{-5}$	$(2.0 \pm 0.0) \times 10^{-6}$

By comparing the values obtained at two different immersion times, the effective diffusion rates for the longer 3.0 min exposure were found to be lower than that for 0.5 min exposure. This difference resulted from the occurrence of higher TAZ amounts in the first two cuts for the longer exposure, which increased the overall amount of TAZ in the wood, c_0 . Therefore, beyond this subsurface level, the TAZ fraction for each particular slice that was used for calculations (Eq. 5) became smaller and so did the effective diffusion coefficients. Thus, the use of a short immersion time (0.5 min) reflected the TAZ movement in the first instants of wood exposure. This effect was averaged out with increasing treatment time when sorption Phase I was masked by a longer subsequent Phase 2 as reflected in the obtained numerical values. A similar observation of increasing effective diffusion coefficients with the penetration depth was reported by Danvind and Ekevad.¹¹³ The results obtained can also be related to the occurrence of a small fraction of the penetrating chemical moving into the wood with significantly higher rates, as observed by Popova et al. for point source diffusion.³³

II.2.2.3 TAZ Distribution in Aged Wood

To investigate a possible redistribution of TAZ in the wood after its removal from the treating solution, the treated wood was aged for one and six months. A comparison of the TAZ distribution in freshly treated and aged wood is shown in Figure 5 for the outer (A) and inner (B) parts of wood slices, respectively, for an immersion time of 3.0 min. No TAZ redistribution in the near-surface wood area was observed as the amounts of TAZ recovered were statistically indistinguishable among any slices but the first one. By comparing the amounts of TAZ found in the

first slice (both surface and the inside wood part) in non-aged wood and in wood aged for six months, the loss of TAZ was approx. 25%, presumably caused by evaporation.

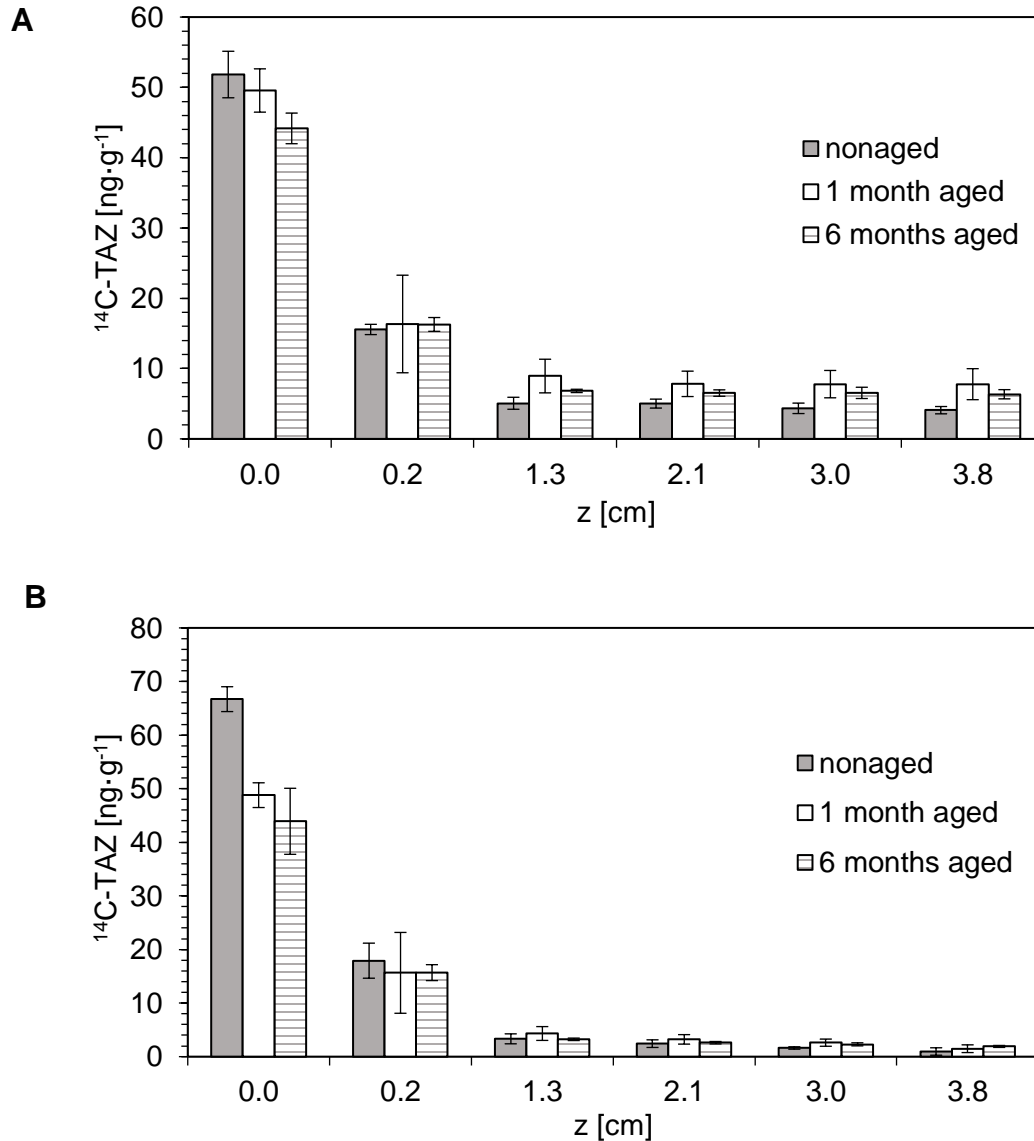


Figure 5. The TAZ distribution profile in freshly treated and aged wood after 3.0 min immersion time for the outer (A) and inner (B) parts of wood slices, thus

reflecting the surface absorption (**A**) and longitudinal diffusion (**B**). Grey, white, and striped bars represent the distribution of TAZ in freshly treated wood, aged wood for 1 months, and aged wood for six months, respectively.

II.2.3 Mass Balance

The amount of solvent absorbed was both measured directly and calculated based on the corresponding TAZ uptake. As shown in Table 4, the calculated amount of solvent accounted for 90% and 87% of the gravimetrically measured amount for the 0.5 and 3.0 min immersion times, respectively.

Similarly, the TAZ amount was both measured directly and calculated based on the corresponding solvent uptake. The measured over calculated TAZ uptake resulted in a 92% mass balance for the 0.5 min and 88% for 3.0 min immersion time (Table 4). The observed mass balance below 100% can be explained by the loss of TAZ in wood dust while cutting wood blocks with a saw. Nevertheless, mass balance was successfully closed for both the solvent and TAZ, thus mutually verifying the conducted measurements.

Table 4. Mass balance closure for TAZ and the solvent performed on wood blocks (15.2 cm x 3.8 cm x 3.8 cm).

	0.5 min	3.0 min
Measured solvent uptake (gravimetrically) [g]	1.33	2.00
Calculated solvent uptake (as radioactivity) [g]	1.20	1.75
[Calculated / Measured solvent uptake] × 100%	90	87
Calculated TAZ uptake (gravimetrically) [g]	0.0029	0.0044
Measured TAZ uptake (as radioactivity) [g]	0.0027	0.0039
[Measured / Calculated TAZ uptake] × 100%	92	88

The conducted experimental study showed that the effective diffusion coefficients of TAZ matched those of the solvent. However, the common model of solvent penetration, based on constant effective solvent diffusivities over significant time ranges, cannot be applied to the description of the TAZ penetration into wood, as the TAZ effective diffusivity continuously changes with time. Thus, a simple numerical model was developed accounting for the penetration of both the solvent and dissolved fungicide.

II.2.4 Data Evaluation

II.2.4.1 Empirical Model for Solvent Diffusion

In order to obtain order-of-magnitude estimates of the effective diffusion coefficients during the different sorption phases, Eq. 1 was solved numerically using the CFD code ANSYS FLUENT by modeling the solvent as a user-defined scalar (UDS) (see section II.1.7). The boundary conditions associated with the

UDS transport equation during the solvent mass uptake simulation are illustrated in Figure 6A. The numerical results reported in this study are presented in terms of normalized solvent concentrations assuming a UDS concentration of unity at the boundaries where the wood block is in contact with the solvent. A logarithmic variation in the effective diffusion coefficient (in the longitudinal direction) as a function of time was initially proposed as shown in Figure 6B. As per this variation, the effective longitudinal diffusion coefficients during Phase 1 (0–1 min) and Phase 2 (1–20 min) were on the order of $10^{-6} \text{ m}^2\cdot\text{s}^{-1}$ and $10^{-7} \text{ m}^2\cdot\text{s}^{-1}$ respectively. The effective surface diffusion coefficients were assumed to be 1% of the effective longitudinal diffusion coefficient prevailing at that time.

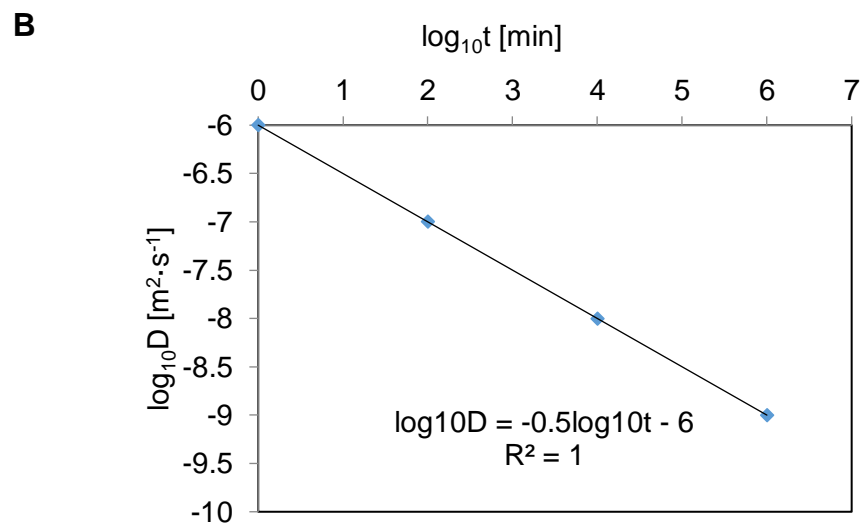
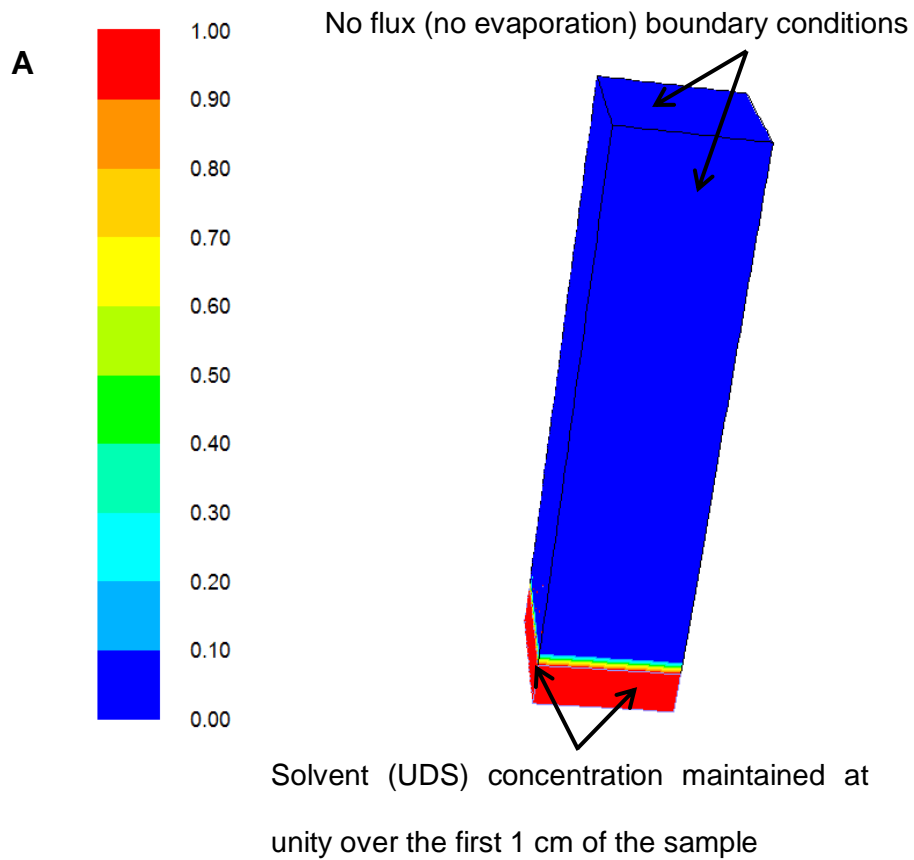


Figure 6. Boundary conditions associated with the user-defined scalars (UDS) during the numerical simulation of the solvent mass uptake (**A**); the logarithmic variation in the effective diffusion coefficient (longitudinal direction) as a function of time employed in the numerical simulations (**B**).

Figure 7A shows the normalized solvent concentration within the wood after 10,000 seconds of solvent mass uptake. In Figure 7B, the measurements spanning four months and numerical predictions of the normalized solvent mass uptake (LHS in Eq. 2) are compared. The normalized mass uptake was estimated numerically as the volume weighted average of the UDS concentration within the wood. A reasonable agreement between the measurements and numerical predictions employing the logarithmic variation in effective diffusivities is notable.

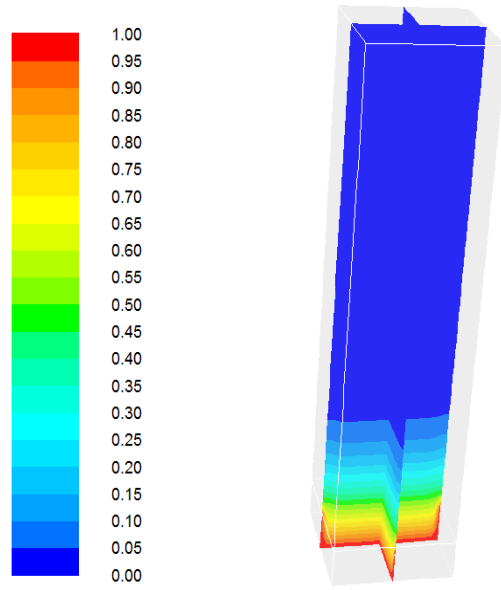
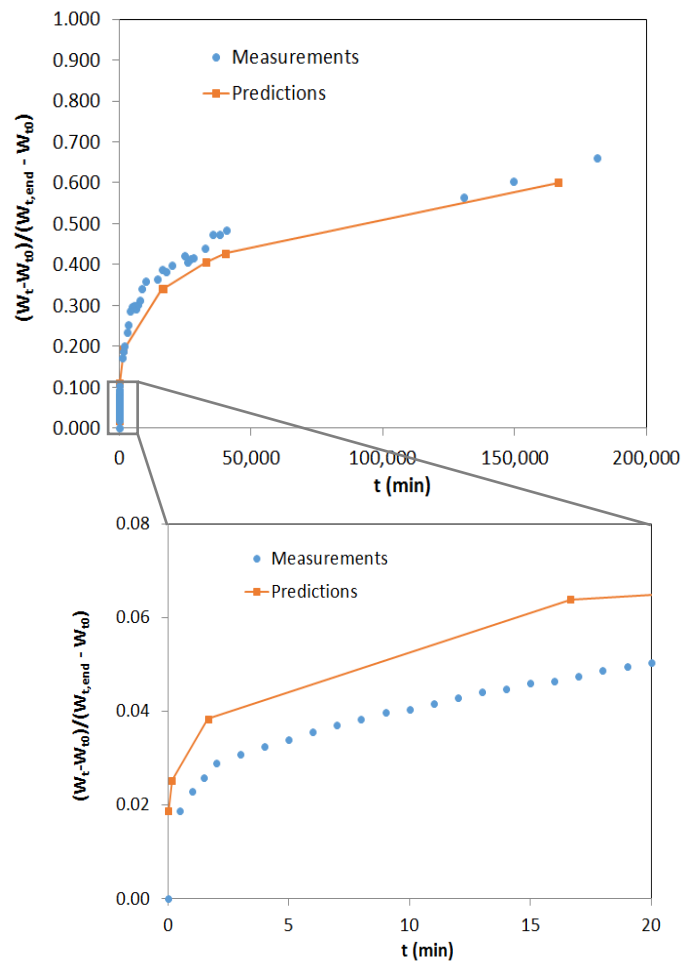
A**B**

Figure 7. Normalized solvent concentration within the wood after 10,000 seconds of solvent mass uptake **(A)**; measurements and numerical predictions of the normalized solvent mass uptake **(B)**.

II.2.4.2 Numerical Modeling of TAZ Diffusion

In order to ascertain if the active fungicide and the solvent were diffusing at the same rate, numerical simulations were carried out by solving the UDS transport equation using the logarithmic variation in the effective diffusion coefficient (longitudinal) shown in Figure 6B. Again, the effective surface diffusion coefficients were assumed to be 1% of the effective longitudinal diffusion coefficient prevailing at that time. Figure 8A shows the UDS boundary conditions employed to simulate the complete immersion process with a normalized TAZ concentration of unity employed across all faces of the wood. Figure 8B and Figure 8C show the normalized TAZ concentration variations across different slices shown in Figure 2. Due to symmetry in the diffusion process along the longitudinal direction during the complete immersion experiments, only one half of the wood samples are shown.

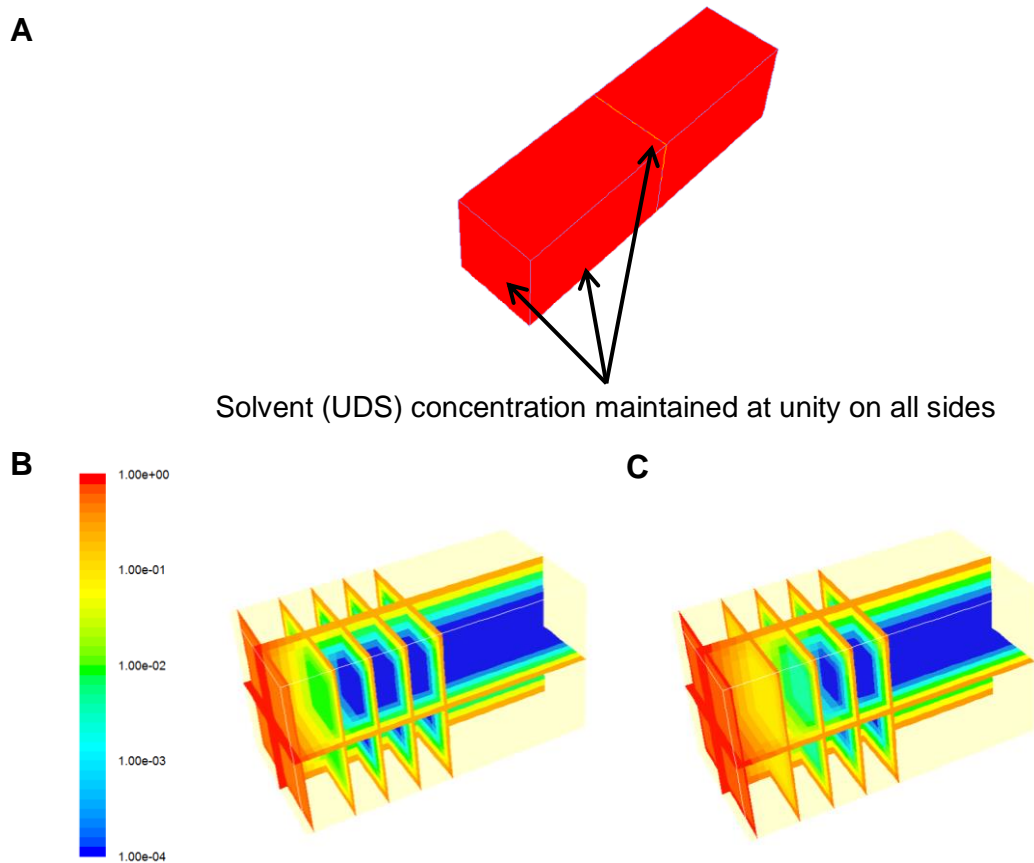
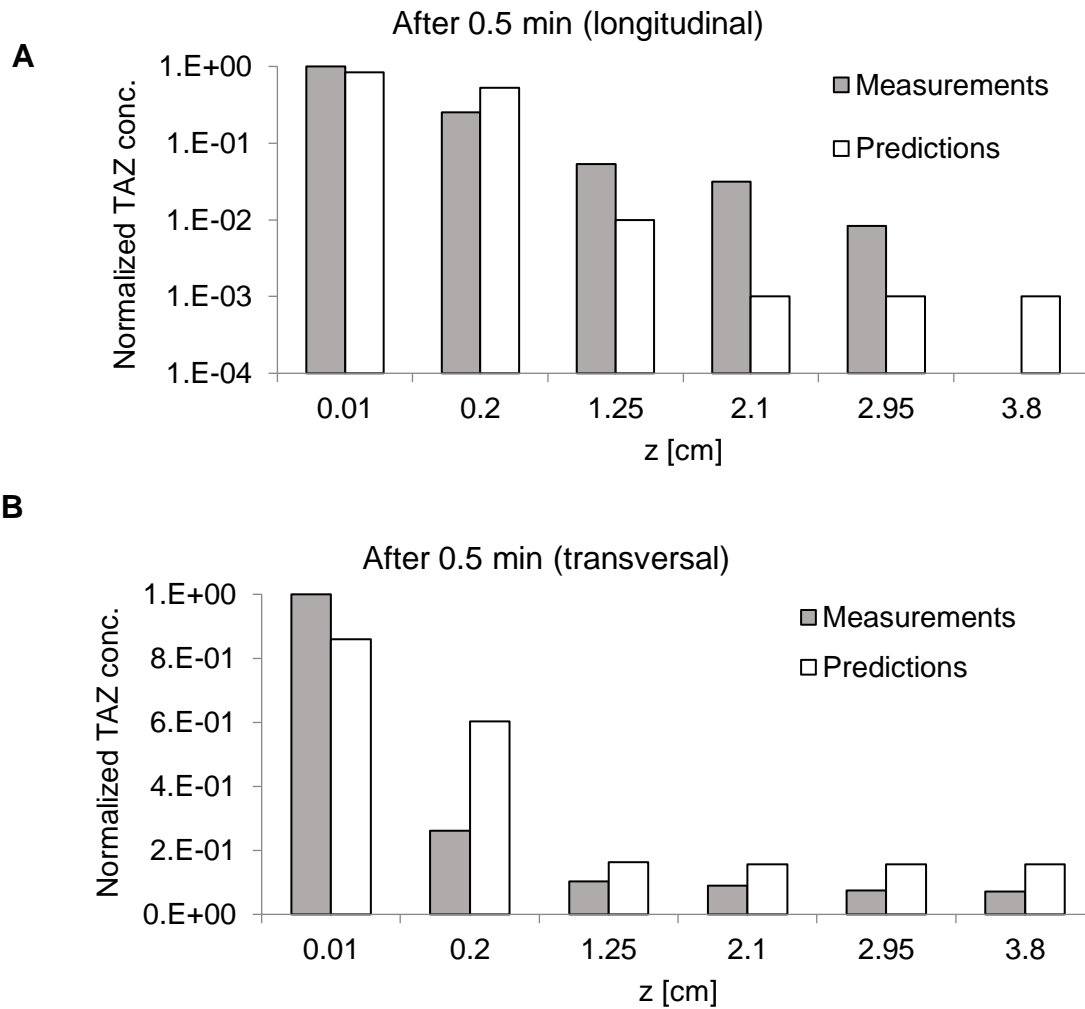


Figure 8. User-defined scalars (UDS) boundary conditions employed to simulate the complete immersion process (**A**); normalized TAZ concentrations across the different sections of the wood after 0.5 min of immersion time (**B**); normalized TAZ concentrations across the different sections of wood after 3.0 min of immersion time (**C**).

Figure 9 compares the numerically estimated distribution profiles of TAZ in the longitudinal and transversal directions across the different sections shown in Figure 2 with their corresponding measured values shown in Figure 4. The reasonable agreement between the numerical predictions and the experimental

measurements using this simplistic log model further confirmed that: (1) the effective diffusion coefficients of TAZ in the longitudinal direction were on the order of $10^{-6} \text{ m}^2 \cdot \text{s}^{-1}$ during Phase 1 (0–1 min) and on the order of $10^{-7} \text{ m}^2 \cdot \text{s}^{-1}$ during Phase 2 (1–10 min); (2) the transversal diffusion coefficients were roughly 1% of the effective longitudinal diffusion coefficient prevailing at that time. Further, these observations confirmed that the active fungicide (TAZ) diffused with the solvent at the same rate.



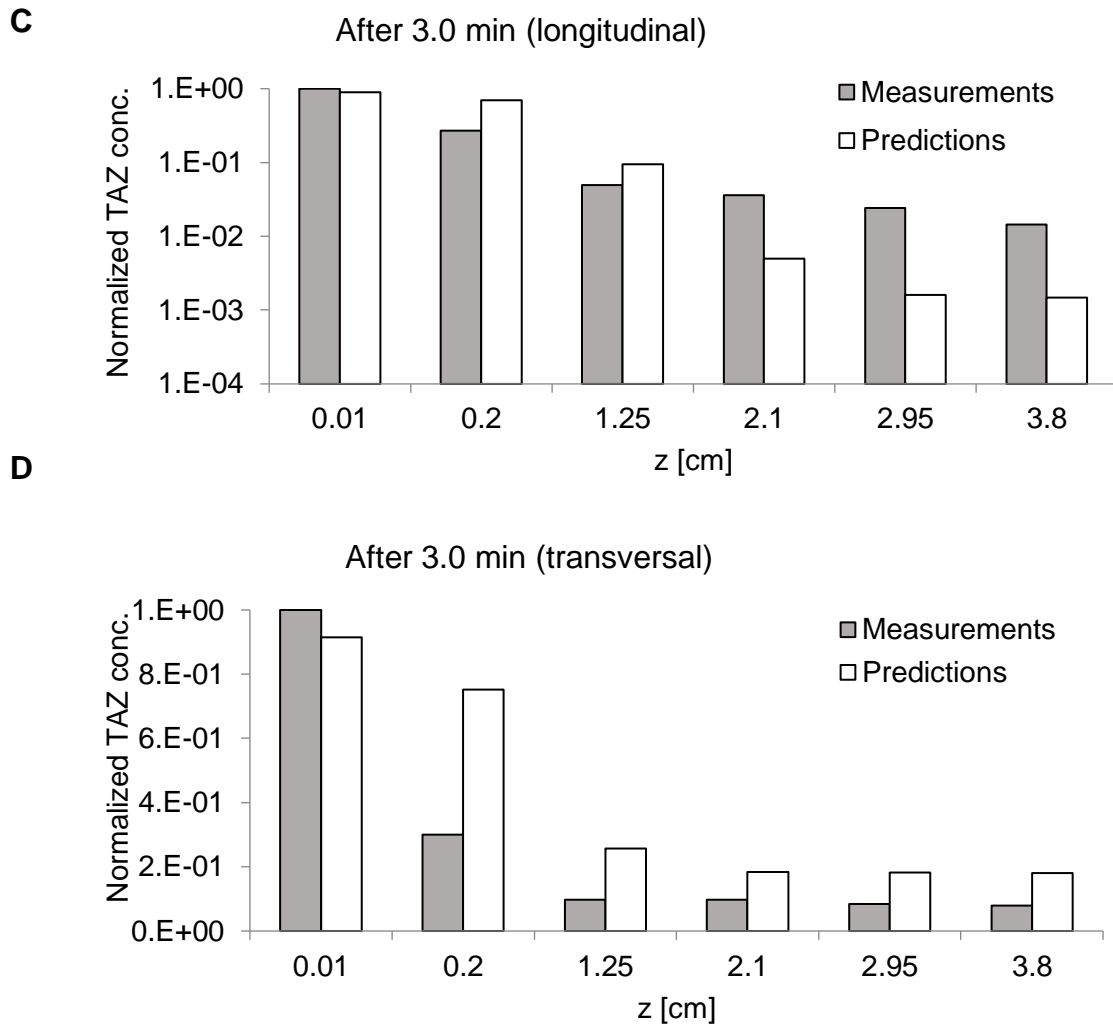


Figure 9. Numerically estimated (using CFD code ANSYS FLUENT) distribution profiles of TAZ in the longitudinal (**A, C**) and transversal directions (**B, D**) across the different sections compared against their corresponding measured values.

II.3 CONCLUSIONS

Woodlife, a hydrocarbon-based solvent for wood treatment, featured three different absorption phases when introduced to ponderosa pine wood under

ambient temperature and pressure. To estimate the effective diffusion coefficients for TAZ, the active component of Woodlife, during the different absorption phases, a numerical model has been proposed featuring a logarithmic variation in the effective diffusion coefficient as a function of time. This model predicted the longitudinal and surface penetration data as well as the mass uptake data reasonably well. Using both numerical modeling and experimental studies, the effective diffusion coefficients for solvent and TAZ were found to be similar, confirming their comparable penetration rates. Furthermore, the mass balance on solvent and TAZ was closed successfully.

The bulk of TAZ was found within 2–4 mm below the end-grain wood surface while only a small fraction penetrated deep (3–4 cm) into the wood in the longitudinal direction. With increasing treatment time, the amount of diffused TAZ increased (mostly near the end-grain wood surface), but the distribution remained similar. The wood block grain sides were treated to a lesser extent but still contained significant TAZ amounts in the 2-mm subsurface layer.

No noticeable TAZ movement was observed in treated wood samples upon laboratory aging for up to six months barring a ca. 25% evaporative surface loss. The TAZ located beyond the thin surface layer thus appears to be useless for wood treatment. Overall, 0.5 min treatment time with no external pressure appears to be sufficient.

III. CHAPTER: FATE OF TRIAZOLES IN SOFTWOOD UPON ENVIRONMENTAL EXPOSURE

III.1. MATERIALS AND METHODS

III.1.1 Chemicals and Reagents

Analytical standards, TAZ, PAZ, IPBC and an internal standard (IS), HAZ, were of > 99% purity and purchased from Sigma-Aldrich (St. Louis, MO, USA), as was sodium azide. Acetone and acetonitrile (LC or GC grade) were purchased from Fisher Scientific (Pittsburgh, PA, USA). Water was purified using a DirectQ Millipore system (Billerica, MA, USA).

Woodlife 111 RTU from Kop-Coat, Inc. (Pittsburgh, PA, USA) was used as a common nonpolar solvent with 0.22% of dissolved fungicides (TAZ, PAZ, and IPBC). For the analysis of fungicide distribution, ¹⁴C-TAZ obtained from Commerce Institute of Isotopes Co., Ltd. (Budapest, Hungary) with a radioactivity of 7.4 MBq·mL⁻¹ was spiked as a tracer to Woodlife resulting in a radioactivity of 0.74 MBq·L⁻¹ of the treatment solution. A scintillation cocktail, Betamax, was obtained from MP Biomedicals, LLC (Solon, OH, USA).

III.1.2 Outdoor Exposure Study

The exposure study was performed on ponderosa pine frame corner sections (41.2 cm × 3.6 cm × 3.6 cm). Each section consisted of two wood blocks, which were ultimately assembled together to comprise a corner piece (Figure 10). For the treatment, conditioned unassembled blocks were fully submerged into the radiolabeled Woodlife solution for 3.0 min. Radiolabeled tracer was used to determine the total TAZ amount in wood including the original TAZ molecule but also its potential degradation products without the need of knowing their structure. Wood blocks were then dried for one week before they were assembled together and shipped to a Marvin Windows and Doors facility (Warroad, MN, USA) where they were painted white using aqueous based paint to mimic the routine industrial handling. After the paint application, selected wood sections were shipped to Hilo, Hawaii in January 2014 and underwent a six-month outdoor study whose detailed experimental layout is described in Table 5. During the exposure, all wood blocks remained assembled.

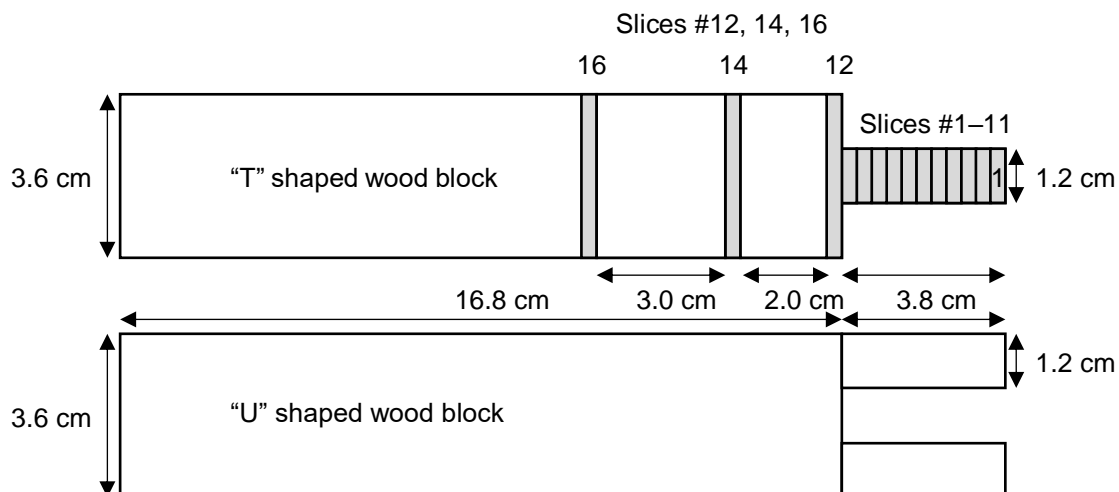


Figure 10. Wood corner section (41.2 cm x 3.6 cm x 3.6 cm, when assembled together) cutting scheme. Each "T" shaped wood block was cut into 2-mm wide wood slices (#1–11, 12, 14, 16) that were subjected to analysis by either liquid scintillation counting or GC-MS.

Table 5. Experimental layout for outdoor study.

No of Wood Sections	Dipping Solution	Exposure Type	No of Slices per Section ¹	Analysis
4	Radiolabeled Woodlife	Direct sun	9	Scintillation
4	Radiolabeled Woodlife	No sun	9	Scintillation
4	Radiolabeled Woodlife (biodegradation control)	Direct sun + NaN ₃	9	Scintillation
4	Radiolabeled Woodlife (control)	Lab freezer	9	Scintillation
4	Woodlife	Direct sun	3	GC-MS
4	Woodlife (control)	Lab freezer	3	GC-MS

¹Number of slices analyzed as illustrated in Figure 10.

Exposures included wood section storage under direct sun, in shade (no sun), and under direct sun with an additional treatment applied before the exposure and each month afterwards. This treatment consisted of a sodium azide (NaN_3) aqueous solution ($10 \text{ g}\cdot\text{L}^{-1}$) applied on the wood surface using a synthetic paint brush to prevent microbial TAZ biodegradation. Exposure to direct sunlight causes wood to dry out fast and shrink. Repeating cycles of wetting and drying (i.e., swelling and shrinking) may cause cracking and checking of the wood surface, which would ultimately decrease wood resistance towards microbial attack. Therefore, the sodium azide treatment was used in combination with direct sun exposure.

After six months, “T” shaped wood blocks were cut with a band saw (Figure B. 1) followed by extraction and analysis of selected 2-mm wide wood slices (#1, 2, 4, 6, 8, 10, 12, 14, and 16) using either liquid scintillation counting (wood blocks treated with radiolabeled Woodlife solution) or gas chromatography - mass spectrometry (GC-MS) for wood blocks treated with non-labeled Woodlife. For the GC-MS analyses, three slices were analyzed (#1, 12, and 14) per each wood block. “U” shaped wood blocks were only used for the assembly of a corner piece of window frames. They were not analyzed as the results from “T” shaped wood blocks were considered to be representative of both assembly parts.

The TAZ amounts in wider wood slices #13 and #15 were approximated by breaking them into 2-mm units for the purpose of calculation and fitting an exponential function between them. The two boundary slices were analyzed and thus the TAZ amounts were known. An exponential relationship was observed for slices #1–11 shown in Figure 13 (only the first two surface slices had higher

amounts of TAZ which then plateaued at a lower value for the distal slices) and was thus used for the calculation of TAZ in wood slices #13 and #15. The total TAZ amount in the entire “T” shaped wood block was then calculated as a sum of TAZ recovered from analyzed slices and the estimated TAZ from slices that were not analyzed (#13 and #15). Comparing the total TAZ amounts in exposed and control wood allowed for TAZ recovery calculations.

III.1.3 Controlled-Environment Study

Smaller-sized wood blocks (30.5 cm × 3.8 cm × 3.8 cm) were used for the experiments conducted in laboratory settings. Even though the wood size was decreased for practical reasons, the treatment remained identical - wood blocks were treated using the procedure described in Section III.1.2 but with a non-labeled Woodlife solution (containing the same amount of fungicides as radioactive Woodlife). In addition to TAZ and PAZ, Woodlife solution contained IPBC. IPBC was previously reported to undergo both thermal and photo-degradation¹¹⁴⁻¹¹⁵ and was used in this study as a negative control confirming that the experimental conditions were severe enough to cause its degradation.

Experimental layout was planned using a fractional factorial design, e.g., Taguchi design (Table 6), using a 3⁴ array (4 factors and 3 levels), which allowed for the robust evaluation of the individual effect of temperature, light, relative humidity (RH), and time on fungicide removal. Each factor was studied on three levels - low, medium, and high. For each wood sample, the non-exposed control was available

allowing the analysis of results as paired data (i.e., changes in the control and desorption experiments).

Table 6. The experimental layout proposed by the Taguchi design evaluating the impact of temperature, RH, UV light and time, on the fate of fungicides in wood. Saturated salt solutions were used to ensure the required humidity levels.

Chamber	Salt	RH [%]	Temperature [°C]	Light source	Time [weeks]
1	none	20	25	dark	10
2	potassium bromide	80	55	dark	16
3	potassium iodide	50	80	dark	26
4	sodium bromide	50	25	daylight	16
5	none	20	55	daylight	26
6	potassium bromide	80	80	daylight	10
7	ammonium chloride	80	25	black light	26
8	urea	50	55	black light	16
9	none	20	80	black light	10

Desorption experiments were performed in small-scale glass chambers (23 cm ID x 35 cm H) shown in Figure 11. To ensure the sufficient exposure to UV light, a 0.13 mm fluoroethylene propylene (FEP) Teflon film was applied to cover the top of the chamber and held in place by rubber bands. Black light was generated by using a Philips Actinic BL PL-S 9W/10/2P 1CT ultraviolet lamp. Wood blocks were placed on permeable ceramic desiccator plates, 18 cm in diameter (obtained from VWR, Radnor, PA, USA), allowing for air circulation. To achieve the allotted

humidity, saturated salt solutions were added to the bottom of the chamber. For experiments performed at higher temperatures, chambers were placed on top of a hot plate. The RH and temperature were initially monitored continuously using the RH/temperature probes (for two months). However, high humidity and salt concentration resulted in fast corrosion (malfunction) of probes, and thus the RH and temperature were monitored in these samples only at selected times to ensure the constant conditions in each chamber.

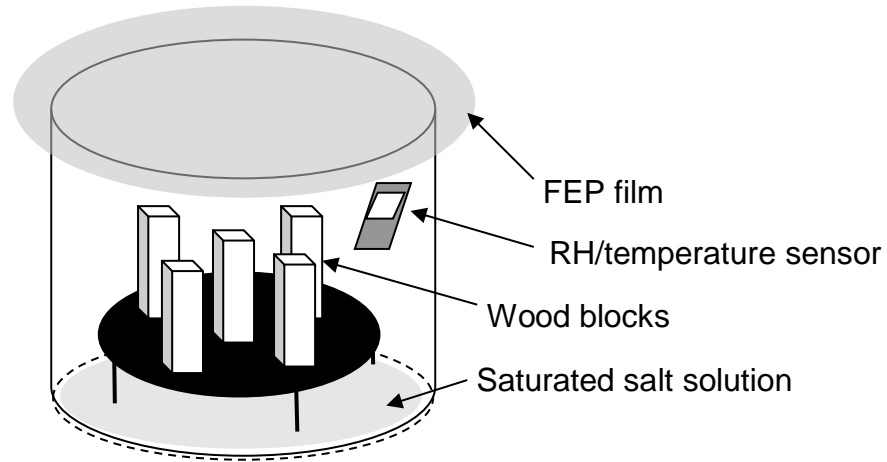


Figure 11. The glass chamber (23 cm ID x 35 cm H) design used for the desorption experiments.

Each wood block was air dried after the treatment and cut in half, then one half was introduced upright into the chamber (with the freshly cut surface facing downward) while the other half was stored in a freezer (used as a control). After exposure for the allotted time, wood blocks were air dried again and the upper

portion of the wood was cut with a band saw so the surface 2-mm slice could be analyzed. Prior to the GC-MS analysis, wood was extracted with acetone using Soxhlet.

III.1.4 Wood Leaching Experiments

To investigate triazole leaching rates, wood corner sections identical to those in the outdoor study were used since the kinetics may be affected by the wood geometry and assembly. The sections were conditioned, treated with a non-labeled Woodlife solution using the same technique as described above, dried and painted white.

Ten assembled wood sections were placed on a raised platform in Rubbermaid roughneck totes (18-gallon volume) under a flowing, recirculating water irrigation system (Figure B.2. 5). The sections were laid horizontally on the platform and water was sprayed in a 90° angle (exposing the radial and tangential wood surface). Wood sections in one tote were exposed to 11.3 L of water per week for a total of four weeks. Since the leaching experiments were conducted within a shorter time period than the outdoor study, an excessive amount of water was used to approximate the leaching potential of triazoles.

A 1.0 L sample from each tote was collected weekly to be analyzed by LC-MS. The control experiment involved the same setup using wood sections that were not treated (1 tote with 10 wood sections). Along with the leachate water samples, 1.0 L of water was analyzed as a blank experiment.

III.1.5 Wood Cutting & Extraction

Wood blocks were cut into slices using a Craftsman 22.9 cm band saw purchased from Sears Brands Management Corporation (Hoffman Estates, IL, USA) in a ventilated laminar hood. The blade used was a Powertec saw blade (157.5 cm x 1.0 cm, 10 teeth per 2.5 cm).

The extraction method employed was designed to exhaustively extract TAZ from wood as well as to assess the extent of TAZ sorption. Wood slices were further cut into smaller pieces using a razor blade and extracted by an exhaustive three-step extraction protocol. The first and second extraction steps were sonication in acetone (3.5 mL, volume adjusted to cover the wood surface) to extract loosely bound TAZ that is either weakly interacting with the wood matrix or sorbed near the wood surface. Extracts from each sonication were collected and analyzed separately. The third step was an overnight Soxhlet extraction with 120 mL of acetone to recover strongly bound TAZ, which remained sorbed within the wood after the two sonication steps. To validate that all extractable TAZ was released with the three-step protocol, an additional Soxhlet extraction in acetone was performed yielding no TAZ.

III.1.6 Analysis & Instrumentation

For the liquid scintillation counting analysis, 1.0 mL of a wood extract in acetone was vortexed with 4.0 mL of the scintillation cocktail and analyzed after an overnight equilibration in a scintillation counter, Beckman Coulter LS 6500, purchased from Beckman Coulter, Inc. (Fullerton, CA, USA). The analysis was run

for 3.0 min in a DPM calculation mode (disintegrations per minute, which is directly proportional to the tracer concentration).

GC-MS protocol was adapted from Stavova et al.⁸⁸ Analyses were performed using a 6890 Series II Plus GC coupled to a 5975C MS detector (Agilent, Santa Clara, CA). Separations were carried out using a 22 m-long DB-5MS column with 0.25 mm internal diameter and 0.25 μm film thickness (J&W Scientific, Rancho Cordova, CA, USA). Further details are provided in Appendix B.1 including fungicide calibration plots, limits of detection (LODs), limits of quantification (LOQs), and example chromatograms.

LC-MS analyses were conducted on an Agilent 1100 LC coupled to a high resolution TOFMS G1689A Series 6200. All LC separations were performed using an Agilent Eclipse Plus C18 150 mm \times 2.1 mm reverse phase LC column with 3.5 μm particle size. A binary solvent system consisting of A: 5% acetonitrile in water with 2.5 mM ammonium acetate and B: acetonitrile with 2.5 mM ammonium acetate was used. A gradient program starting with 40% B and ending with 90% B was run at a flow rate of 0.2 mL \cdot min⁻¹. The total analysis time was 35 min. The column oven temperature was set to 30 °C and injection volume was 20 μL . ESI was performed in a positive mode with drying gas (N_2) set to 350 °C at a flow rate of 12 L \cdot min⁻¹ and the nebulizer gas (N_2) pressure set to 25 psig. The capillary and fragmentor voltages were 4350 V and 125 V, respectively. Further details are provided in Appendix B.2 including fungicide calibration plots, limits of detection (LODs), limits of quantification (LOQs), and example chromatograms.

III.1.7 Statistical Data Processing

All experiments were performed in quadruplicate and the results were reported as mean values. Comparison of data sets was done using a two-sample t-test at 95% confidence level.

The controlled-environment study was designed using a DOE fractional factorial design, the Taguchi design, which is commonly used in industry for its robustness.¹¹⁶ The use of a fractional factorial design was a necessity due to a large number of variables prohibiting the use of a one-variable-at-a-time approach. The Taguchi design uses orthogonal arrays, which estimate the effects of factors on the response mean and variation.¹¹⁷¹¹⁷ The design is thus balanced so that factor levels are weighted equally. As a result, each factor can be assessed independently of all the other factors, so the effect of one factor does not affect the estimation of a different factor. Taguchi design evaluates the individual impact of main factors as opposed to their interactions, which are generally less significant. Minitab statistical software was used to design the experimental setup and analyze the results. Four factors (%RH, temperature, light and time) were studied on 3 levels (low, medium, and high). Results were reported as p -values where factors with $p \leq 0.05$ were considered to be statistically significant.

III.2 RESULTS AND DISCUSSION

III.2.1 Loosely and Strongly Bound TAZ

TAZ loss from wood due to environmental exposure was apparent from the first and second sonication steps (Figure 12). This loss was attributed to the loosely bound TAZ, which may be either weakly interacting with the wood matrix or sorbed near the wood surface (more accessible by the solvent), and consequently readily removed during exposure. The TAZ amount recovered through the third step, Soxhlet extraction, was similar for the exposed and control wood and is referred to as strongly bound TAZ. Loosely bound TAZ accounted for $85 \pm 5\%$ of the total TAZ while strongly bound TAZ represented the remaining $15 \pm 5\%$, and this distribution remained constant for both surface and distal slices. Therefore, evaluation of the TAZ loss during the outdoor study was based only on the loosely bound TAZ fraction that was prone to be removed from the wood.

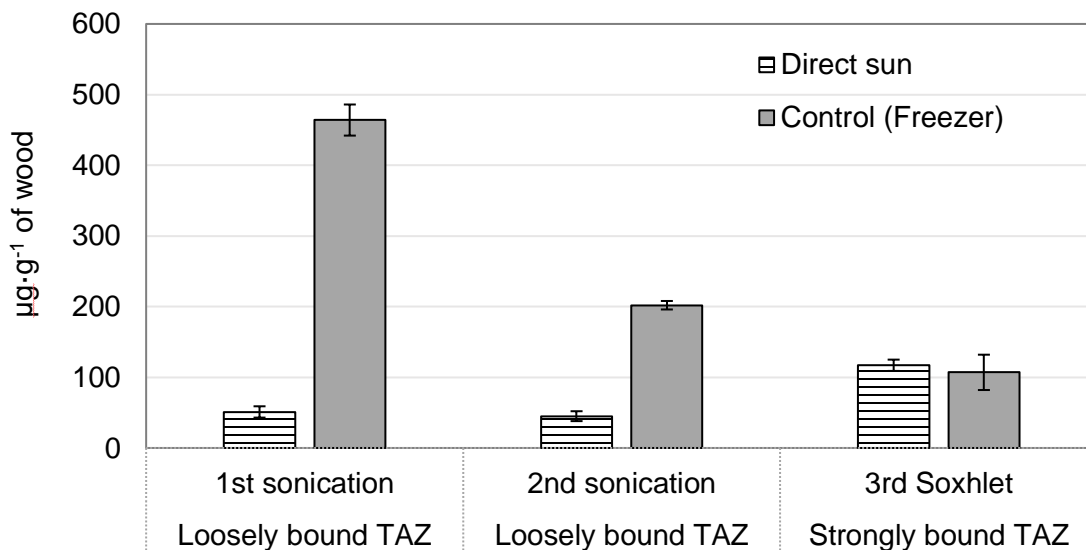


Figure 12. The TAZ amount recovered from slice #12 for sun-exposed and control wood employing a three-step extraction protocol. Individual extracts were analyzed and quantified using GC-MS.

III.2.2 TAZ Loss upon Environmental Exposure

The outdoor exposure of treated wood led to a TAZ loss from the surface slices (e.g., wood frame corner) accompanied by minor losses from the nearest subsurface slices. The spatial distribution of loosely bound TAZ in a “T” shaped wood block for various environmental exposures was based on ¹⁴C-TAZ determination and is shown in Figure 13. A depletion of loosely bound TAZ was observed from surface wood slices #12 and 1, and subsurface slice #2. The losses in slices #1 and #2 were not as significant as for slice #12, the full-size surface slice. Based on the loss observed from slice #2, further minor losses may be expected in the wood slice adjacent to slice #12.

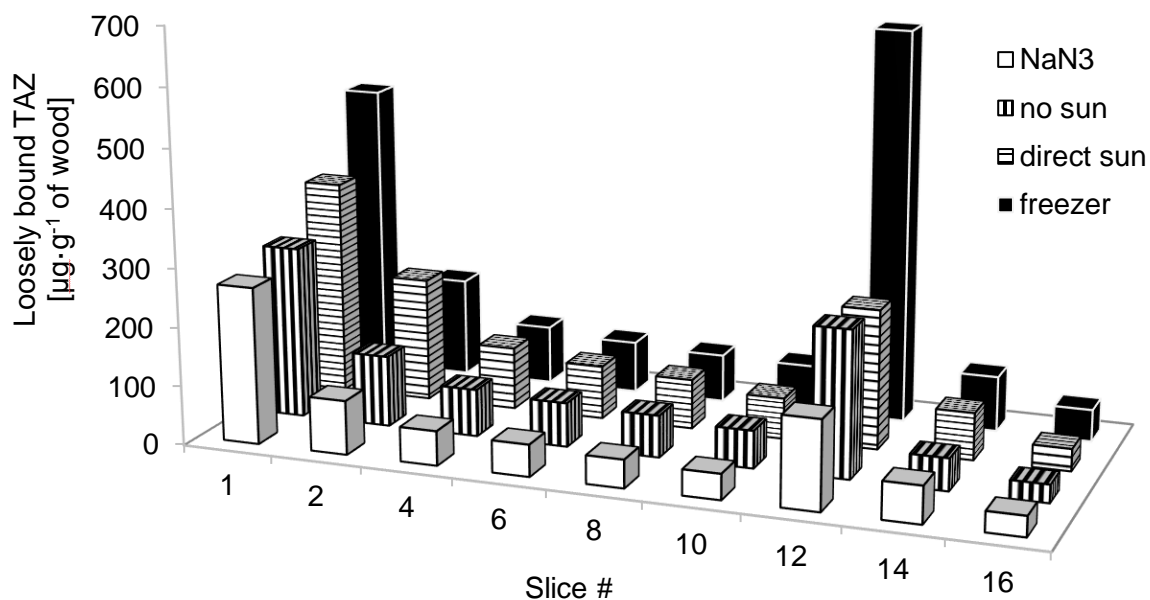


Figure 13. The spatial distribution of loosely bound TAZ (recovered through two consecutive sonications) in a “T” shaped wood block after various environmental exposures.

The depletion of loosely bound TAZ did not appear to affect wood preservation. Since the wood surface (slices #1, and 12) contained the highest amount of sorbed TAZ, a significant amount remained in this region despite the exposure to harsh conditions. The quality of wood seemed to remain intact as long as the active fungicide was present in all wood slices in sufficient amounts. So even though surface slices #1 and #12 lost up to 75% of the originally present loosely bound TAZ, the remaining $\mu\text{g}\cdot\text{g}^{-1}$ concentration was still more than twice the concentration

present in inner slices. Additionally, each slice contained the strongly bound TAZ ($15 \pm 5\%$ of total TAZ), which is not accounted for in Figure 13. Strongly bound TAZ was not affected by outdoor conditions and thus remained sorbed in wood increasing the amount of total TAZ in each slice.

The recoveries of loosely bound TAZ from the entire wood block were ~80% of the initially sorbed amount and seemed to be unaffected by the exposure type (Figure 14). TAZ recoveries from wood exposed to direct sunlight were comparable to recoveries from wood stored in the shade (no sun exposure). Also, the sodium azide treatment did not appear to impact the TAZ loss. Since sodium azide was applied to prevent biodegradation and protect the wood from deterioration, its negligible effect on TAZ retention may be interpreted as indirect evidence of biodegradation being insignificant compared to the evaporation and leaching. This preliminary conclusion was further confirmed in the next section by comparing TAZ amounts quantified by GC-MS to the scintillation data to verify that all carbon-14 was present in the non-degraded TAZ molecule.

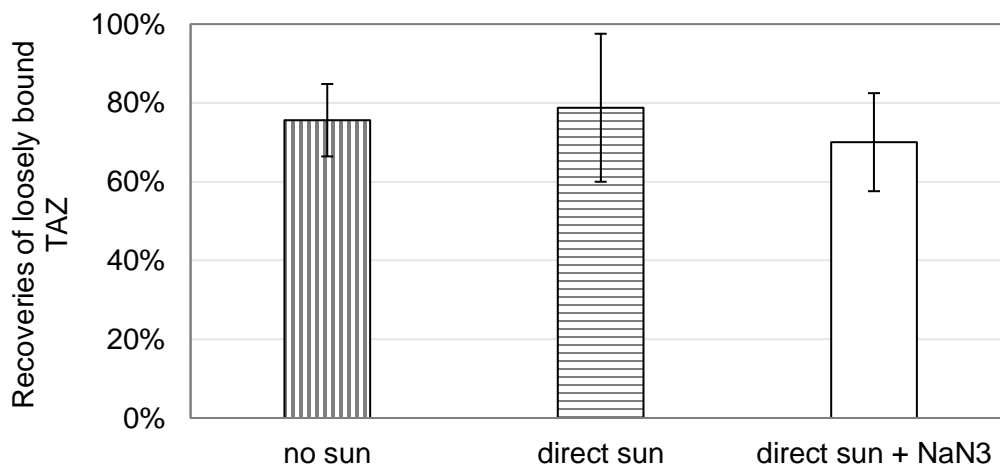


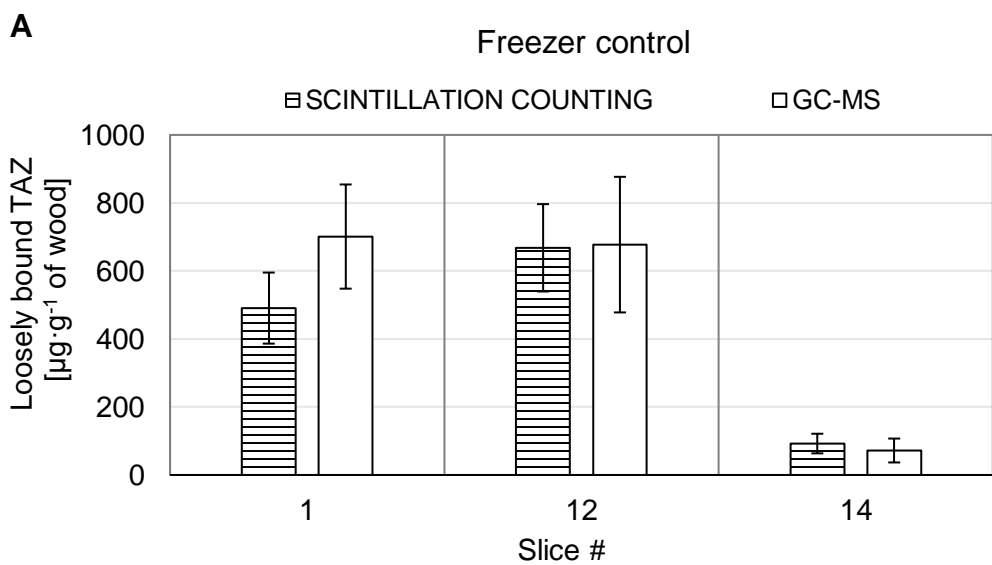
Figure 14. Recoveries of loosely bound TAZ from a "T" shaped wood block after varying environmental exposures for six months.

III.2.3 Evaluation of Triazole Degradation

The outdoor study conducted in the previous section monitored carbon-14 originally present in a TAZ molecule. However, upon the environmental exposure, TAZ may undergo degradation or transformation yielding still radiolabeled but inactive products.⁶⁴ Therefore, TAZ potential degradation products were investigated by GC-MS using exposed wood treated with non-labeled Woodlife.

The close match of GC-MS results with scintillation counting indicated that the majority of carbon-14 remained present in the non-degraded TAZ structure (Figure 15). Comparison of the loosely bound TAZ amounts recovered in selected wood slices as quantified by either liquid scintillation counting (detecting carbon-14) or GC-MS (quantifying TAZ) showed no statistical difference between these amounts. Results from a two-sample t-test are provided in Table 7. Considering

the higher standard deviations, degradation could not be completely ruled out, however it would represent only a minor contribution to the depletion of loosely bound TAZ. Also, additional MS screening for potential degradation products containing chlorine molecules (showing a distinct chlorine isotopic pattern in the obtained mass spectra) did not reveal their presence, thus the TAZ thermal, photo- or biological degradation was deemed to be negligible.



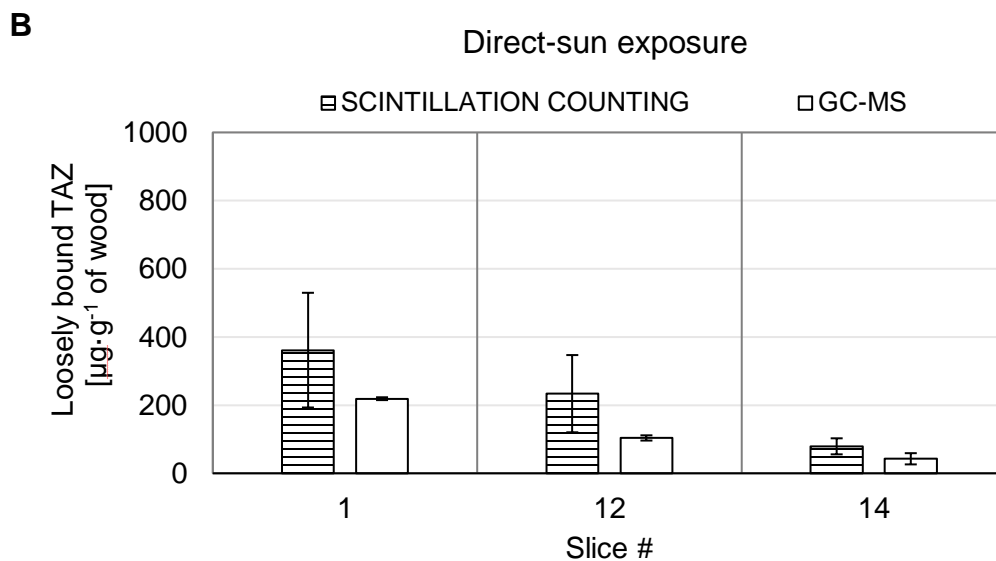


Figure 15. Comparison of the loosely bound TAZ amounts (results from first and second sonication) recovered in selected wood slices after freezing (**A**) or direct-sun (**B**) exposure quantified by either liquid scintillation counting or GC-MS. Their difference was found to be statistically insignificant.

Table 7. Application of two-sample t-test for comparison of TAZ amounts recovered from various wood slices and quantified by GC-MS and scintillation counting. The two data sets were not found to be statistically different ($p > 0.05$).

	N^1	Pooled StDev ²	DF^3	t -value	p -value
Sun exposure					
Wood slice #1	3	118.83	4	1.46	0.217
Wood slice #12	3	80.10	4	1.99	0.118
Wood slice #14	3	19.81	4	2.23	0.090

Table 7 cont.

	<i>N</i> ¹	Pooled StDev ²	<i>DF</i> ³	<i>t</i> -value	<i>p</i> -value
Freezer control					
Wood slice #1	3	130.81	4	1.97	0.121
Wood slice #12	3	167.31	4	0.07	0.951
Wood slice #14	3	32.14	4	0.76	0.488

¹*N* – sample size (3 = replicate); ²Pooled StDev - pooled standard deviation; ³*DF* - total degrees of freedom

PAZ degradation was also considered negligible as PAZ recoveries from control and sun-exposed wood were similar to TAZ recoveries (Figure 16). Due to this similarity of PAZ and TAZ behavior in wood, the same conclusions as for TAZ can be drawn. Also, GC-MS was used to screen for previously published PAZ degradation products and other compounds containing chlorine atoms, though none were found.⁶⁹⁻⁷⁰

Lastly, a discussion on IPBC degradation is outside of the scope of this section, and is discussed in Appendix B.1 (Figure B.1. 4).

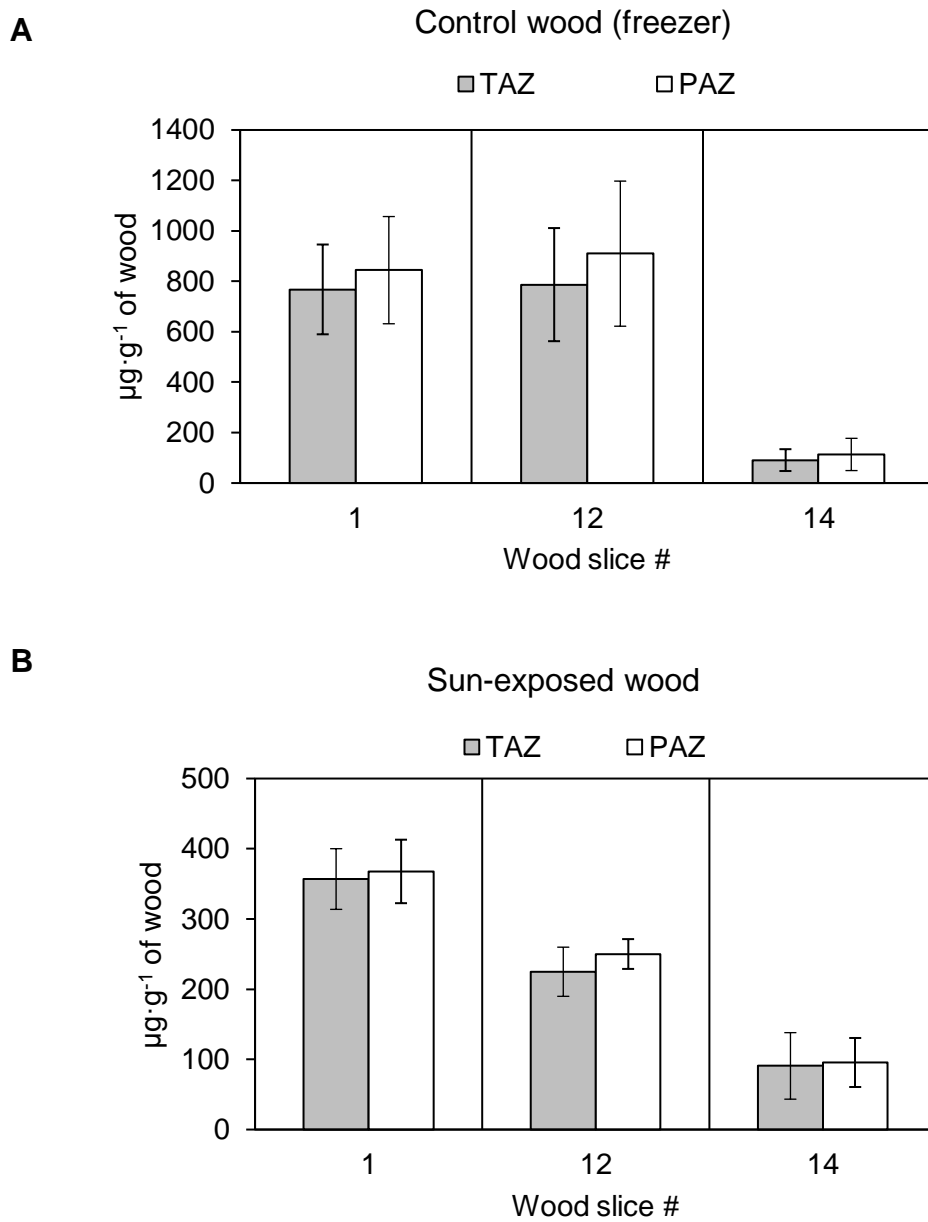


Figure 16. Comparison of TAZ and PAZ amounts found in control (**A**) and sun-exposed (**B**) wood. Amounts recovered from various slices were quantified by GC-MS.

III.2.4 Environmental Factors Contributing to Triazole Loss

A controlled-environment study using the Taguchi design was carried out to further investigate the cause of fungicides' depletion from the wood surface. The aging conditions targeted were temperature, light, RH, and exposure time. The study monitored both triazoles, TAZ and PAZ in the surface layer of wood over the period of 21 weeks. Additionally, the Woodlife solution contained IPBC, which was used as a control chemical to compare our findings to the reported thermal and photo-degradation data.

Judging based on *p*-values, temperature followed by the exposure time appeared to be the most strongly contributing factors for both TAZ and PAZ (Table 8). Assuming no degradation of triazoles (as inferred in the previous section), evaporation can be viewed as an important path of their depletion from wood. The emission rate of triazoles was found to be $\sim 1 \mu\text{g m}^{-2}\cdot\text{h}^{-1}$ for exposure at 25 °C, which is similar to the rate of $0.5 \mu\text{g}\cdot\text{m}^{-2}\cdot\text{h}^{-1}$ reported by Horn et al.⁶⁰ With increasing temperature, the emission rates increased exponentially to $55 \mu\text{g}\cdot\text{m}^{-2}\cdot\text{h}^{-1}$ at 55 °C and $200 \mu\text{g m}^{-2}\cdot\text{h}^{-1}$ at 80 °C, which are the upper bounds of effective temperatures on the wood surface during summers in temperate and hot climates, respectively. However, considering the moderate temperatures in Hilo during the outdoor study (21–26 °C), evaporation could have accounted for a TAZ loss of 5–10 $\mu\text{g}\cdot\text{g}^{-1}$ of wood, which would represent a negligible contribution to the total observed TAZ loss ($\sim 600 \mu\text{g}\cdot\text{g}^{-1}$ of wood). Therefore, evaporation could not be attributed to the TAZ loss from wood exposed to ambient temperatures.

Table 8. Application of Taguchi design for the evaluation of four factors on fungicide removal from wood. The highlighted factors were of a significance ($p \leq 0.05$).

TAZ						
Source	<i>DF</i> ¹	Seq SS ²	Adj SS ³	Adj MS ⁴	<i>F</i> ⁵	<i>p</i> ⁶
% RH	2	27501	33680	16840	1.41	0.257
Temp	2	1696729	1699182	849591	71.21	0.000
Light	2	56662	56633	28316	2.37	0.108
Time	2	76902	76902	38451	3.22	0.052
Error	35	417605	417605	11932		
Total	43	2275398				

PAZ						
Source	<i>DF</i>	Seq SS	Adj SS	Adj MS	<i>F</i>	<i>p</i>
% RH	2	46843	61089	30545	2.10	0.137
Temp	2	1817824	1827573	913786	62.93	0.000
Light	2	79378	80736	40368	2.78	0.076
Time	2	113198	113198	56599	3.90	0.030
Error	35	508198	508198	14520		
Total	43	2565442				

IPBC						
Source	<i>DF</i>	Seq SS	Adj SS	Adj MS	<i>F</i>	<i>p</i>
% RH	2	118	257.6	129	0.58	0.568
Temp	2	22145	22425	11213	50.06	0.000
Light	2	1592	1679	840	3.75	0.033
Time	2	1572	1572	786	3.51	0.041
Error	35	7839	7839	224		
Total	43	33268				

¹ *DF* - total degrees of freedom; ² Seq SS - sequential sums of squares; ³ Adj SS - adjusted sum of squares; ⁴ Adj MS - adjusted mean squares; ⁵ *F*-value; ⁶ *p*-value

For IPBC control, light factor was shown to significantly affect its loss, thus photo-degradation of IPBC during the exposure was likely. Vaporization and thermal

degradation of IPBC could not be ruled out since the temperature and time were also among the significant factors. These findings agreed with previously reported thermal and photo-degradation of IPBC¹¹⁴⁻¹¹⁵ and thus confirmed that the effect of experimental conditions was observable via the Taguchi design.

Contrary to the expectations based on the published data on leaching experiments,⁴³⁻⁴⁴ the air humidity did not affect the fungicide loss. The reason could be the lack of wood saturation with water (water-filled pores), which was previously reported to be essential for fungicide leaching.¹¹⁸

III.2.5 Triazole Leaching

To approximate the contribution of leaching to the triazoles loss from environmentally exposed wood, kinetic data for TAZ and PAZ leaching were obtained (Table B.2. 2). The triazole loss from wood was virtually independent of time, i.e., yielding a constant amount every week, but dependent on the amount of applied water (Figure 17). The TAZ and PAZ leaching rates related to the amount of water were approximated using linear functions, but with increasing amounts of applied water, the leaching curves would eventually level off¹¹⁹ due to the inability of water to access and dissolve the sorbed triazole from either distantly located or poorly accessible sites within the wood matrix. The TAZ leaching rate was slightly higher than that for PAZ, even though the TAZ solubility in water is three times lower at room temperature. The observed higher TAZ leaching rate may be due to the different interactions of each fungicide with the wood matrix.

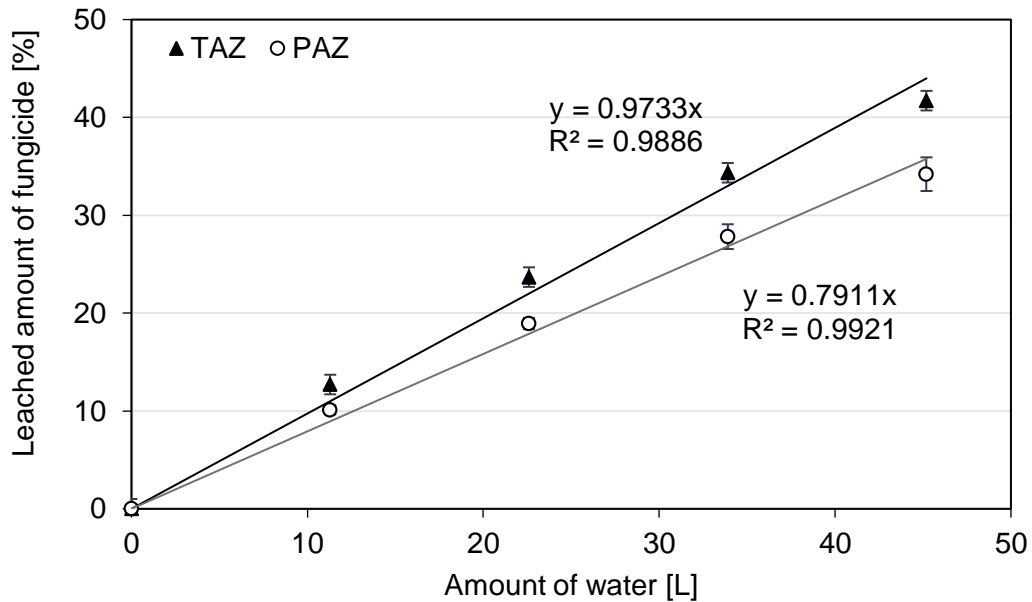


Figure 17. Leaching of TAZ and PAZ from wood corner sections with respect to the amount of water applied.

The use of identical wood sections as in the outdoor study allowed for an approximation of triazole amounts that could have leached during the six-month exposure. Based on the on-site measurements in Hilo, Hawaii, the precipitation in 2014 was 63" per six months (1.6 m). Considering the surface area of each wood section exposed to rain (0.02 m²), the amount of water fallen on each section over six months was estimated as being as high as 32 L. Using the leaching kinetic data shown in Figure 17, approximately 32% of TAZ and 26% of PAZ could have leached into water, if all this estimated amount of rain actually fell on the given wood sections. Since the TAZ loss during the outdoor study was ~20% (Figure 14), leaching would represent a major path of its removal. This finding agrees with

previously reported 21.0–25.5% of leached TAZ from wood upon seven months of outdoor exposure.⁵⁴

The observed six-month losses represent the upper boundary of TAZ depletion due to the high amount of rains in Hawaii during this season. The amount of retained fungicide in wood may be further increased by triazole chemical modification that will decrease its polarity, thus rendering it less water-soluble and more wood-bound.

III.3 CONCLUSIONS

A six-month outdoor study exposing treated wood corner sections (representing window frame corners) to harsh environmental conditions revealed TAZ losses from the 2-mm wide cross-sectional surface followed by minor losses from the nearest subsurface. The total depletion of loosely bound TAZ was not affected by the type of exposure and amounted to ~20% of the originally sorbed TAZ in wood exposed to rain, wind and sunlight. Since the total TAZ amount in wood remained high, the depletion of loosely bound fungicide did not seem to affect the product preservation.

Using a fractional factorial design (Taguchi design), significant factors contributing to TAZ and PAZ losses were found to be temperature and time of exposure. Therefore, evaporation of triazoles appeared to be a significant path of their removal. However, considering the moderate temperature during the outdoor study, evaporation could only account for a minor portion of the observed TAZ loss.

Additionally, bio-, photo- and thermal degradation were negligible since no degradation products were found and light was not among the significant factors affecting triazole loss.

Controlled experiments revealed that up to 32% of TAZ (and 26% of PAZ) could have leached from the exposed wood during the six-month exposure suggesting water leaching to be the major route of triazole losses from wood. Leaching rate was found to be slightly higher for TAZ than for PAZ.

IV. CHAPTER: THE EXTENT OF TEBUCONAZOLE LEACHING FROM UNPAINTED AND PAINTED SOFTWOOD

IV.1 MATERIALS AND METHODS

IV.1.1 Chemicals

Uniformly ^{14}C -labeled TAZ obtained from the Commerce Institute of Isotopes Co., Ltd. (Budapest, Hungary) with a radioactivity of 7.4 MBq mL^{-1} was spiked as a tracer to a commercial wood preservative formulation, Woodlife 111 RTU from Kop-Coat, Inc. (Pittsburgh, PA, USA), resulting in a radioactivity of 0.74 MBq L^{-1} and ^{14}C -TAZ concentration of 0.12 mg L^{-1} . In addition to the radiolabeled tracer, Woodlife contained 0.21% of dissolved fungicides (TAZ, propiconazole, and 3-iodo-2-propynylbutylcarbamate), therefore, the ratio of ^{14}C -TAZ to TAZ was 14,000:1. A scintillation cocktail, Betamax, was obtained from MP Biomedicals, LLC (Solon, OH, USA) and acetone (GC grade) was purchased from Fisher Scientific (Pittsburgh, PA, USA). The applied exterior wood primer was from Akzo Nobel Coatings Inc. (High Point, NC, USA), and white paint was made by The Valspar Corporation (Minneapolis, MN, USA). Both the primer and paint were water-based.

IV.1.2 Wood Treatment

Size-reduced samples ($5.0 \times 2.5 \times 1.5 \text{ cm}^3$) of conditioned ponderosa pine sapwood (randomized grain selection) were dip treated with vigorously-mixed and sonicated radiolabeled Woodlife formulation for 1.0 min. The uptake of ^{14}C -TAZ based on the control samples was $56 \pm 2 \text{ ng}$. Wood was then placed on wooden skewers and dried in a hood for 24 hours (Figure C. 1). Half of the samples were directly placed into the chambers while the other half were coated on all sides using a foam brush with one layer of the primer and two layers of paint, where each coating was followed by drying for 24 hours before the next layer was applied (Figure C. 2).

IV.1.3 Wood Exposure

Experiments were performed in triplicate using painted and unpainted wood. The exposure conditions included low humidity, high humidity, continuous leaching (i.e., continuous rain), and weekly alternating leaching and drying (i.e., intermittent rain). Control samples consisted of treated wood blocks wrapped in aluminum foil that were placed in an enclosed bag into a freezer (e.g., to prevent any TAZ evaporation and leaching). Further experimental details are provided in Table 9 and illustrated in Appendix C (Figure C. 3 and Figure C. 4). The exposures were maintained for sufficient time to observe the leveling off the TAZ leaching curve, which was found to be 8–10 weeks.

Table 9. Experimental layout including the exposure types with corresponding chamber conditions. For all experiments, conditioned ponderosa pine wood was dip-treated with Woodlife containing ^{14}C -TAZ.

Wood Type	Exposure Type	Temperature [°C]	RH [%]	Exposure Time [weeks]
Unpainted	Freezer control	-18	–	8
Unpainted	Low humidity	rt*	~40	8
Unpainted	High humidity	rt	80	8
Unpainted/ Painted	Continuous leaching (continuous rain)	rt	~40	8
Unpainted/ Painted	Leaching/drying (intermittent rain)	rt	~40	10

*rt = room temperature (e.g., 15–21 °C)

For moderate and high humidity conditions, individual wood samples were placed in separate glass chambers on a glass platform and purged weekly with air, maintaining the temperature and relative humidity similar to the indoor environment (i.e., 15–21 °C and ~40%, respectively). The 80% relative humidity was achieved by placing a sufficient amount of saturated ammonium sulfate solution on the bottom of the chambers, below the glass platform, to prevent any contact with wood. For leaching experiments, wood was placed on a platform under a 50° angle with part A being at the top. Deionized water was dripped onto the transversal surface of part A from a volumetric pipette (the flow was manually adjusted to ~0.1 mL min⁻¹) and descended towards part D and then into the run-off collection flask,

as illustrated in Figure 18. As a result of this design, several water droplets were continuously accumulating near the end-grain side of part D. For the intermittent rain, wood blocks were periodically transferred into an enclosed chamber after a week of leaching and left to dry for another week.

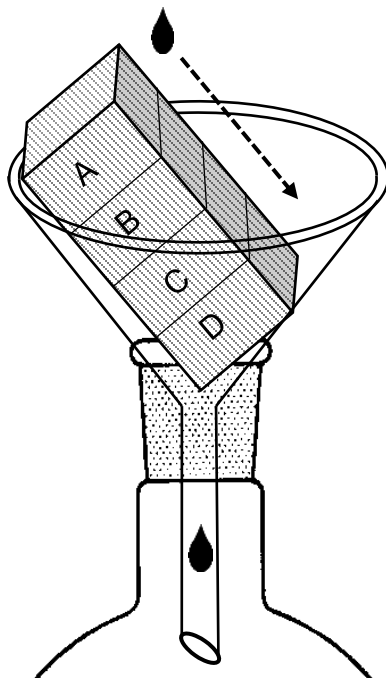


Figure 18. Experimental design of TAZ-treated wood exposure to simulated rain.

IV.1.4 Extraction & Analysis

After the exposure, wood samples were sheared with a hammer and knife into four equal parts ($\sim 1.25 \times 2.5 \times 1.5 \text{ cm}^3$), where parts A and D were those originally located next to the end-grain side whereas parts B and C were the two middle sections (Figure 18). Each wood part was further sheared into smaller pieces to allow for an exhaustive TAZ extraction, which was carried out for 16 hours using a

Soxhlet apparatus with 130.0 mL of acetone. The extract was evaporated to dryness using a vacuum rotary evaporator and reconstituted in 1.5 mL of acetone. For the liquid scintillation counting analysis, 1.5 mL of an acetone dissolved sample was vortexed with 3.5 mL of the scintillation cocktail and analyzed after an overnight equilibration in a scintillation counter, Beckman Coulter LS 6500, purchased from Beckman Coulter, Inc. (Fullerton, CA, USA). The analysis was run in duplicate for 10.0 min in a DPM calculation mode (disintegrations per minute, which is directly proportional to the tracer concentration). The detection limits equaled to two-times the DPM reading of a background sample (i.e., 70 DPM), which amounted to 0.16 ng of ^{14}C -TAZ.

Water run-off was collected several times per week and the volume was recorded. As with the wood extracts, run-off water was evaporated to dryness using a vacuum rotary evaporator and reconstituted in 1.5 mL of acetone, which was analyzed using a scintillation counting analysis as described above.

IV.1.5 Estimate of Maximum Leachable TAZ

To readily estimate the maximum TAZ amount that can be leached from wood, a simplistic model was employed, which can be adapted for the purpose of industrial and environmental assessments. Specifically, TAZ leaching curves were plotted as the amount of applied water onto wood versus the cumulative leached ^{14}C -TAZ amount. These curves were simplified into Eq. 1 based on the perceived analogy to Langmuir isotherm, where $[TAZ_W]$ referred to the cumulative amount of leached TAZ, $[H_2O]$ was the amount of applied water, $[TAZ_{MAX}]$ was the highest TAZ

amount that could be leached from treated wood, and K represented an affinity constant.

$$[TAZ_W] = [TAZ_{MAX}] \times \frac{[H_2O]}{K+[H_2O]} \quad \text{Eq. 6}$$

In order to calculate $[TAZ_{MAX}]$, sigmoidal curves were transformed into a linear function by plotting $[H_2O]^{-1}$ on the x axis and $[TAZ_W]^{-1}$ on the y axis (Eq. 7), where the intersection of this linear function with the y axis represented $[TAZ_{MAX}]^{-1}$. The slope of the function was defined by $K/[TAZ_{MAX}]$.

$$\frac{1}{[TAZ_W]} = \frac{K}{[TAZ_{MAX}]} \times \frac{1}{[H_2O]} + \frac{1}{[TAZ_{MAX}]} \quad \text{Eq. 7}$$

IV.1.6 Data Analysis

To compare the ^{14}C -TAZ amounts recovered from wood exposed to various conditions and to examine the mass balance closure, a one-way analysis of variance (ANOVA) was used. Specifically, Tukey's method was employed to compare results from multiple wood exposures using a family error rate of 0.05 (i.e., 95% simultaneous confidence level). All data were processed using Minitab 18 software.

IV.2. RESULTS AND DISCUSSION

In order to monitor the leaching extent of triazole fungicides from painted and unpainted softwood, ^{14}C -labeled TAZ was used as a fungicide tracer. The overall impact of the several aqueous environmental exposures shows no losses under either of two extreme humidity settings, 15 and 80% (Figure 19). By contrast, when wood was exposed to the simulated continuous rain conditions, a moderate TAZ depletion was found to occur from the end grain (14–33%) accompanied by smaller losses from the unpainted transverse surfaces (not accounted in Figure 19), thus being attributed to leaching. As expected, lower TAZ leaching was observed in painted wood. The mass balance was not closed for intermittent rain conditions suggesting that the additional TAZ losses may have occurred due to water enhanced vaporization. Nevertheless, the experimental setup allowed for the investigation of mechanistic aspects of TAZ leaching, providing the insights on spatial losses from wood and the leaching kinetics.

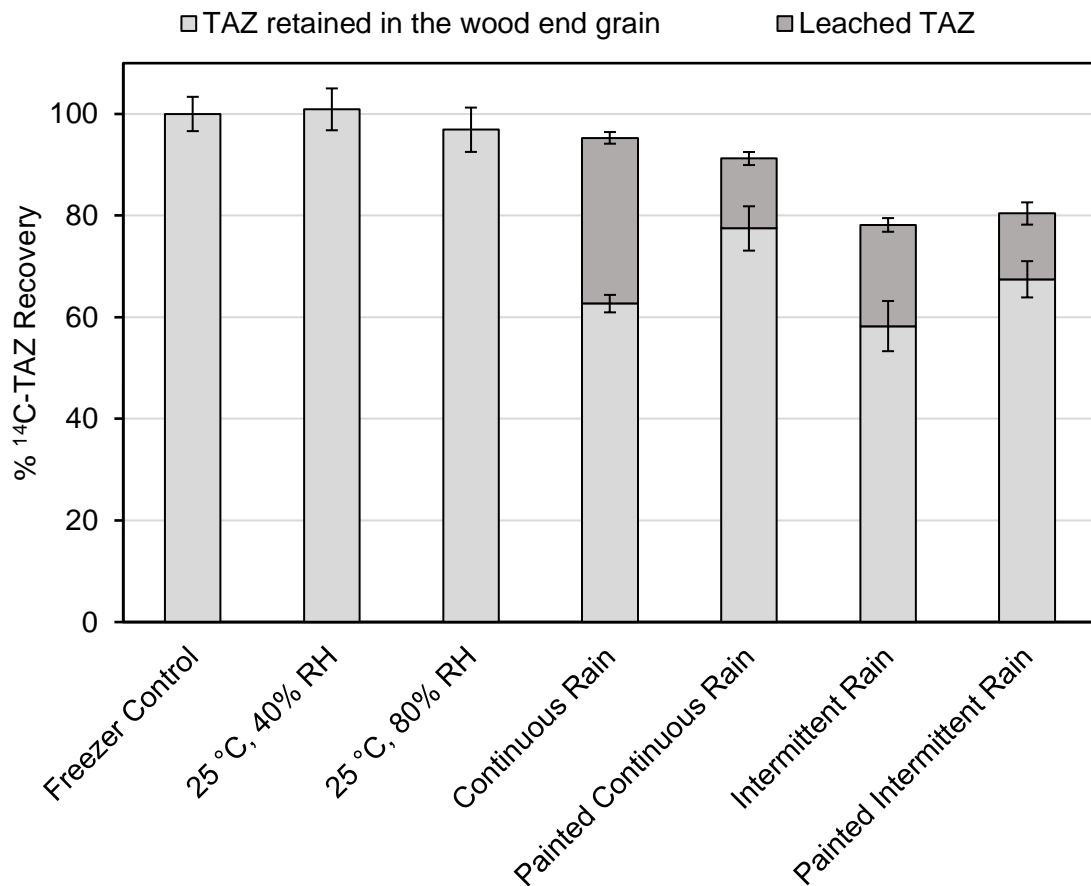


Figure 19. Percent ^{14}C -TAZ recoveries from end grains of painted and unpainted treated wood exposed to various humidity and simulated rain conditions, complemented by ^{14}C -TAZ recoveries from the run-off water. The error bars represent one standard deviation and RH denotes relative humidity.

IV.2.1 ^{14}C -TAZ Distribution and Recoveries from Wood End Grain and Middle Sections

The TAZ amounts recovered from the parts located next to the end grain (i.e., Figure 20, parts A and D) were significantly higher than those found in the middle

sections (i.e., parts B and C) due to a significant contribution of longitudinal TAZ penetration. By contrast, the middle sections contained TAZ sorbed only via the transversal uptake (e.g., a combination of capillary adsorption and diffusion). This observation is consistent with the previously shown TAZ distribution in wood as a result of dip treatment, where the sorption in the transversal direction distributed small amounts of TAZ evenly onto the wood surface, while the diffusion in the longitudinal direction mediated its large deposition near the end grain.¹²⁰

As shown above, the exposure to moderate and high humidity did not impact the sorbed TAZ ($\alpha = 0.05$), while the exposure to simulated rain led to a sizable TAZ depletion from end grain surfaces. The less pronounced TAZ loss from part A (compared to D) was due to the water application, where only the transversal surface was exposed to the simulated rain (the end-grain side remained untouched), which was not sufficient to cause TAZ leaching. Conversely, the end grain of part D was fully accessible to water and became soaked into the aqueous phase after a few days of exposure, which led to TAZ leaching. For both unpainted and painted wood exposed to intermittent rain, a moderate TAZ depletion was observed from part A as well, and these losses are discussed further in the next section with respect to TAZ leaching kinetics.

Even though the TAZ recoveries from the middle sections (i.e., parts B and C) varied between exposures (Figure 20), the differences were not as pronounced as for the end grain parts. Exposures to moderate and high humidity did not significantly impact the sorbed TAZ in the middle sections, while exposures to continuous and intermittent rain decreased the TAZ amounts. This decrease was

only observed for unpainted wood exposed to simulated rain, and so it was attributed to leaching from transverse surfaces. As discussed above, the TAZ amounts deposited on the transverse surfaces were low compared to the amounts that penetrated in the longitudinal direction. Thus, leaching from the middle sections was deemed minimal compared to the end-grain leaching, and it was eliminated by paint application.

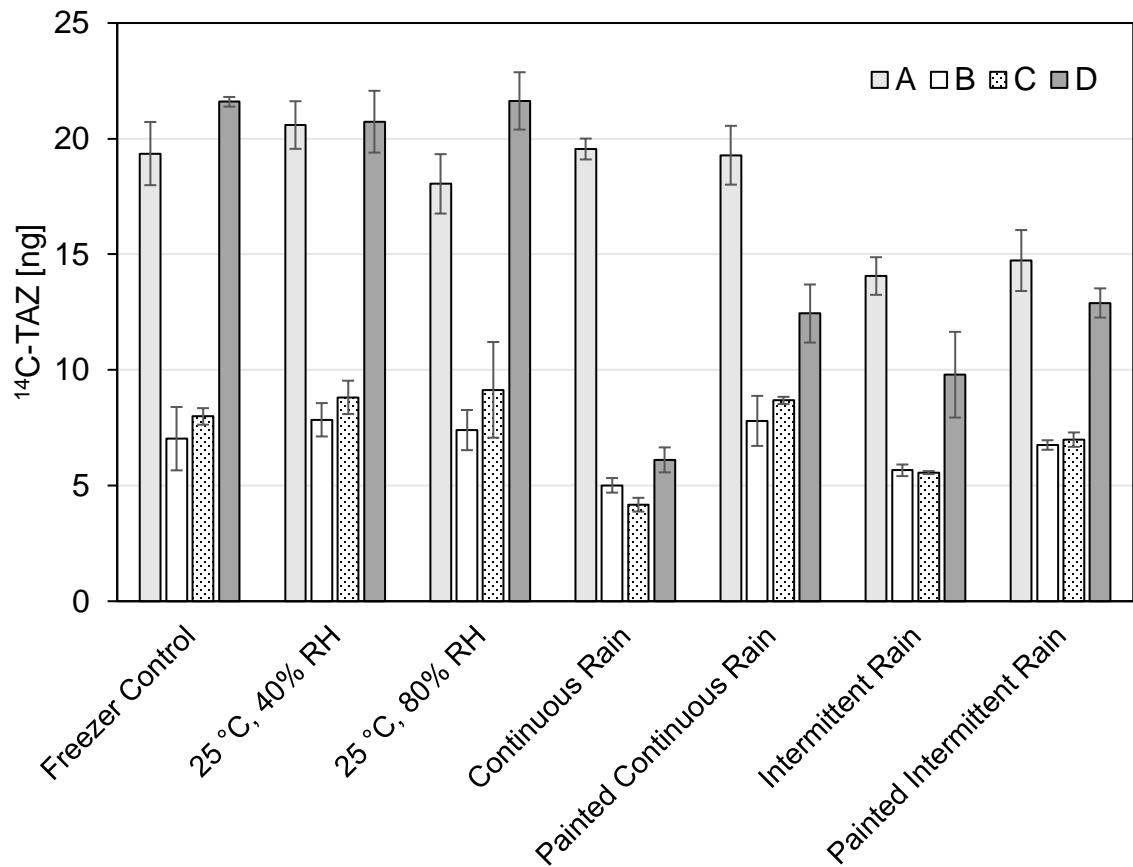


Figure 20. Distribution of ¹⁴C-TAZ recovered from the exposed wood.

IV.2.2 ¹⁴C-TAZ Leaching Kinetics

The TAZ leaching rate was investigated with respect to the amount of water applied on the wood surface and was found to be the highest for the unpainted wood exposed to continuous rain (Figure 21). After two months of continuous rain exposure, 13.5 ng of TAZ leached from the unpainted wood representing ~25% of the originally sorbed TAZ. The paint application reduced the leached TAZ amount to 6.0 ng (~11%). The observed reduction of TAZ leaching from painted wood can be explained by the effect of coatings, such as paints and primers, which is expected to reduce the water transport in and out of wood by creating a physical barrier that partially repels water. The rate of water sorption was previously shown to be the highest for uncoated wood, followed by wood painted with a water-based coating and slowest for wood painted with a solvent-based coating.²⁷ Likewise, end-grain sealing is commonly employed in industry to reduce the decay of windows, which is often initiated in the end grain within joints.¹²¹

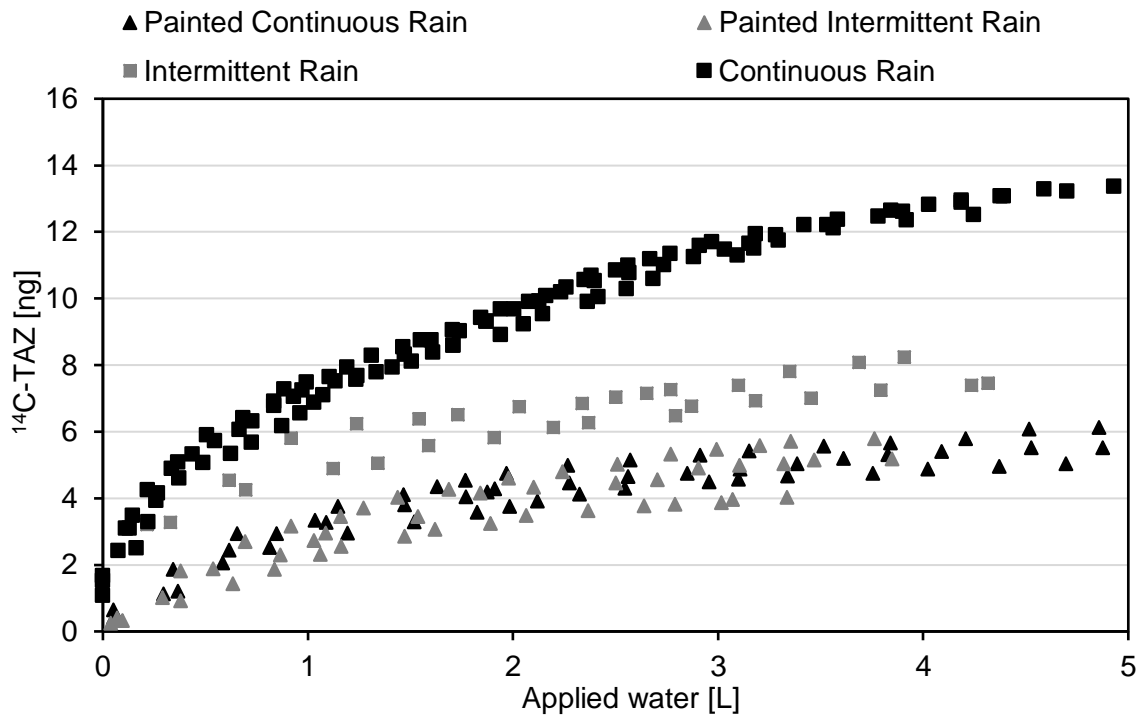


Figure 21. $^{14}\text{C-TAZ}$ recovered in the collected run-off water from unpainted and painted wood exposed to simulated continuous and intermittent rain.

Wood exposure to intermittent rain led to a reduced TAZ leaching rate from unpainted wood and similar leaching rate from painted wood compared to the continuous rain (Figure 21). Similar observations pertinent to the unpainted wood were previously shown on TAZ depletion from polymer renders, where pores that were constantly filled with water (i.e., saturated) led to significantly higher leaching rates than the dried and then wetted pores.¹¹⁸ It is plausible that wood exposed to intermittent rain had to be re-saturated after each drying period for leaching to occur. In this case, with unlimited time, the intermittent rain exposure of unpainted wood would result in the same leached amount of TAZ as the continuous rain. For

painted wood, drying intervals did not have a visible impact on the TAZ leaching kinetics likely due to the reduced water transport in and out of wood, which resulted in less effective wood drying between the leaching periods hence faster re-saturation.

In addition, intermittent rain exposure led to the TAZ depletion from wood parts A, which was not the case for continuous rain. Furthermore, this additional TAZ loss was not reflected in the run-off water analysis and was thus not caused by leaching. For painted wood, the TAZ leaching curves observed for continuous and intermittent rain were similar (Figure 21) as well as the recovered TAZ amounts from wood parts D (Figure 20), suggesting that TAZ presumably leached from part D. The same trend was observed for unpainted wood, where the leaching rate was higher for continuous rain exposure and consequently the TAZ amount recovered from wood part D was lower compared to the intermittent rain exposure.

This unexpected TAZ loss from wood part A was seen only after introducing drying intervals between water exposures, therefore we hypothesize that the loosely bound fungicide co-evaporated from this end grain with water. When wood was saturated with water, TAZ was depleted exclusively through leaching as water completely sealed the pores and hindered evaporation. Thus, no vaporization was observed for part A of continuously leached wood. However, as wood started drying, the pores were no longer fully saturated so the association with water (possibly via hydrogen bonding) enabled loosely bound surface TAZ to evaporate along with water (enhanced vaporization). Moreover, during drying of water-saturated wood, wicking occurs at the end grain, which further moves the nearby

TAZ to the end-grain surface thereby promoting the enhanced evaporation. This loosely bound TAZ is prone to removal and is easily leached from end grain part D during the initial leaching interval, so no evaporative losses are observed from this part afterwards. Also, since the TAZ depletion from wood part A was not observed when wood was exposed to 80% RH, we assume that the TAZ association with water occurred only when pores were first saturated. Finally, it is important to note that both end grains of wood used in windows and doors are sealed or otherwise protected, thus eliminating the possibility of enhanced vaporization.

IV.2.3 TAZ Depletion from Wood Exposed to the Outdoor Environment

In our previous study, the TAZ depletion from painted softwood after a six-month environmental exposure (involving high humidity, rain, wind, etc.) was found to be ~20% of the originally sorbed TAZ; however, it was unclear whether these losses were final or would increase with the exposure time.¹²² The present study shows that even though a portion of TAZ is prone to be leached from the end grain possibly due to its weak fixation within the wood matrix, this amount is limited as evident from the leaching curve levelling off for each exposure type. In order to estimate the highest TAZ amount that can be leached from treated wood of similar proportions as used in this study (i.e., 5.3 ratio of end-grain surfaces to lateral surfaces), ¹⁴C-TAZ results from continuous leaching exposure were transformed into a linear relationship (Figure 22) as described in Section IV.1.5. For unpainted wood, the maximum leachable TAZ amounted to 22 ng or 40% of the originally sorbed amount, while for painted wood, the maximum leachable TAZ was

calculated to not exceed 12% (6.7 ng). These results corresponded to TAZ leached from one wood end-grain side (wood part D), therefore, the maximum leachable TAZ would double for exposures where leaching from both sides was plausible. Besides the change in TAZ_{MAX} , the affinity constant K also decreased for painted wood (K was 3.7 for unpainted compared to 0.5 for painted wood).

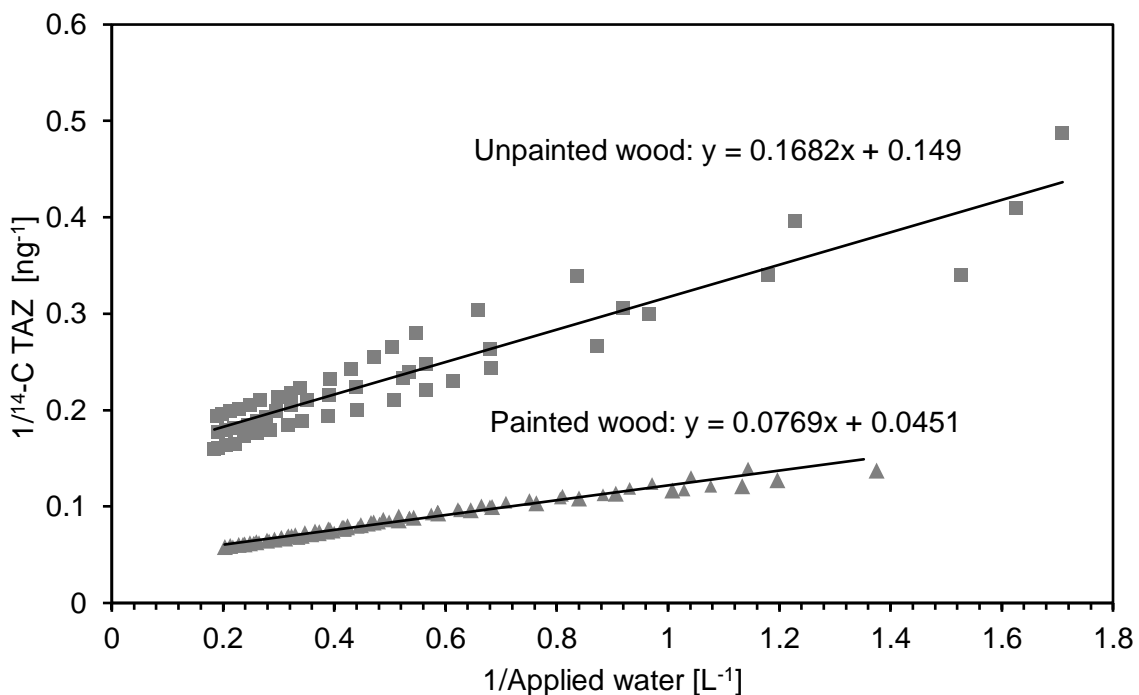


Figure 22. Determination of the highest ¹⁴C-TAZ amount that can be leached using the results obtained from wood exposure to continuous rain.

During the outdoor study,¹²² painted wood was exposed to rain and dry weather conditions and the leaching was facilitated only via one wood side, which are similar settings to the intermittent rain exposure applied in this study. However,

since the wood proportions differed (i.e., 9.3 vs 5.3 ratio of end-grain surfaces to lateral surfaces), the maximal TAZ leaching is expected to be 1.7 times higher, amounting to ~20%. The experimentally observed (20 ± 10)% TAZ loss in the wood exposed to the outdoor environment is similar to the estimate based on the maximum ^{14}C -TAZ loss calculated in the current indoor study (20%), thus demonstrating the relevance of laboratory measurements. On the other hand, data collected in a controlled indoor environment for a limited amount of time may lack some external variables occurring under natural weathering conditions, such as wood splitting in service.

IV.2.4 Impact of TAZ Loss on Wood Protection

The amounts of TAZ that could potentially be depleted from wood are an insignificant part of the total triazole amounts entering the environment, thus are rather negligible from the standpoint of environmental pollution. However, the TAZ loss is important from the product perspective as it may affect wood integrity if extensive. The TAZ amounts added to wood formulations (0.21%)¹²³ are one to two orders of magnitude smaller than those present in agricultural mixtures that are intended for crop protection (7–50%)¹²⁴⁻¹²⁵. Additionally, a window frame absorbs a similar volume of formulation as is typically sprayed on just 4 acres. Therefore, the TAZ amount that is depleted from wood over its lifetime does not significantly contribute to the total TAZ released into the environment, but may affect the durability and quality of wood products. In this study, more than 70% of ^{14}C -TAZ was shown to remain in the painted wood despite the exposure to water. TAZ was depleted mainly from the end grain, which contained the highest amount

of sorbed TAZ. Despite the loss, a significant TAZ amount stayed in this region - either greater or similar TAZ amount as was in the inner wood parts, thus the wood remained protected. On the other hand, since the end grain represents the most vulnerable part of windows and the maximum leachable ^{14}C -TAZ amount for an unpainted end grain was shown to be 40% of the initially sorbed amount, any means of end grain protection, such as sealing with a primer and paint, would be beneficial and enhance wood protection across its lifespan.

IV.3 CONCLUSIONS

Despite an eight-week exposure of treated wood to laboratory-simulated environmental conditions, more than 60% of originally sorbed ^{14}C -TAZ remained in the wood for all exposure types. While the high humidity environment did not impact the sorbed TAZ, water application led to a TAZ depletion mainly from the end grain. Since this region initially contained the highest TAZ amount, the loss did not impact the overall wood protection as a sufficient amount persisted in all wood parts.

The ^{14}C -TAZ leaching rate was found to be the highest for unpainted wood exposed to simulated continuous rain. Upon extensive water application, up to 40% of the originally sorbed TAZ may leach from end grain based on the obtained kinetic data. The TAZ leaching rate from unpainted wood exposed to intermittent rain declined since wood was allowed to dry between weeklong rain intervals, yet it might eventually result in a comparable TAZ loss. Additionally, primer and paint coatings led to a substantial reduction of TAZ depletion with the maximum

leachable TAZ fraction of 12%. Therefore, end-grain sealing was found to be beneficial as it enhanced the wood protection in the long run by acting as a physical barrier and decreasing the wood affinity for water.

V. CHAPTER: METHOD DEVELOPMENT FOR TRIAZOLE AND IPBC QUANTIFICATION IN WOOD LEACHATE USING SPE FOLLOWED BY LC-ESI-TOFMS DETECTION

V.1 MATERIALS AND METHODS

V.1.1 Chemicals and Reagents

Analytical standards, TAZ, PAZ, AZA, HAZ, and IPBC, were of > 99% purity and purchased from Sigma-Aldrich (St. Louis, MO, USA). Solvents (e.g., acetone, methanol, and acetonitrile of LC or GC grade) and electrolytes (e.g., acetic acid, formic acid, ammonium acetate, and ammonium formate) were obtained from Fisher Scientific (Pittsburgh, PA, USA). Water was purified using a DirectQ Millipore system (Billerica, MA, USA). Supelco HLB cartridges (3 cm³, 60 mg sorbent) were also purchased from Sigma-Aldrich, and PRiME HLB cartridges (3 cm³, 60 mg sorbent) were from Waters Corporation (Milford, MA, USA).

V.1.2 Wood Matrix Extract for SPE Validation

An aqueous wood extract was prepared by extracting wood with acetone to obtain highly concentrated solution, and subsequently evaporating the acetone and re-dissolving the wood matrix components in water. Specifically, untreated ponderosa pine wood samples stored under standard conditions of an air-conditioned building (22 ± 2 °C, ambient pressure and ca. 50% relative humidity) were sheared with a

hammer and knife into smaller pieces to allow for an exhaustive wood extraction, which was carried out for 16 hours using a Soxhlet apparatus with 130.0 mL of acetone.¹²² The wood extract was then evaporated to dryness under a gentle stream of nitrogen, re-dissolved in water, and filtered through 0.2 μm syringe filters. The resulting aqueous wood matrix extract was spiked with a fungicide stock solution in methanol (MeOH) to achieve the desired analyte concentration (~20 ppm, w/v) in 10% MeOH solution. This 10% MeOH wood extract was only used to evaluate the SPE method as it represented the worst-case scenario wood leachate with each aliquot (0.5 mL) containing matrix from 0.5 g of wood.

V.1.3 Industrial Wood Leachate Samples

Industrial leachate samples were prepared at Marvin Windows and Doors facility (Warroad, MN, USA) by direct aqueous leaching of wood preserved with fungicides. Specifically, ponderosa pine wood sections (1.5 x 1.5 x 8") were dip-treated with a commercially available Woodlife 111 solution (containing 0.22% of TAZ and PAZ, made by Kop-Coat, Inc., Pittsburgh, PA, USA), dried and painted white (aqueous white paint manufactured by The Valspar Corporation, Minneapolis, MN, USA). Ten wood sections were placed on a raised platform in Rubbermaid roughneck totes (18-gallon volume) under a flowing, recirculating water irrigation system. The sections were laid horizontally on the platform and water was sprayed in a 90° angle (thus exposing both the radial and tangential wood surface). Wood sections were exposed to 11.3 L of water per week for a total of four weeks. A control experiment involved the same setup using 10 wood sections that were not treated with preservatives. Because this wood leachate did

not contain any fungicides, it was used for determining the matrix-affected LOD and LOQ.

V.1.4 SPE-HLB

To achieve the retention of triazoles and IPBC within the solid phase while eluting interfering water-soluble components, reversed-phase SPE cartridges were employed. The method was developed on two types of HLB cartridges, Supelco HLB and PRiME HLB cartridges, using the protocol described in Table 10, with PRiME HLB cartridges not requiring conditioning. To evaluate the method performance, 0.5 mL of wood extract in 10% MeOH solution was used (preparation described in Section V.1.2), while for analyzing industrial leachate samples, 3 mL were loaded. The fungicides collected in ACN with 2% ammonium hydroxide solution were evaporated down to 0.3 mL under a gentle stream of nitrogen, mixed with 0.7 mL of water, and spiked with IS prior to the LC-ESI-TOFMS analysis.

Table 10. The SPE-HLB protocol developed for retention of fungicides present in wood leachate.

HLB SPE protocol	
Cartridge conditioning (Supelco HLB)	3 mL MeOH 3 mL 10% MeOH solution
Sample load	0.5 mL of wood matrix extract in 10% MeOH or 3 mL of industrial wood leachate

Table 10 cont.

HLB SPE protocol	
Matrix wash	3 mL 10% MeOH solution
Analyte collection	3 mL ACN with 2% ammonium hydroxide

V.1.5 ESI-TOFMS Optimization

ESI-TOFMS optimization consisted of two parts. At first, an initial screening was performed to select the suitable solvent system and electrolyte using a representative triazole, TAZ, and IPBC. Then, ESI voltages and the electrolyte concentrations were thoroughly optimized. A DOE methodology, specifically response surface design, was used to find the optimal electrolyte concentrations, capillary voltage, and fragmentor voltage for TAZ, PAZ, and IPBC.

As in our previous studies,^{103, 126} all optimization experiments were conducted using a flow injection analysis (FIA), where samples containing fungicides and the electrolytes (concentration range 4–400 mM) in the evaluated solvent system (MeOH/ACN and water 50:50, v/v) were injected into a mobile phase flow (MeOH/ACN and water, 50:50, v/v). The concentration of electrolyte in the sample was four times higher than the desired concentration in the ESI chamber (Table 11) to account for the dilution in the mobile phase (i.e., 50 μ L sample injection into 0.2 mL·min⁻¹ flow). The final concentration of fungicide standards in the ESI chamber was ~10 ppm. Since no column was employed for fungicide separation,

all standards were detected having the same retention time. An illustrative chromatogram is shown in Figure D. 1.

V.1.5.1 Screening of ESI-TOFMS Conditions

Screening of ESI-TOFMS conditions included the evaluation of organic solvent (e.g., ACN or MeOH) and the electrolyte type. Previously we observed significant interactions between the electrolyte type and its concentration, thus for each electrolyte, various concentrations were examined (Table 11).^{103, 126} Since two solvent systems were used, 32 runs were required for full optimization. Also, TAZ and IPBC were screened separately, yielding 64 experiments.

Table 11. Electrolytes and their concentrations evaluated in both MeOH-water and ACN-water solvent systems as part of the screening of ESI-TOFMS conditions.

Experiment #	Electrolyte	Conc. [mM]
1		1
2	formic acid	10
3		100
4		1
5	ammonium formate	5
6		10
7	ammonium formate + formic acid (50:50, v/v)	1
8		10
9		1
10	acetic acid	10
11		100

Table 11 cont.

Experiment #	Electrolyte	Conc. [mM]
12		1
13	ammonium acetate	5
14		10
15	ammonium acetate + acetic acid (50:50, v/v)	1
16		10

V.1.5.2 Optimization of ESI-TOFMS Using DOE Response Surface Design

To optimize the ESI-TOFMS conditions and assess the expected curvature, DOE response surface design was used. The ACN-water system and the ammonium acetate as an electrolyte were employed based on the screening results. The main factors included the electrolyte concentration (factor A), capillary voltage (i.e., electrospray voltage, factor B), and fragmentor voltage (i.e., collision induced dissociation voltage, factor C). For each factor, low and high levels were selected, and are summarized in Table 12. The design was created using Minitab and yielded 20 runs, which are described in Table D. 1.

Table 12. Factors and levels used for the optimization of ESI-TOFMS conditions using DOE response surface design. Ammonium acetate was chosen as the electrolyte based on the screening experiments.

Factor	Low level	High level
A: electrolyte concentration [mM]	2.5	5
B: capillary voltage [V]	4500	5000

Table 12 cont.

Factor	Low level	High level
C: fragmentor voltage [V]	125	150

V.1.6 Instrumentation

Both FIA and LC-ESI-TOFMS analyses were conducted on an Agilent 1100 LC coupled to a high resolution TOFMS G1689A Series 6200. LC separations were performed using an Agilent Eclipse Plus C18 150 mm × 2.1 mm reverse phase LC column with 3.5 μm particle size. The flow rate was 0.2 mL·min⁻¹. The optimized LC method employed a solvent system consisting of A: 5% ACN in water with 1.7 mM ammonium acetate and B: ACN with 1.7 mM ammonium acetate. The gradient elution was evaluated starting at 20, 30, 40, or 50% ACN, but the final program began at 30% B and increased to 55% B in 21 min followed by a further increase to 65% B in 5 min (time 26 min). It reached 90% B in 1 min (time 27 min) and was held at 90% B for an additional 1 min (time 28 min). The %B was then decreased back to 30% in 1 min (time 29 min) and held there for an additional 11 min to provide sufficient time for column equilibration. The total analysis time was 40 min. During the analysis, the flow was first diverted into a waste container for initial 7 min, and then into the TOFMS to minimize contamination of the ESI chamber with salts and early eluting species. The column oven temperature was set to 30 °C and injection volume was 20 μL. ESI was performed in positive mode with drying gas (N₂) set to 350 °C at a flow rate of 12 L·min⁻¹ and the nebulizer gas (N₂)

pressure set to 25 psig. The capillary and fragmentor voltages were 4350 V and 115 V, respectively.

V.1.7 Data Processing

The LC-ESI-TOFMS data were processed using Analyst QS 1.1 (Applied Biosystems) and MassHunter Workstation Quantitative Analysis B.04.00 (Agilent Technologies). Fungicides were identified based on their retention times and mass spectra matching those of individual standards. Quantification was accomplished by integrating the extracted ion current (EIC) chromatograms of the corresponding protonated molecular ions $[M+H]^+ \pm 0.03$ m/z listed in Table 13 employing an IS method.

Table 13. Protonated molecular ions used for the analyte LC-MS quantitation.

Fungicide	$[M+H]^+$
TAZ	308.153
PAZ	342.077
AZA	300.030
HAZ (IS)	314.082
IPBC	281.999

Minitab 16.1.1 was used for statistical analysis. DOE response surface design was employed for the optimization of ESI-TOFMS ionization, where factors and

interactions were considered significant when the p -value was lower than 0.10 (i.e., 90% confidence level). Response surface design methodology is routinely used when curvature in the response surface is suspected, and it was previously reported as a systematic approach for the optimization of analytical methods.¹²⁷⁻
¹²⁸ A response surface optimizer function was further employed to find the settings yielding the highest MS response of all fungicides. By selecting a target value (i.e., MS peak area), Minitab calculated an optimal solution based on the conducted experiments.

Instrumental and matrix-affected LODs and LOQs were calculated from the calibration curves generated using a least square linear regression. Only the calibration points that were within one order of magnitude of the LODs were used. The calculation was based on the following equations: $LOD = 3.3 \times s_y/m$ and $LOQ = 10 \times s_y/m$, where s_y is a standard error of the predicted y -value for each x -value and m is a slope of the calibration curve. To calculate matrix-affected LODs and LOQs, the control industrial wood leachate (i.e., generated from untreated wood; see Section V.1.3) was purified using the developed SPE protocol (e.g., 3 mL of leachate per calibration standard), evaporated to 0.3 mL, mixed with 0.7 mL of water, and spiked with IS and fungicides in the concentration range of one order of magnitude of LOD.

V.2 RESULTS AND DISCUSSION

V.2.1 SPE-HLB Recoveries and Purification

Fungicide SPE-HLB recoveries were evaluated using a wood matrix extract spiked with standards, and were 94–102% (Table 14). These high recoveries were achieved despite the presence of wood matrix interferences, and were reproducible with $RSD \leq 5\%$.

Table 14. Fungicide recoveries using SPE-HLB protocol.

SPE-HLB Recoveries			
TAZ	PAZ	AZA	IPBC
96 ± 4%	102 ± 3%	102 ± 2%	94 ± 5%

Aside from SPE-HLB analyte recoveries, the extent of wood matrix purification (i.e., removal of matrix interferences) was assessed. The LC-ESI-TOFMS chromatograms of wood matrix extract containing fungicides before and after SPE are shown in Figure 23. A partial purification could be seen from the decrease of TIC response and the peak intensities in the first 8 min of analysis, where polar and mid-polar wood compounds eluted. Generally, the SPE-HLB purification is expected to vary as wood leachate composition changes with respect to wood type, age, and location; nevertheless, by extracting the protonated molecular ions (Figure 23), no interfering compounds were observed. Yet, as the sample clean-

up was not extensive, the final method included diversion of the mobile flow into a waste container instead of MSTOF for the initial 8 min to minimize contamination of the ESI chamber with these early-eluting species. Additionally, the high fungicide retention and their efficient collection from the cartridge were found beneficial for their pre-concentration, since their amounts in industrial wood leachate, although significant, may be near the method's limits of detection. Thus, the SPE-HLB step was employed for analyte pre-concentration purposes rather than purification.

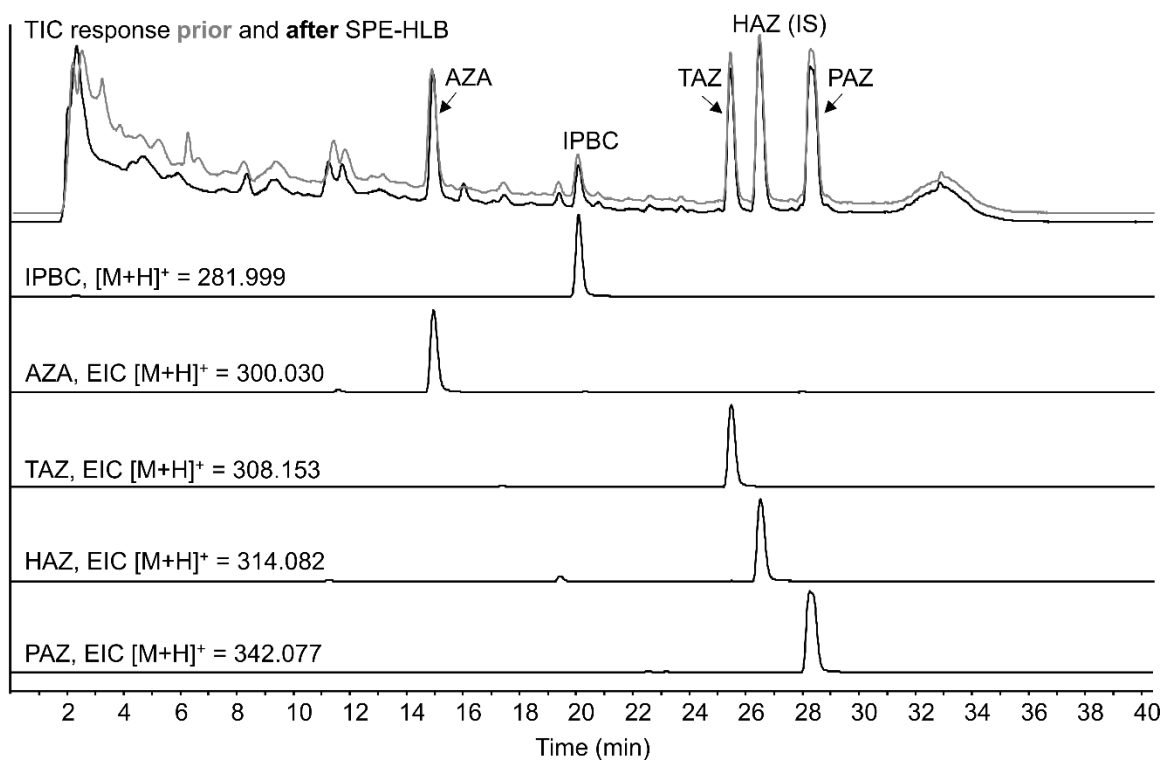


Figure 23. LC-ESI-TOFMS total ion current (TIC) chromatograms of unpurified wood matrix extract containing fungicides (grey) and an SPE-HLB purified sample

(black), followed by EIC chromatograms for IPBC, AZA, TAZ, HAZ, and PAZ in the purified sample.

V.2.2 Screening of the Solvent System and Electrolyte

The organic solvent selection did not seem to affect the fungicide MS response as both ACN and MeOH yielded similar results (Figure 24 vs Figure D. 2). As a result, ACN was selected since it was also employed to elute fungicides from the SPE-HLB cartridge. In addition, an ACN-water system yields lower column backpressures, and exhibits a lower UV cut-off wavelength, which is desirable as many LC-MS instruments offer a secondary UV detection.

On the other hand, neither the choice of electrolyte nor its concentration had an impact on the fungicide MS response. For all 32 conditions (Figure 24 and Figure D. 2), the TAZ response was ~2x higher than the IPBC response, indicating a lower ionization efficiency for the latter. For both TAZ and IPBC, the MS response was higher when acetic acid and ammonium acetate were used compared to formic acid and ammonium formate. In general, 1 mM ammonium acetate provided the highest ionization efficiency for both TAZ and IPBC. It was of note that the high concentration of acetic acid was even more effective for TAZ ionization, but had a detrimental effect on the ionization of IPBC, and so it was not further evaluated.

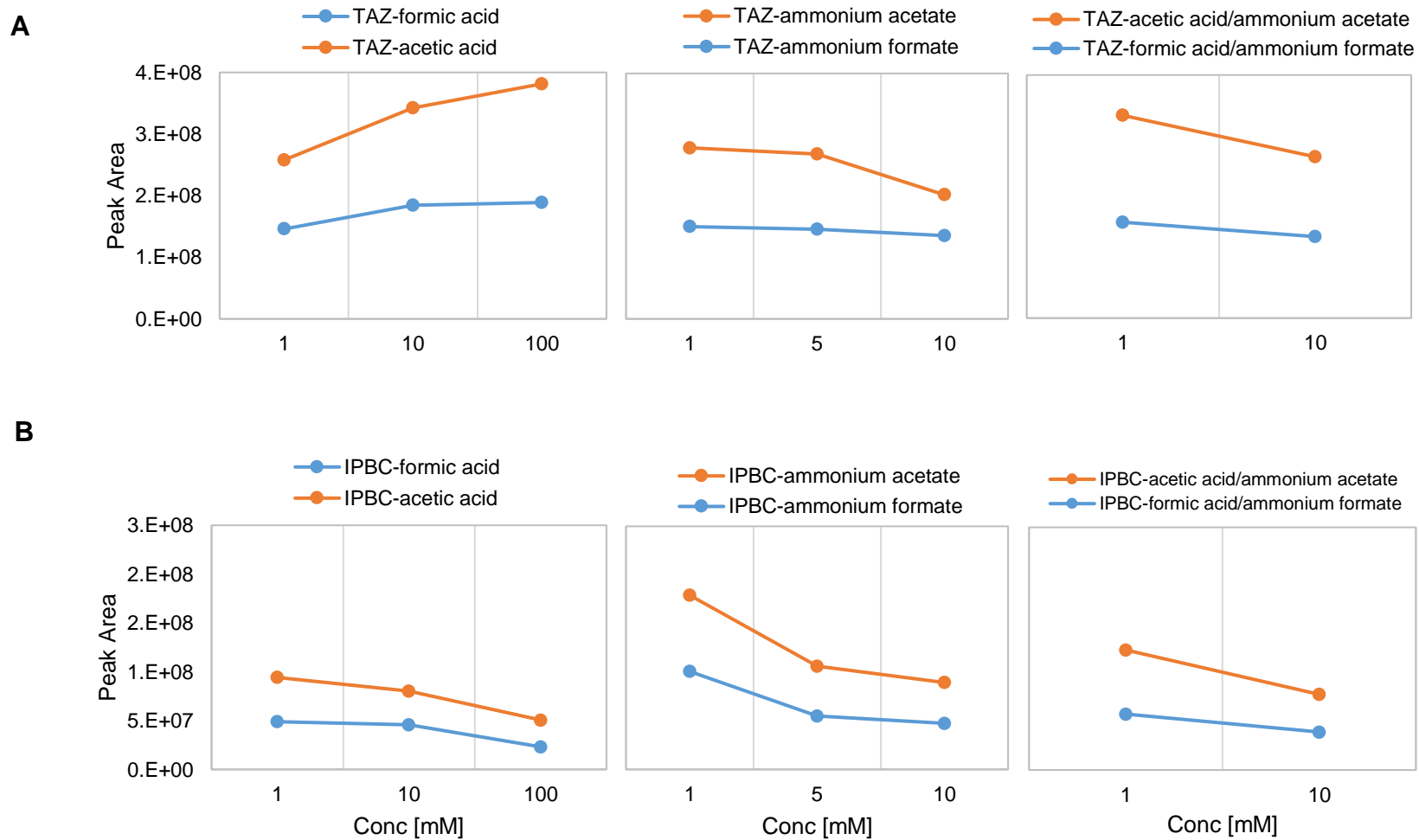
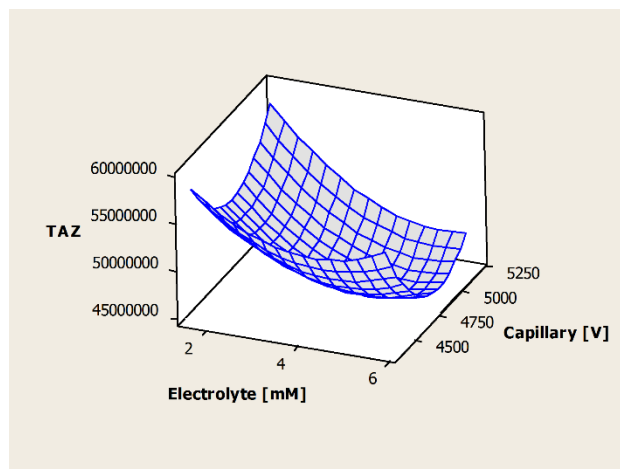


Figure 24. Impact of electrolyte type and its concentration in ACN-water system (50:50, v/v) on TAZ (A) and IPBC (B) MS response.

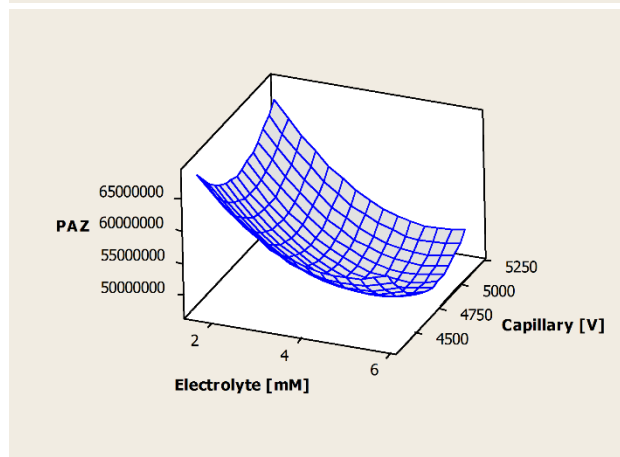
V.2.3 Detailed ESI-TOFMS Optimization

A detailed optimization of ESI-TOFMS conditions was performed using ACN-water solvent system and ammonium acetate as an electrolyte (based on the LC screening), focusing on the interaction of ammonium acetate concentration with the capillary and fragmentor voltages. In general, the electrolyte concentration ($0.005 \leq p \leq 0.090$) and the capillary voltage ($0.065 \leq p \leq 0.085$) were the two most influential factors for TAZ and PAZ detection (Table D. 2, Figure D. 3, and Figure D. 4). By contrast, the IPBC response was significantly impacted by the electrolyte concentration and the fragmentor voltage (both $p = 0.000$, Figure D. 5). The response surface plots constructed using these two factors for each fungicide were found to be curved (Figure 25), thus demonstrating the need for simultaneous optimization of the electrolyte concentration and ESI voltages. The conditions yielding the highest fungicide responses are further summarized in Table 15. Also, as observed previously, IPBC exhibited the lowest MS response compared to TAZ and PAZ.

A



B



C

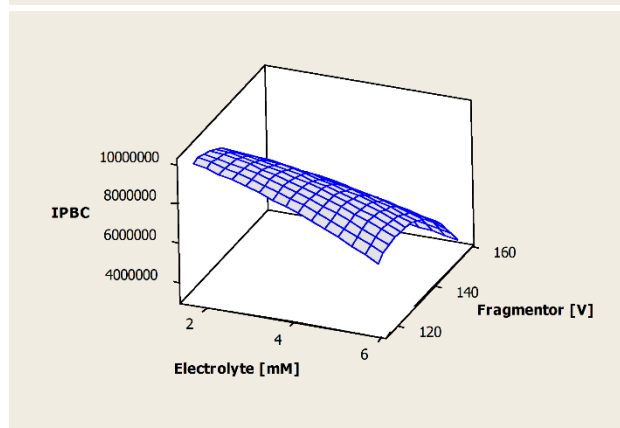


Figure 25. Surface plots for TAZ (A), PAZ (B), and IPBC (C) constructed using the two most influential factors. The highest points of the surface plots illustrate the ESI-TOFMS experimental conditions yielding the largest fungicide peak areas.

Table 15. ESI-TOFMS conditions yielding the highest fungicide response based on the response surface optimization.

Analyte	Factor	Conditions yielding highest MS response
TAZ	electrolyte conc.	< 1.6 mM
	capillary voltage	< 4450 V or > 5150 V
PAZ	electrolyte conc.	< 2.0 mM
	capillary voltage	< 4450 V or > 5100 V
IPBC	electrolyte conc.	< 3.0 mM
	fragmentor voltage	< 133 V

To find the optimal ESI-TOFMS conditions, DOE response optimizer was used with the goal of maximizing the response for the three analytes simultaneously using the same factor levels (Figure D. 6 and Figure D. 7). The conditions were predicted based on the obtained experimental data, and consisted of 1.7 mM ammonium acetate, capillary voltage of 4330 V, and fragmentor voltage of 116 V (Figure 26). Since the MassHunter software did not allow for the same voltage input, the capillary and fragmentor voltages were adjusted to the nearest value, 4350 V and 115 V, respectively.

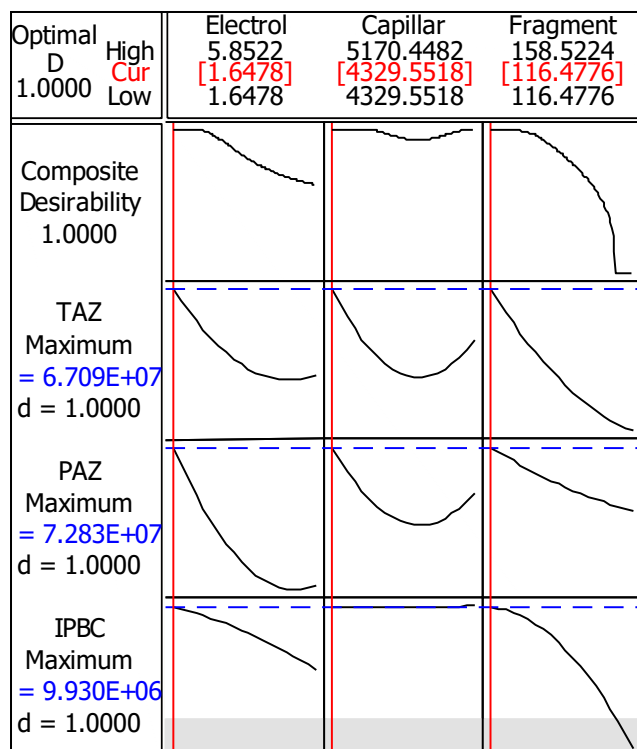


Figure 26. Optimal ESI-TOFMS conditions predicted by DOE response optimizer to maximize TAZ, PAZ, and IPBC responses.

V.2.4 Matrix-Affected LOD and LOQ

Instrumental LOD and LOQ were found using fungicide standards in pure solvents, while matrix-affected values were calculated from standards spiked into SPE-purified industrial wood leachate control (Section V.1.7). The instrumental LODs for triazoles varied between 10–13 ng·L⁻¹, and LOQs were 27–43 ng·L⁻¹ (Table 16). For IPBC, a higher instrumental LOD and LOQ were found, 30 ng·L⁻¹ and 97

ng·L⁻¹, respectively. While triazole LODs and LOQs were only slightly affected by the wood leachate matrix, those of IPBC increased by a factor of 2.

Table 16. Instrumental and matrix-affected LODs and LOQs for triazoles and IPBC expressed in ng·L⁻¹ concentrations.

	Instrumental [ng·L ⁻¹]				Matrix-affected [ng·L ⁻¹]			
	AZA	IPBC	TAZ	PAZ	AZA	IPBC	TAZ	PAZ
LOD	13	30	10	10	20	63	13	13
LOQ	43	97	27	27	60	187	40	40

To compare our results to previously developed LC-ESI-TOFMS methods for triazole quantification in aqueous samples, the matrix-affected LOQs for triazoles, ≤ 60 ng·L⁻¹, were taken into account. This value is between those reported by Robles-Molina *et al.* (LOQs < 10 ng·L⁻¹),¹⁰⁴ and Amelin and Andoralov (LOQs of 60,000 ng·L⁻¹ for TAZ and 20 ng·L⁻¹ for PAZ)¹⁰⁵. However, the reported methods did not aim for simultaneous IPBC quantification, and were not developed with respect to wood leachate matrix. Also, the SPE-HLB pre-concentration step employed in this study aids in the quantification of fungicide amounts that are below the matrix-affected LOQs.

V.2.5 Method Application to Industrial Wood Leachate

The developed method was applied to quantification of TAZ and PAZ in industrial wood leachate received from Marvin Windows and Doors (Section V.1.3). A total of four samples were analyzed (i.e., leachate from weeks 1–4), by pre-concentrating samples on SPE-HLB cartridges. Figure 27 shows the efficiency of SPE-HLB by comparing the LC-ESI-TOFMS chromatograms of leachate samples analyzed either directly (0.5 mL) or after the pre-concentration (3.0 mL), where an increase in the TAZ and PAZ responses is clearly seen for both TIC and EIC. Also, besides the six-fold increase in fungicide responses, the response of wood leachate components increased comparatively less and did not interfere with the fungicide detection.

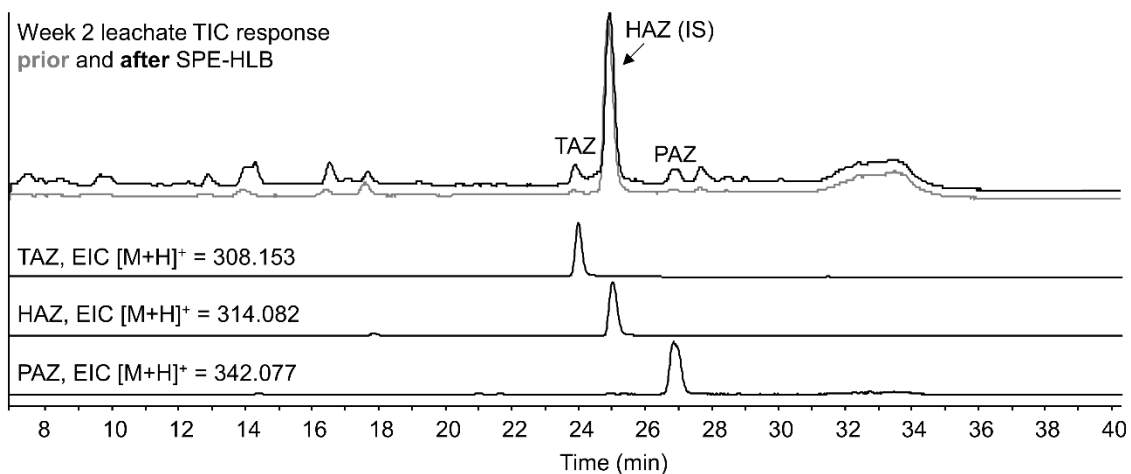


Figure 27. LC-ESI-TOFMS TIC chromatograms of week 2 industrial wood leachate containing TAZ and PAZ (grey) and an SPE-HLB pre-concentrated

sample (black), followed by EIC chromatograms for TAZ, HAZ, and PAZ in the pre-concentrated sample.

The quantified TAZ and PAZ amounts in the industrial leachate are summarized in Table 17. The amount of leached fungicide decreased each week with the TAZ concentration being slightly greater than that of PAZ, which is in agreement with the previously published results.¹²² The intra-day repeatability of the LC-ESI-TOFMS analysis was investigated by analyzing the wood leachate obtained in the first and second week in triplicate. Good repeatability with the relative standard deviations (RSDs) $\leq 2\%$ was achieved for the two analytes. Also, the inter-day repeatability was assessed by repeating the analysis after 4 days. The RSDs ranged between 1% and 7%, which was considered acceptable.

Table 17. Intra- and inter-day repeatability of triazole determination in industrial wood leachate samples.

	TAZ [$\mu\text{g}\cdot\text{L}^{-1}$]		PAZ [$\mu\text{g}\cdot\text{L}^{-1}$]	
	AVG	% RSD	AVG	% RSD
Inter-day Repeatability (4 days)				
Week 1 leachate	342	5	251	5
Week 2 leachate	213	5	166	1
Week 3 leachate	134	4	108	4
Week 4 leachate	72	4	62	7
Intra-day Repeatability (n = 3)				
Week 1 leachate	356	1	263	1
Week 2 leachate	220	2	172	1

V.3 CONCLUSIONS

An optimized LC-ESI-TOFMS method for triazole and IPBC quantification in wood leachate was developed employing SPE-HLB sample pre-concentration and exhibiting 91-102% analyte recoveries. The optimal LC-ESI conditions included an ACN-water solvent system and ammonium acetate as an electrolyte. Using a DOE response surface design, the optimal electrolyte concentration was found to be 1.7 mM, with a capillary voltage of 4330 V and a fragmentor voltage of 116 V. The matrix-affected LODs for triazoles varied between 13–20 ng·L⁻¹, and the matrix-affected LOQs were 40–60 ng·L⁻¹. For IPBC, a higher matrix-affected LOD and LOQ were found, 63 and 187 ng·L⁻¹, respectively. The developed method was applied to the analysis of industrial wood leachate. The intra-day repeatability was ≤ 2%, and the inter-day repeatability varied between 1–7%.

APPENDICES

APPENDIX A

Liquid scintillation counting procedure to measure ^{14}C -TAZ in acetone wood extracts

The following protocol describes the analysis procedure as used on a Beckman Coulter LS6500 liquid scintillation counter.

To prepare automatic counting, racks need to be organized in the manner described below and shown in Figure A. 1:

- a) The 1st rack is blue and contains a 14-C standard in the first position. It also contains a magnetic *calibration card* labeled "AUTO CALIBRATE" starting in the position labeled L and extending to the right (see image below, the magnetic card is facing the instrument's back, the L is visible on the red rack).
- b) The 2nd rack is yellow and contains samples to be measured. Start with a blank sample and follow with the remaining samples. This rack contains two magnetic cards - a *rack card* to the left of position L and a *program card* starting at position L and extending right. In this case, method 5 was used so the *program*

- card* is labeled "USER NO. 5". The *rack card* is labelled "RACK NO. 1". Each yellow rack can hold 12 samples. If you have more samples, install more yellow racks. Each of the latter must contain the *rack card* in the left slot (to the left of position L), but only the first rack contains the *program card*.
- c) The last rack is red and does not contain any samples. It only holds one *card* labelled "HALT" starting in the L position and extending right. This will terminate the automatic counting.

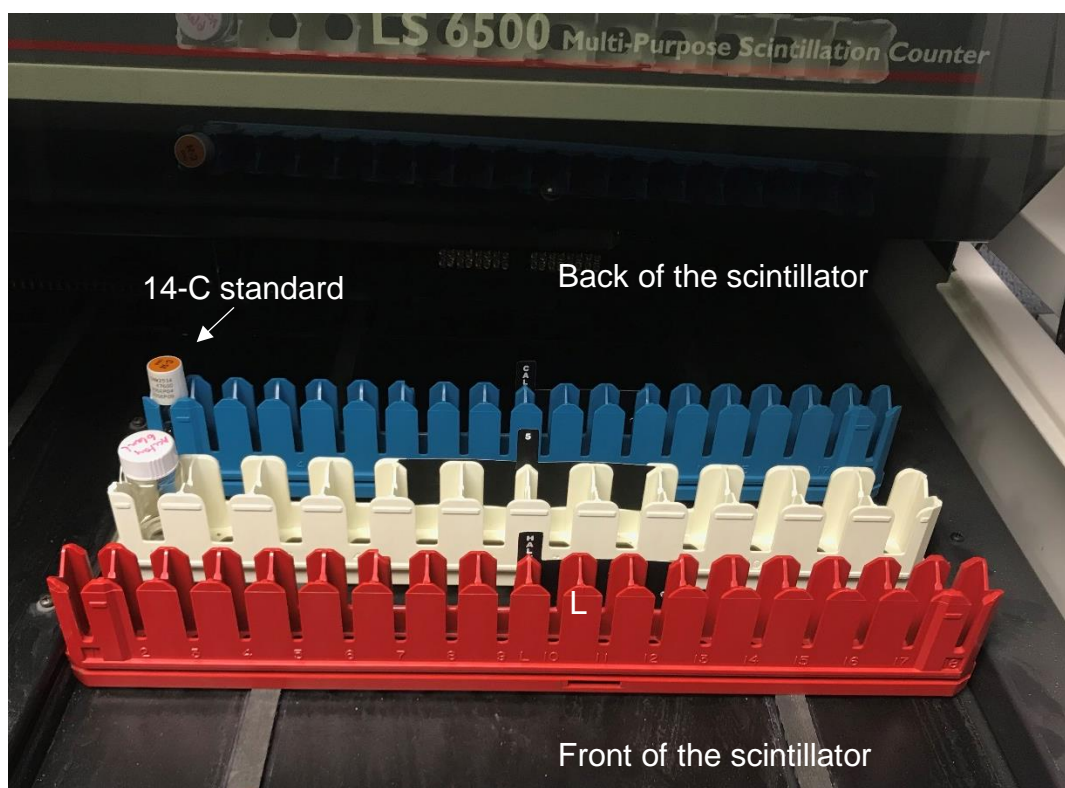
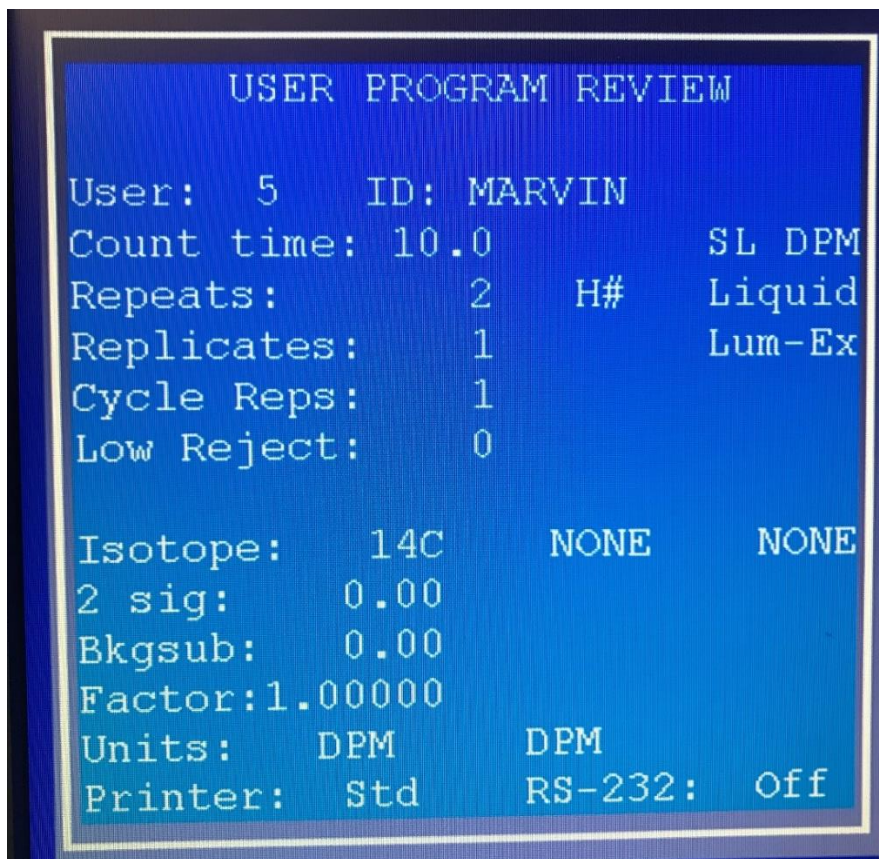


Figure A. 1. Setup of racks for automatic counting analysis on a Beckman Coulter LS6500.

Before you run the automatic analysis, make sure a printer is connected and is full on paper. All results are printed and not stored in the computer.

The method details are provided below in Figure A. 2. Shortly, the isotope of interest was carbon-14. The counting time was ten minutes and each sample was counted twice (i.e., two repeats). The liquid counting mode was SL DPM and the method included automatic correction for quenching (#H) and luminescence (Lum-Ex).



```
USER PROGRAM REVIEW

User: 5      ID: MARVIN
Count time: 10.0      SL DPM
Repeats:      2      H#      Liquid
Replicates:      1      Lum-Ex
Cycle Reps:      1
Low Reject:      0

Isotope:      14C      NONE      NONE
2 sig:      0.00
Bkgs sub:      0.00
Factor: 1.00000
Units:      DPM      DPM
Printer:      Std      RS-232: Off
```

Figure A. 2 Scintillation method used to detect ¹⁴C-TAZ in wood extracts.

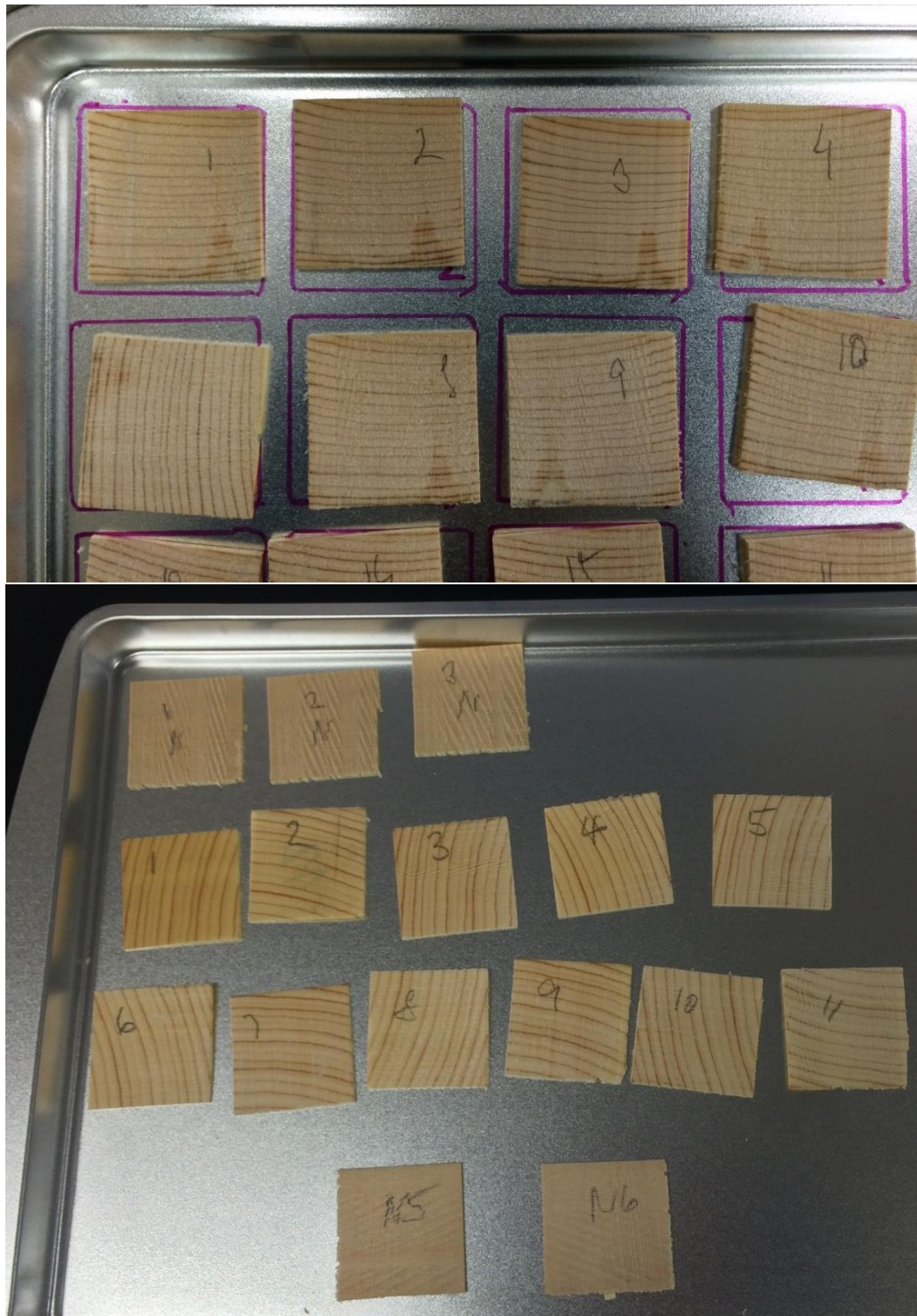


Figure A. 3. Smaller wood slices (0.2 cm x 3.8 cm x 3.8 cm) cut using a Craftsman 9" band saw.



Figure A. 4. Protective hood enclosure to eliminate ^{14}C -wood dust contamination. The enclosure contained two chambers separated by a plastic sheet. Entrance to the first chamber is shown on the left, while the second chamber attached to the hood is shown on the right.

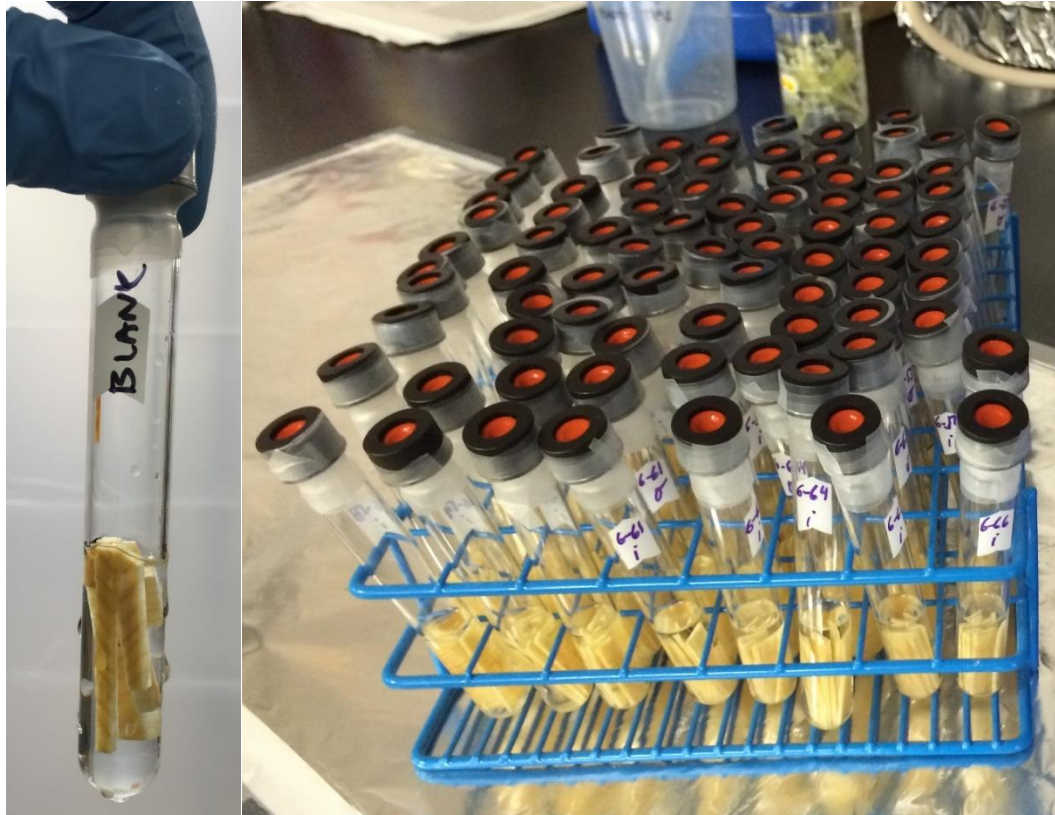


Figure A. 5. Glass tubes containing smaller wood pieces (cut with a blade) and 3.5 mL of acetone.

APPENDIX B



Figure B. 1. Cutting of “T” wood sections with a band saw into 2-mm wide wood slices (#1–12, 14, and 16).

APPENDIX B.1

GC-MS quantification of TAZ, PAZ, and IPBC in acetone wood extracts

TAZ, PAZ, and IPBC were identified based on their retention times and quantifying ion with the highest signal to noise ratio (e.g., m/z 125 for TAZ, m/z 173 for PAZ, and m/z 165 for IPBC). The IS method was used to quantify the analytes with HAZ added to each sample resulting in ~150 ppm IS concentration. Two PAZ stereoisomers were separated in the GC chromatograms (Figure B.1. 1), and their peak areas were summed for the quantitation.

Calibration consisted of nine calibration standards containing TAZ, PAZ, and IPBC in the range of 0.02–120 ppm ran at the beginning and the end of a sequence. Two sets of calibration curves were used for quantification of fungicides based on the analyte concentration divided by IS concentration, A/A (IS). High calibration curves included c/c (IS) higher than 0.01 (i.e., 2 ppm of fungicide), while low calibration curves included c/c (IS) lower than 0.01 (Figure B.1. 2 and Figure B.1. 3). For c/c (IS) 0.009, four data points are shown as this calibration standard was analyzed twice between wood sample runs in addition to the calibration sets.

Instrumental LODs and LOQs (Table B.1. 1) were calculated from the calibration curves generated using a least square linear regression. The following equations were used: $LOD = 3*s_y/k$ and $LOQ = 10*s_y/k$, where s_y is a standard error of the predicted y value for each x -value and k is a slope of a calibration curve. For the

LOD calculations, only the points within one order of magnitude of the LOD were used.

Table B.1. 1. GC-MS LOD and LOQ values for TAZ, PAZ, and IPBC calculated from calibration curves.

	TAZ, PAZ		IPBC	
	A/A (IS)	Conc [ppm]	A/A (IS)	Conc [ppm]
LOD	0.001	0.2	0.001	0.3
LOQ	0.004	0.6	0.009	1.9

Additionally, GC-MS quantification of IPBC in three wood slices of sun-exposed wood and control wood is shown in Figure B.1. 4. Significantly higher losses of IPBC were discovered in comparison to triazole losses. Also, in contrast to triazoles where losses were restricted only to the surface and first subsurface slices, the IPBC losses were apparent for distal slices as well (slice #14). This indicated that IPBC, unlike triazoles, undergoes additional thermal degradation (in all slices) accompanied by photodegradation (in the surface slices) as previously reported. Notably, as for the triazoles, these losses correspond to the unbound compound and do not represent the overall IPBC loss.

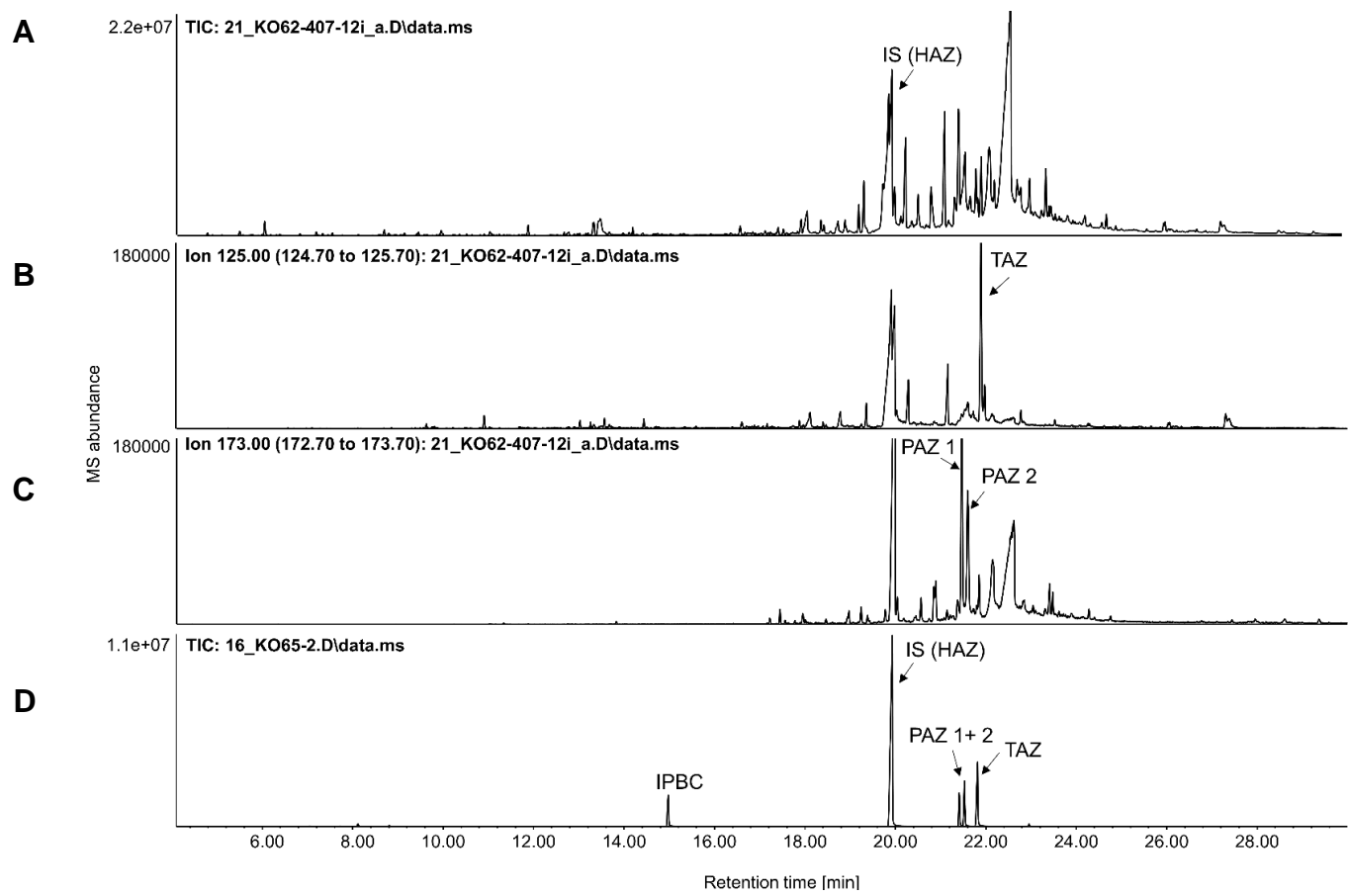


Figure B.1. 1. A: GC-MS chromatogram of acetone wood extract displayed as TIC, B: extracted m/z 125 corresponding to TAZ, C: extracted m/z 173 corresponding to PAZ, and D: TIC of a calibration sample.

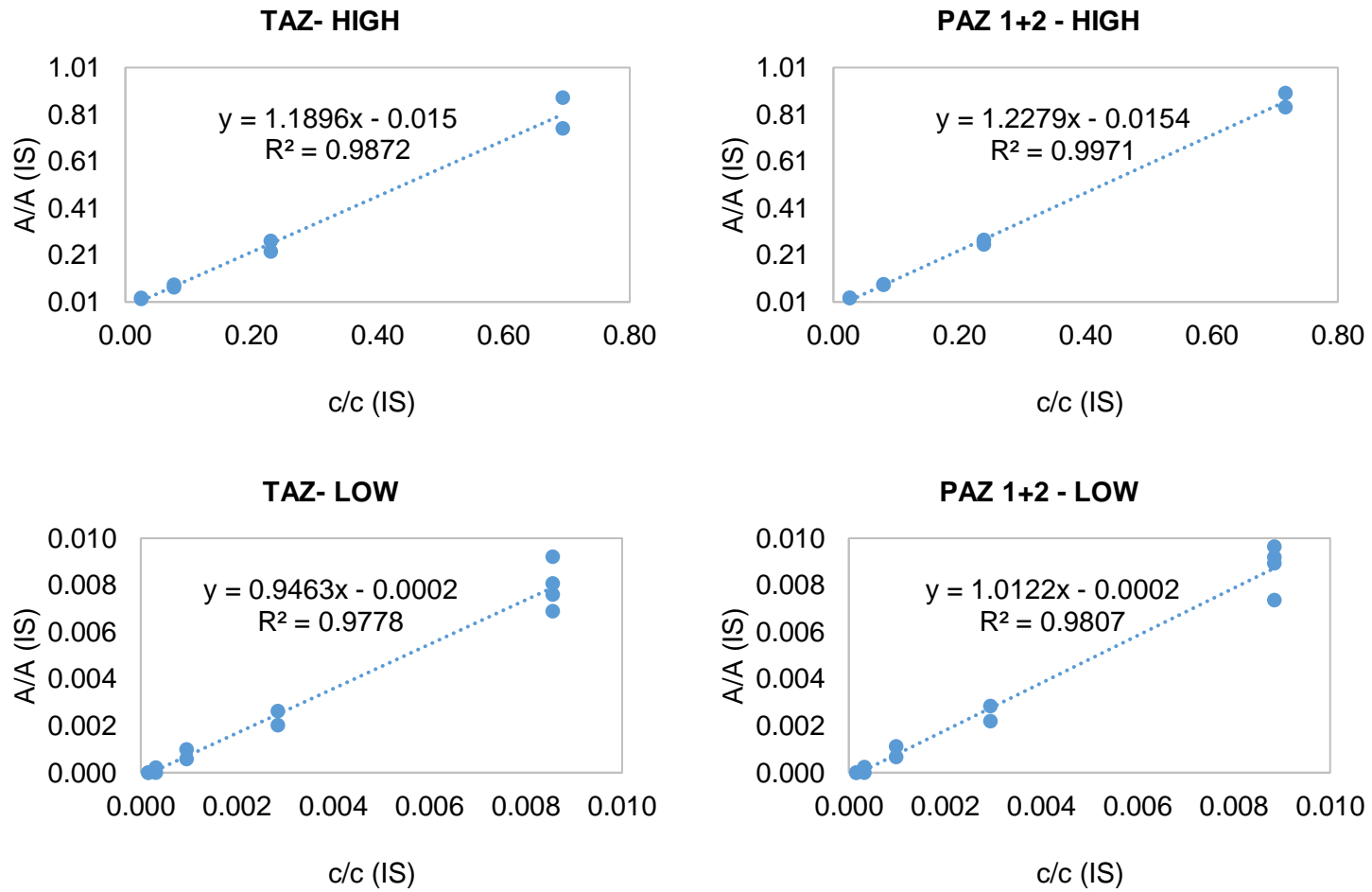


Figure B.1. 2. High and low calibration curves for TAZ and PAZ.

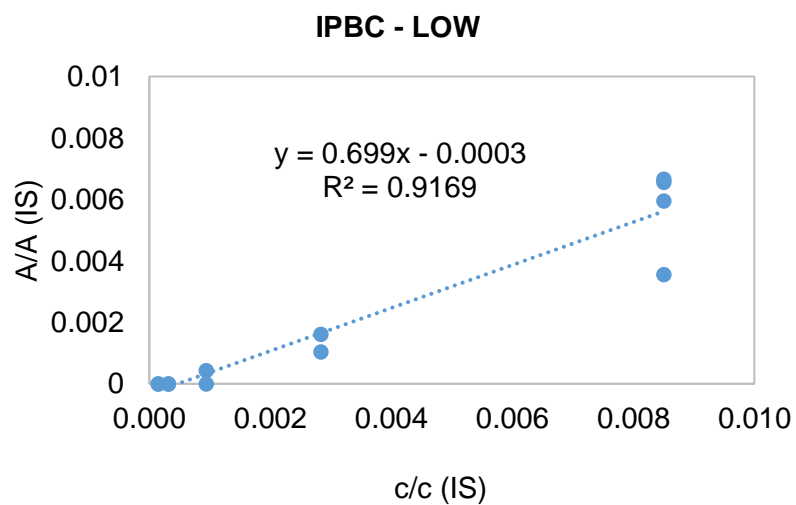
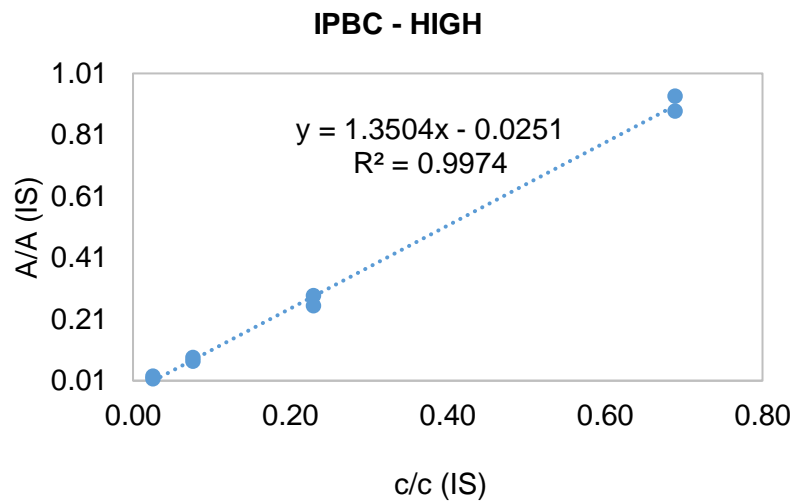


Figure B.1. 3. High and low calibration curves for IPBC.

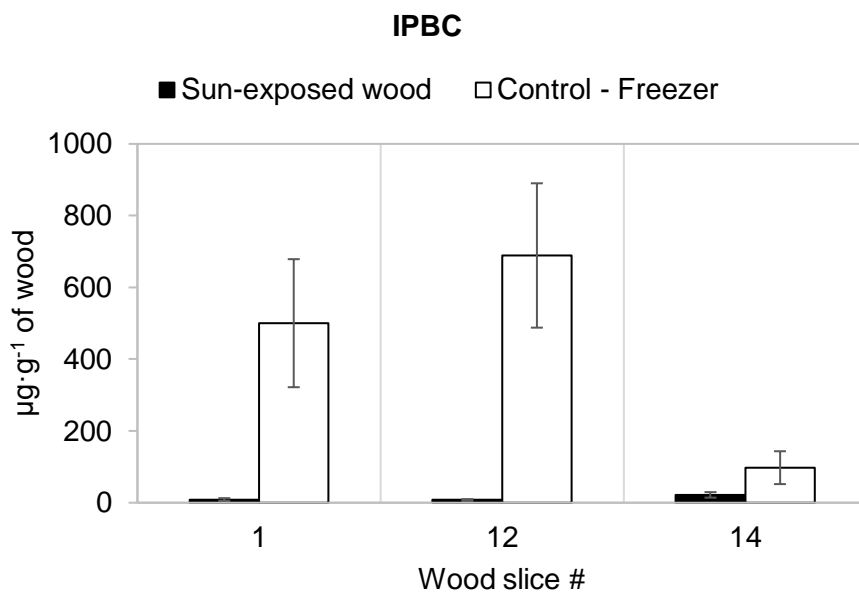


Figure B.1. 4. Comparison of the unbound IPBC amounts recovered in selected wood slices from sun-exposed and control wood. The IPBC amounts were quantified in extracts from first and second sonication using GC-MS.

APPENDIX B.2

LC-MS quantification of TAZ, PAZ, and IPBC in wood leachate

TAZ, PAZ, and IPBC were identified based on their retention times and $[M+H]^+$ ion (e.g., 308.156 for TAZ, 342.081 for PAZ, and 282.006 for IPBC). The IS method was used to quantify the analytes with HAZ added to each sample resulting in ~20 ppm IS concentration.

Calibration consisted of seven calibration standards containing TAZ, PAZ, and IPBC in the concentration range of 0.02–100 ppm ran at the beginning and the end of a sequence (Figure B.2. 1). A mid-concentration standard was run repeatedly throughout the analysis to assure the repeatability of results. To plot calibration curves, only standards in the concentration range of 0.02–7 ppm were used (Figure B.2. 2 and Figure B.2. 3) as the analyte response in the wood leachate samples fell in this range.

Instrumental LODs and LOQs (Table B.2. 1) were calculated from the calibration curves generated using a least square linear regression. The following equations were used: $LOD = 3*s_y/k$ and $LOQ = 10*s_y/k$, where s_y is a standard error of the predicted y value for each x-value and k is a slope of a calibration curve. For the LOD calculations, only the points within one order of magnitude of the LOD were used.

Table B.2. 1. LC-MS LOD and LOQ values for TAZ, PAZ, and IPBC calculated from calibration curves.

	TAZ		PAZ		IPBC	
	A/A (IS)	Conc [ppm]	A/A (IS)	Conc [ppm]	A/A (IS)	Conc [ppm]
LOD	0.01	0.05	0.01	0.05	0.01	0.53
LOQ	0.03	0.17	0.03	0.18	0.03	1.75

An example LC-MS chromatogram is shown in Figure B.2. 4 containing extracted molecular ions for TAZ, PAZ, and IPBC. However, IPBC was not found in any leachate sample. Table B.2. 2 summarizes the results of the analysis with respect to concentrations of TAZ and PAZ in each bin. Lastly, the experimental setup is illustrated in Figure B.2. 5.

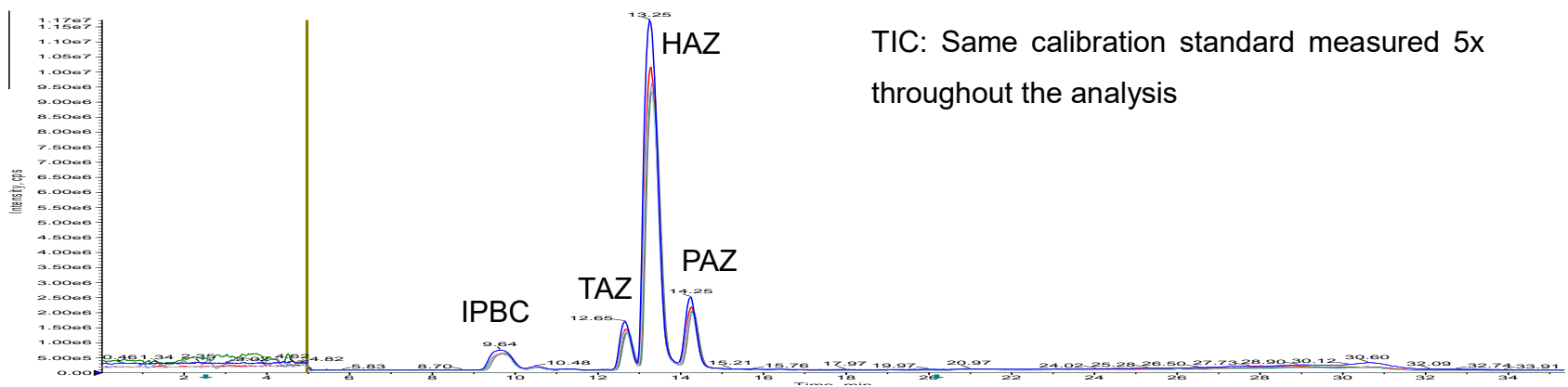
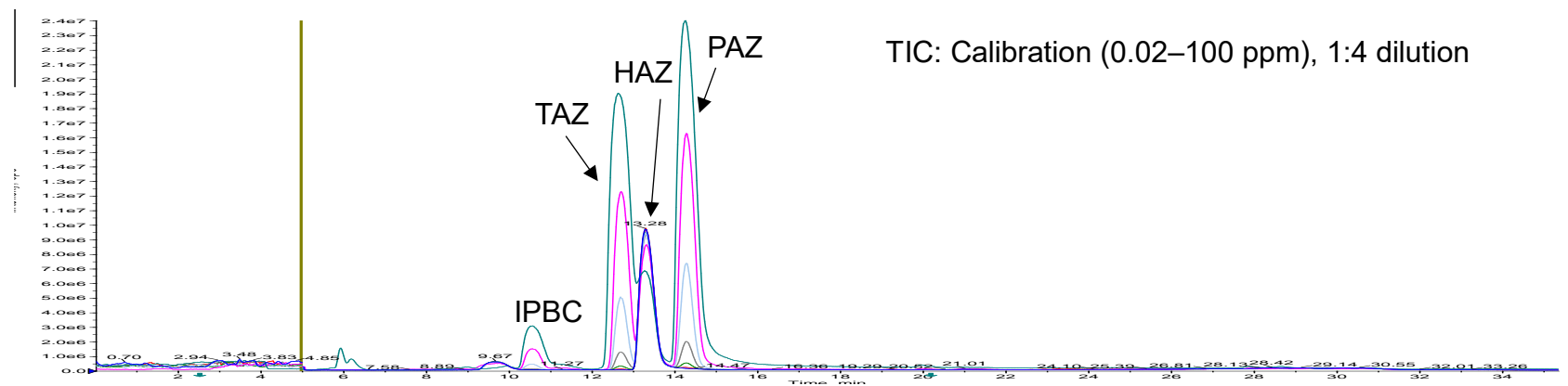


Figure B.2. 1. LC-MS calibration of fungicides in the full concentration range (0.02–100 ppm) accompanied by overlaid chromatograms of the same calibration standard ran five times throughout the analysis demonstrating good repeatability.

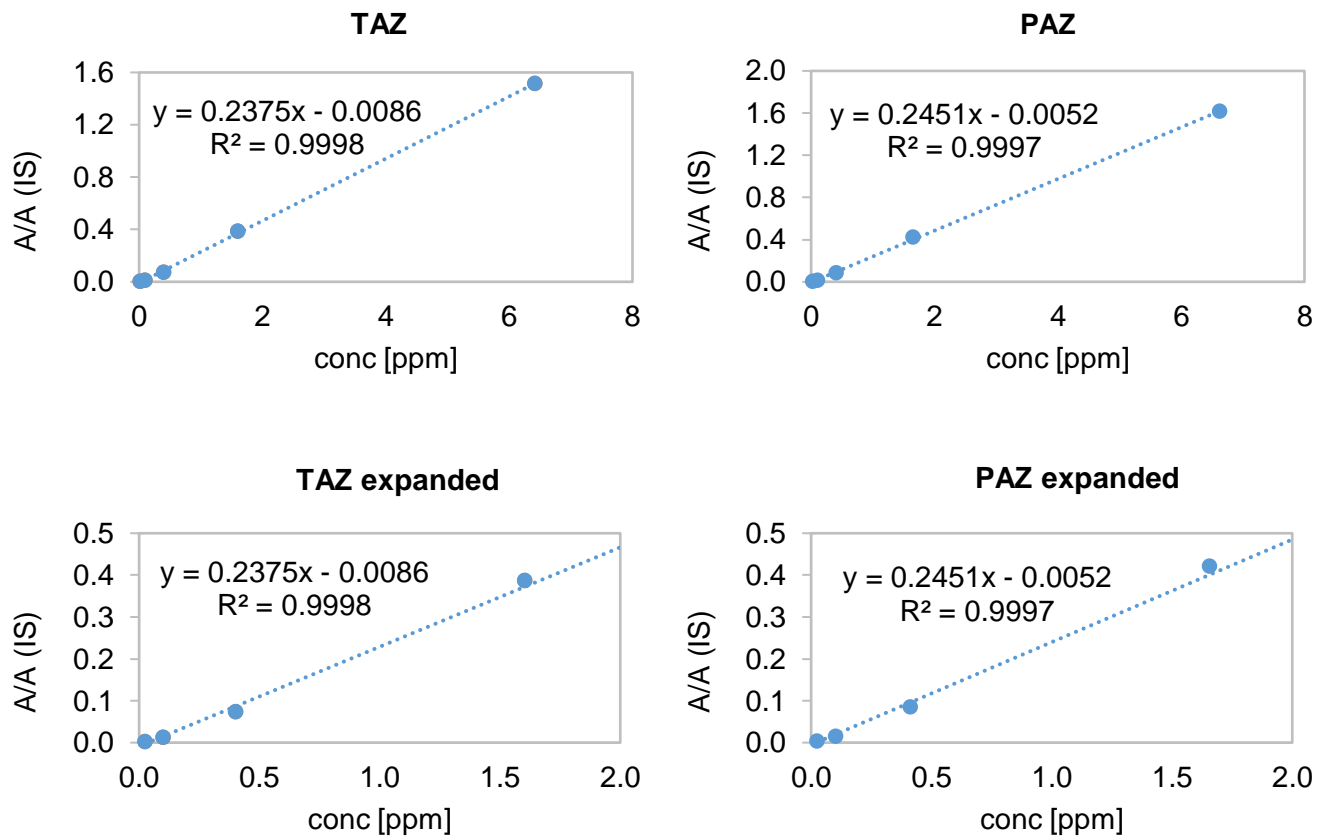


Figure B.2. 2. TAZ and PAZ LC-MS calibration curves plotted using standards in the concentration range of 0.02–7 ppm. The full calibration curve is displayed on the top and an expanded view is located below demonstrating the fit of low ppm standards.

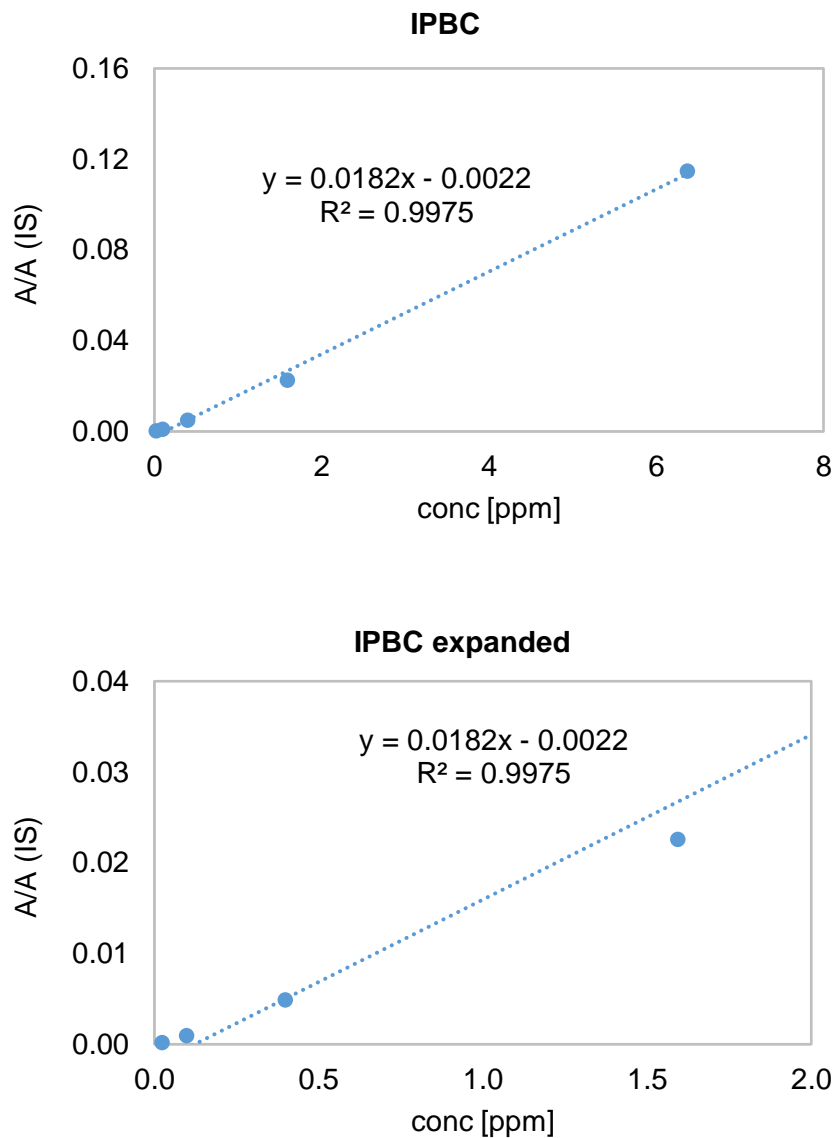


Figure B.2. 3. IPBC LC-MS calibration curve plotted using standards in the concentration range of 0.02–7 ppm. The full calibration curve is displayed on the top and an expanded view is located below demonstrating the fit of low ppm standards.

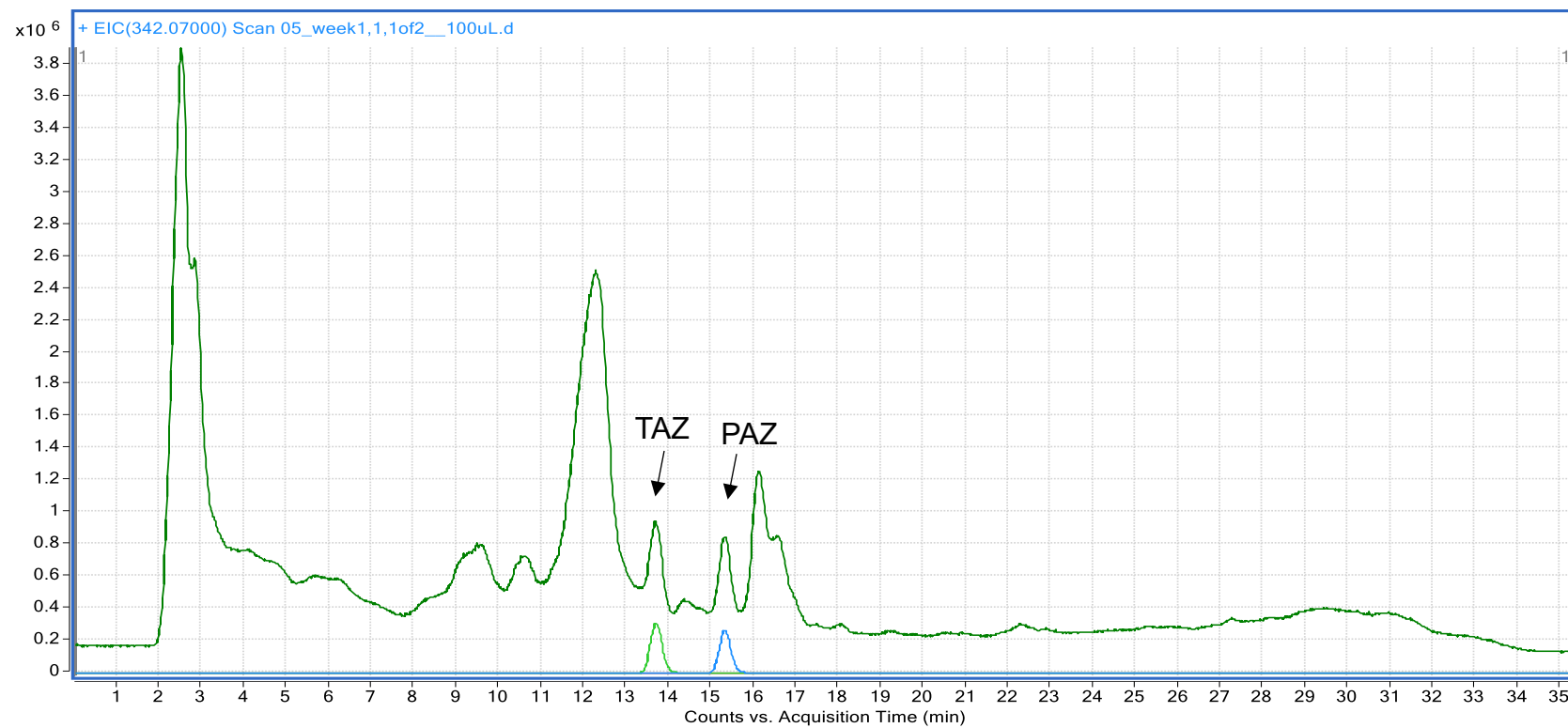


Figure B.2. 4. TIC chromatogram of Week 1, Bin 2 sample (dark green) with extracted molecular ions corresponding to TAZ (light green) and PAZ (blue). IPBC was not found in any of the wood leachate samples.

Table B.2. 2. TAZ and PAZ concentrations in wood leachate. The experimental setup is shown in Figure B.2. 5.

Bin #	TAZ [mg·L ⁻¹]				PAZ [mg·L ⁻¹]			
	Week 1	Week 2	Week 3	Week 4	Week 1	Week 2	Week 3	Week 4
1	1.06 ± 0.05	0.72 ± 0.02	0.47 ± 0.04	0.29 ± 0.02	0.88 ± 0.04	0.58 ± 0.01	0.40 ± 0.03	0.26 ± 0.01
2	1.21 ± 0.06	0.87 ± 0.03	0.58 ± 0.05	0.41 ± 0.01	0.95 ± 0.04	0.70 ± 0.04	0.50 ± 0.04	0.37 ± 0.00
3	1.16 ± 0.11	0.75 ± 0.03	0.52 ± 0.06	0.38 ± 0.03	0.93 ± 0.11	0.62 ± 0.03	0.44 ± 0.04	0.33 ± 0.02
4	N/A	N/A	N/A	N/A	N/A	N/A	N/A	N/A
5	N/A	N/A	N/A	N/A	N/A	N/A	N/A	N/A

*Bins 1, 2, and 3 contained each 10 wood sections (5 painted and 5 unpainted) dipped into Woodlife 111 for 15 seconds

*Bin 4 contained 10 untreated control sections (5 painted and 5 unpainted)

*Bin 5 was DI water that was collected from the tap, but was not irrigated

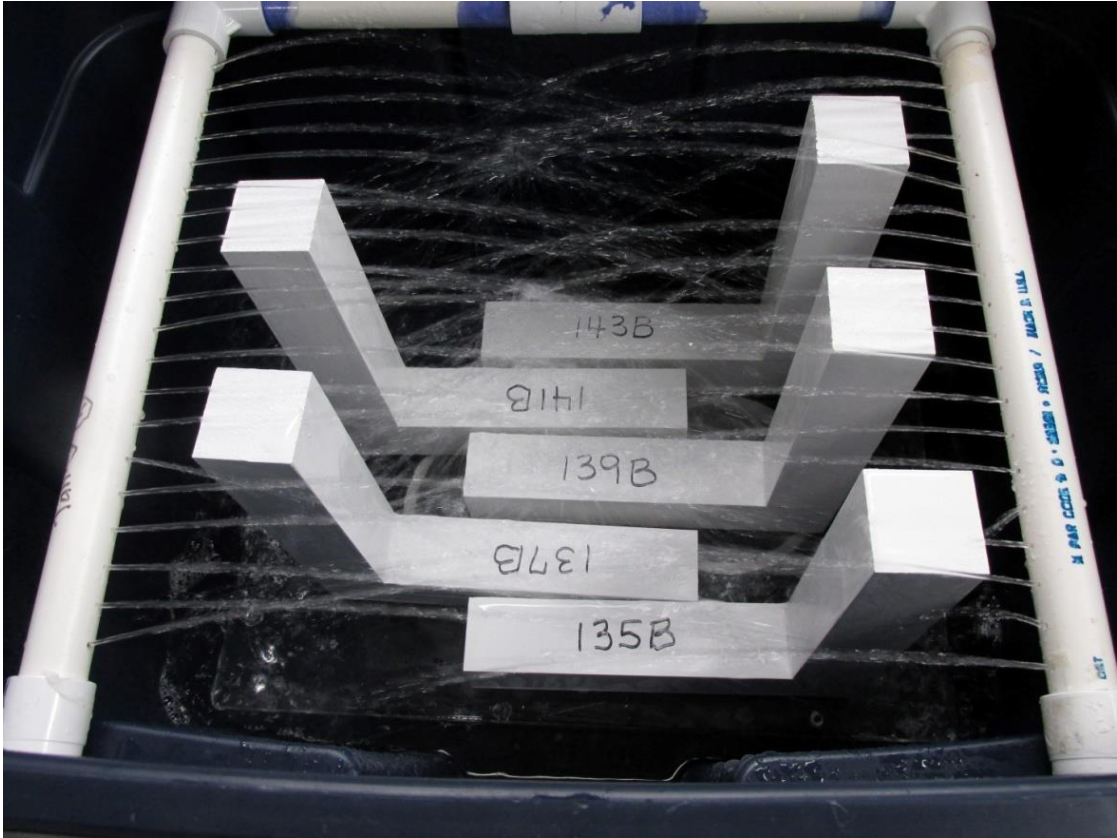


Figure B.2. 5. Assembled wood sections placed on a raised platform in Rubbermaid roughneck totes (18-gallon volume) under a flowing, recirculating water irrigation system. The sections were laid horizontally on the platform and water was sprayed in a 90° angle (exposing the radial and tangential wood surface).

APPENDIX C



Figure C. 1. Ponderosa pine wood samples ($5.0 \times 2.5 \times 1.5 \text{ cm}^3$) dipped in the radiolabeled Woodlife solution and placed on wooden skewers to dry for 24 hours.

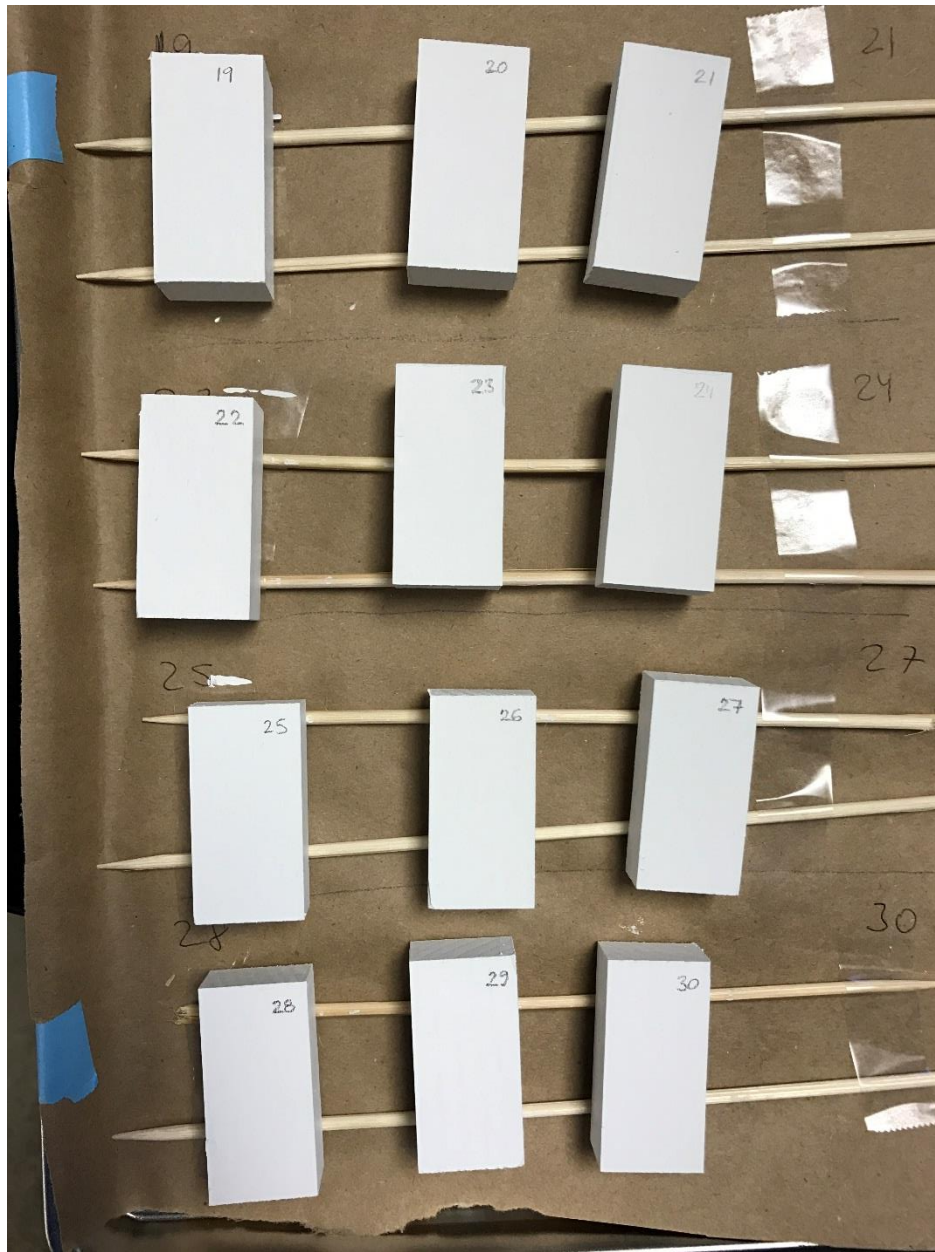
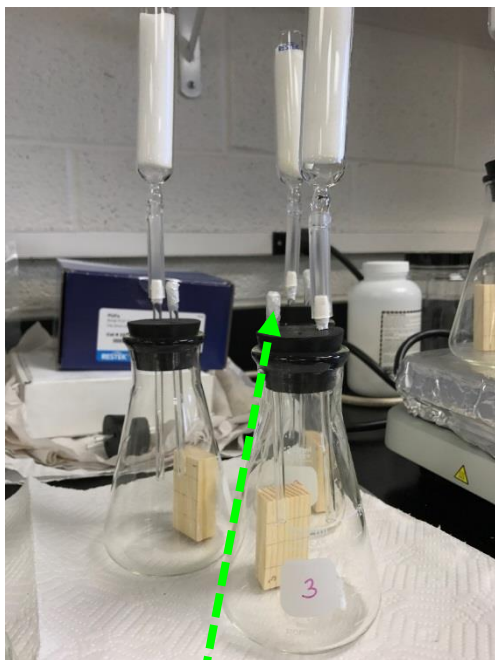


Figure C. 2. Drying of primed and painted ponderosa pine wood samples.

Low humidity (20 °C, 15% R.H.)



Closed system,
weekly purged with air

High humidity (20 °C, 80% R.H.)



Glass beads to
reduce void volume



Saturated $(\text{NH}_4)_2\text{SO}_4$ - maintains 80% RH

Figure C. 3. Experimental setup of wood exposure to low and high humidity.

Dripping DI water (~100 mL per day)



Leachate collection

Figure C. 4. Experimental setup of wood exposure to continuous and intermittent rain.

APPENDIX D

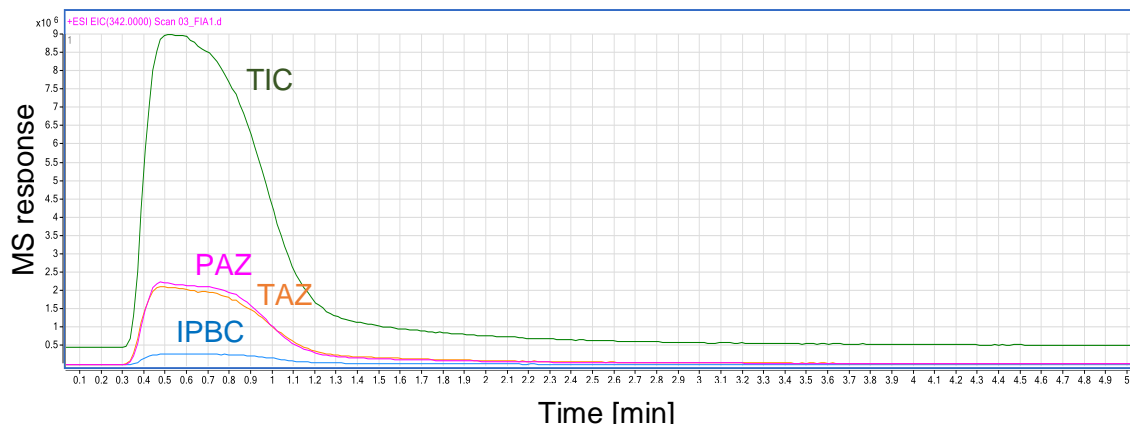


Figure D. 1. FIA LC-ESI-MS chromatogram illustrating the TIC and EIC for TAZ, PAZ, and IPBC. The TIC is shown as a green line, while the EIC for fungicide molecular ions are shown in orange (TAZ), magenta (PAZ), and blue (IPBC).

Table D. 1. Response surface experimental design.

RunOrder	PtType	Blocks	Electrolyte [mM]	Capillary [V]	Fragmentor [V]
1	1	1	2.5	4500	125
2	1	1	5	4500	125
3	1	1	2.5	5000	125
4	1	1	5	5000	125
5	1	1	2.5	4500	150
6	1	1	5	4500	150
7	1	1	2.5	5000	150
8	1	1	5	5000	150
9	-1	1	1.6	4750	138
10	-1	1	5.9	4750	138
11	-1	1	3.8	4330	138
12	-1	1	3.8	5170	138
13	-1	1	3.8	4750	116
14	-1	1	3.8	4750	159
15	0	1	3.8	4750	138
16	0	1	3.8	4750	138
17	0	1	3.8	4750	138
18	0	1	3.8	4750	138
19	0	1	3.8	4750	138
20	0	1	3.8	4750	138

Table D. 2. DOE response surface design including integrated peak areas of TAZ, PAZ, and IPBC molecular ions.

Electrolyte [mM]	Capillary [V]	Fragmentor [V]	TAZ	PAZ	IPBC
2.5	4500	125	60685236	64279358	9574610
5	4500	125	53310556	54051661	7583547
2.5	5000	125	55741766	58878522	9403341
5	5000	125	48656155	50572548	7361554
2.5	4500	150	51143986	58010858	5744568
5	4500	150	49948586	55140082	5098184
2.5	5000	150	52658896	59300962	6413595
5	5000	150	46266219	51229606	5182647
1.6	4750	138	47987757	59023869	8186163
5.9	4750	138	44856097	45053605	6909178
3.8	4330	138	49043499	52975152	7546801
3.8	5170	138	48445572	51991648	8392666
3.8	4750	116	43742193	43032159	8435766
3.8	4750	159	46681498	51401984	4204216
3.8	4750	138	47728432	51379320	7871391
3.8	4750	138	47181661	50436022	8005784
3.8	4750	138	46714946	50271194	7725021
3.8	4750	138	46336975	49892126	7754212
3.8	4750	138	45215185	48712146	7680432
3.8	4750	138	45355250	48653465	7630754

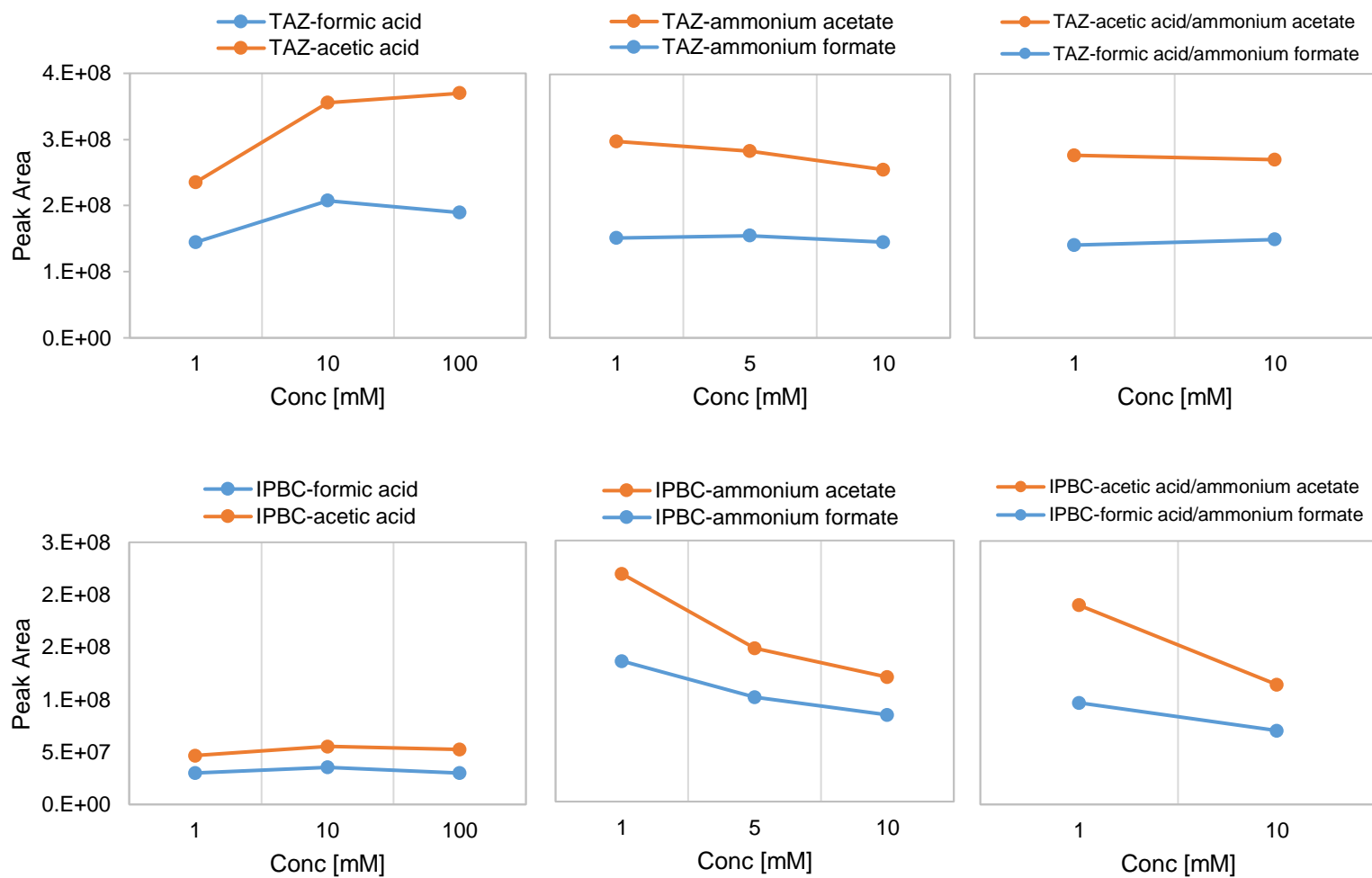


Figure D. 2. Impact of electrolyte type and its concentration in MeOH-water system (50:50) on TAZ and IPBC MS response.

Response Surface Regression: TAZ versus Electrolyte, Capillary [V, ...

The analysis was done using coded units.

Term	Coef	SE Coef	T	P
Constant	46244933	1604415	28.824	0.000
Electrolyte [mM]	-3363766	1790257	-1.879	0.090
Capillary [V]	-1572693	1790257	-0.878	0.400
Fragmentor [V]	-1654192	1790257	-0.924	0.377
Electrolyte [mM]*Electrolyte [mM]	3274361	2930972	1.117	0.290
Capillary [V]*Capillary [V]	5596970	2930972	1.910	0.085
Fragmentor [V]*Fragmentor [V]	2064280	2930972	0.704	0.497
Electrolyte [mM]*Capillary [V]	-1735314	3933853	-0.441	0.669
Electrolyte [mM]*Fragmentor [V]	2429695	3933853	0.618	0.551
Capillary [V]*Fragmentor [V]	2627048	3933853	0.668	0.519

S = 3933853 PRESS = 1.146115E+15
R-Sq = 52.11% R-Sq(pred) = 0.00% R-Sq(adj) = 9.01%

Source	Adj MS	F	P
Regression	1.87120E+13	1.21	0.383
Linear	2.65960E+13	1.72	0.226
Electrolyte [mM]	5.46333E+13	3.53	0.090
Capillary [V]	1.19425E+13	0.77	0.400
Fragmentor [V]	1.32123E+13	0.85	0.377
Square	2.42679E+13	1.57	0.258
Electrolyte [mM]*Electrolyte [mM]	1.93137E+13	1.25	0.290
Capillary [V]*Capillary [V]	5.64311E+13	3.65	0.085
Fragmentor [V]*Fragmentor [V]	7.67626E+12	0.50	0.497
Interaction	5.27204E+12	0.34	0.797
Electrolyte [mM]*Capillary [V]	3.01131E+12	0.19	0.669
Electrolyte [mM]*Fragmentor [V]	5.90342E+12	0.38	0.551
Capillary [V]*Fragmentor [V]	6.90138E+12	0.45	0.519
Residual Error	1.54752E+13		
Lack-of-Fit	2.99562E+13	30.13	0.001
Pure Error	9.94251E+11		
Total			

Estimated Regression Coefficients for TAZ using data in uncoded units

Term	Coef
Constant	1081414140
Electrolyte [mM]	-5390701
Capillary [V]	-338027
Fragmentor [V]	-2981138
Electrolyte [mM]*Electrolyte [mM]	740903
Capillary [V]*Capillary [V]	31.6612
Fragmentor [V]*Fragmentor [V]	4670.93
Electrolyte [mM]*Capillary [V]	-1963.28
Electrolyte [mM]*Fragmentor [V]	54977.7
Capillary [V]*Fragmentor [V]	297.217

Figure D. 3. Data analysis of TAZ MS response using Minitab.

Response Surface Regression: PAZ versus Electrolyte, Capillary [V, ...

The analysis was done using coded units.

Term	Coef	SE Coef	T	P
Constant	49703069	1604122	30.985	0.000
Electrolyte [mM]	-6523176	1789929	-3.644	0.005
Capillary [V]	-1619914	1789929	-0.905	0.387
Fragmentor [V]	1228476	1789929	0.686	0.508
Electrolyte [mM]*Electrolyte [mM]	5616663	2930436	1.917	0.084
Capillary [V]*Capillary [V]	6061326	2930436	2.068	0.065
Fragmentor [V]*Fragmentor [V]	794998	2930436	0.271	0.792
Electrolyte [mM]*Capillary [V]	-1159251	3933133	-0.295	0.774
Electrolyte [mM]*Fragmentor [V]	2684014	3933133	0.682	0.510
Capillary [V]*Fragmentor [V]	2213095	3933133	0.563	0.586

S = 3933133 PRESS = 1.145416E+15
R-Sq = 69.40% R-Sq(pred) = 0.00% R-Sq(adj) = 41.87%

Source	Adj MS	F	P
Regression	3.89913E+13	2.52	0.083
Linear	7.51385E+13	4.86	0.025
Electrolyte [mM]	2.05458E+14	13.28	0.005
Capillary [V]	1.26704E+13	0.82	0.387
Fragmentor [V]	7.28683E+12	0.47	0.508
Square	3.73535E+13	2.41	0.127
Electrolyte [mM]*Electrolyte [mM]	5.68290E+13	3.67	0.084
Capillary [V]*Capillary [V]	6.61833E+13	4.28	0.065
Fragmentor [V]*Fragmentor [V]	1.13853E+12	0.07	0.792
Interaction	4.48186E+12	0.29	0.832
Electrolyte [mM]*Capillary [V]	1.34386E+12	0.09	0.774
Electrolyte [mM]*Fragmentor [V]	7.20393E+12	0.47	0.510
Capillary [V]*Fragmentor [V]	4.89779E+12	0.32	0.586
Residual Error	1.54695E+13		
Lack-of-Fit	2.98235E+13	26.73	0.001
Pure Error	1.11558E+12		
Total			

Estimated Regression Coefficients for PAZ using data in uncoded units

Term	Coef
Constant	1068595750
Electrolyte [mM]	-14755622
Capillary [V]	-359099
Fragmentor [V]	-1853320
Electrolyte [mM]*Electrolyte [mM]	1270906
Capillary [V]*Capillary [V]	34.2880
Fragmentor [V]*Fragmentor [V]	1798.87
Electrolyte [mM]*Capillary [V]	-1311.54
Electrolyte [mM]*Fragmentor [V]	60732.3
Capillary [V]*Fragmentor [V]	250.383

Figure D. 4. Data analysis of PAZ MS response using Minitab.

Response Surface Regression: IPBC versus Electrolyte, Capillary [V, ...

The analysis was done using coded units.

Term	Coef	SE Coef	T	P
Constant	7784507	124789	62.381	0.000
Electrolyte [mM]	-992290	139244	-7.126	0.000
Capillary [V]	219545	139244	1.577	0.146
Fragmentor [V]	-2290603	139244	-16.450	0.000
Electrolyte [mM]*Electrolyte [mM]	-351795	227967	-1.543	0.154
Capillary [V]*Capillary [V]	70268	227967	0.308	0.764
Fragmentor [V]*Fragmentor [V]	-1579474	227967	-6.929	0.000
Electrolyte [mM]*Capillary [V]	-224608	305970	-0.734	0.480
Electrolyte [mM]*Fragmentor [V]	762091	305970	2.491	0.032
Capillary [V]*Fragmentor [V]	405438	305970	1.325	0.215

S = 305970 PRESS = 6.575254E+12

R-Sq = 97.45% R-Sq(pred) = 82.10% R-Sq(adj) = 95.16%

Source	Adj MS	F	P
Regression	3.97664E+12	42.48	0.000
Linear	1.01070E+13	107.96	0.000
Electrolyte [mM]	4.75426E+12	50.78	0.000
Capillary [V]	2.32731E+11	2.49	0.146
Fragmentor [V]	2.53341E+13	270.61	0.000
Square	1.55768E+12	16.64	0.000
Electrolyte [mM]*Electrolyte [mM]	2.22942E+11	2.38	0.154
Capillary [V]*Capillary [V]	8894676569	0.10	0.764
Fragmentor [V]*Fragmentor [V]	4.49405E+12	48.00	0.000
Interaction	2.65204E+11	2.83	0.092
Electrolyte [mM]*Capillary [V]	50448855368	0.54	0.480
Electrolyte [mM]*Fragmentor [V]	5.80782E+11	6.20	0.032
Capillary [V]*Fragmentor [V]	1.64380E+11	1.76	0.215
Residual Error	93617346868		
Lack-of-Fit	1.68198E+11	8.84	0.016
Pure Error	19036200323		
Total			

Estimated Regression Coefficients for IPBC using data in uncoded units

Term	Coef
Constant	-3340481
Electrolyte [mM]	-1039022
Capillary [V]	-8608.25
Fragmentor [V]	591326
Electrolyte [mM]*Electrolyte [mM]	-79602.1
Capillary [V]*Capillary [V]	0.397497
Fragmentor [V]*Fragmentor [V]	-3573.94
Electrolyte [mM]*Capillary [V]	-254.115
Electrolyte [mM]*Fragmentor [V]	17244.1
Capillary [V]*Fragmentor [V]	45.8701

Figure D. 5. Data analysis of IPBC MS response using Minitab.

Response Optimization

Parameters

	Goal	Lower	Target	Upper	Weight	Import
TAZ	Maximum	45000000	61000000	61000000	1	1
PAZ	Maximum	45000000	65000000	65000000	1	1
IPBC	Maximum	4500000	9600000	9600000	1	1

Global Solution

Electrolyte = 1.64776
Capillary [V = 4329.55
Fragmentor [= 116.478

Predicted Responses

TAZ = 67092623 , desirability = 1.000000
PAZ = 72828529 , desirability = 1.000000
IPBC = 9929775 , desirability = 1.000000

Composite Desirability = 1.000000

Figure D. 6. Results from Minitab response optimizer.

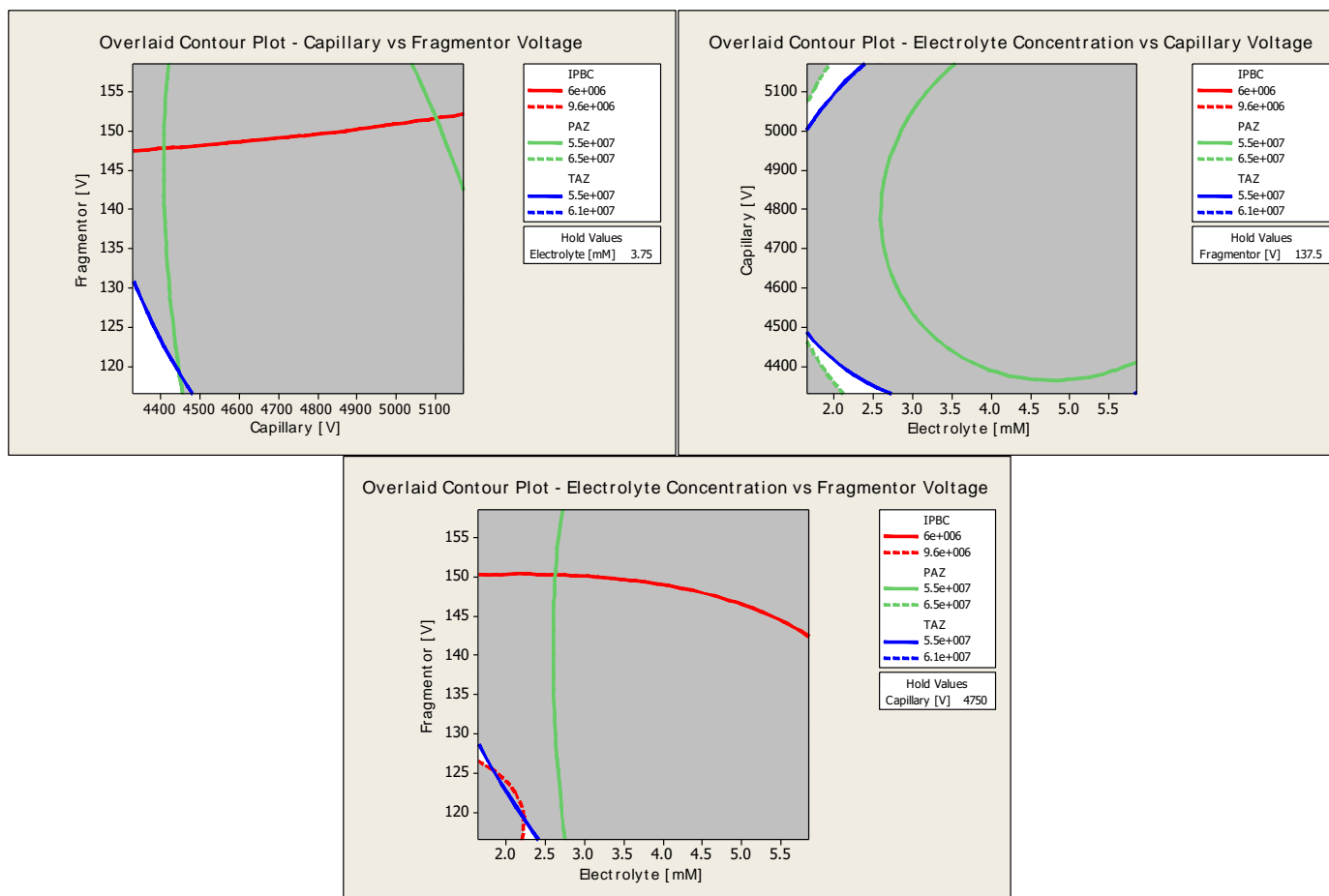


Figure D. 7. Overlaid contour plots for fungicide ESI-MS response. The factors included electrolyte concentrations, capillary voltage and fragmentor voltage. The optimal working range yielding the highest fungicide MS responses is colored white.

REFERENCES

1. Sathre, R.; González-García, S. Chapter 14 - Life Cycle Assessment (LCA) of Wood-Based Building Materials. In *Eco-Efficient Construction and Building Materials*; Woodhead Publishing: Cambridge, 2014; pp 311–337.
2. Waldron, L.; Cooper, P. A. Modeling of Simultaneous Three-Dimensional Leaching and Chemical Reaction of CCA Components in Unfixed Wood Exposed to Water. *Wood Sci. Technol.* **2010**, *44* (1), 129–147.
3. Mercer, T. G.; Frostick, L. E. Leaching Characteristics of CCA-Treated Wood Waste: A UK Study. *Sci. Total Environ.* **2012**, *427–428*, 165–174.
4. Dubey, B.; Townsend, T.; Solo-Gabriele, H. Metal Loss from Treated Wood Products in Contact with Municipal Solid Waste Landfill Leachate. *J. Hazard. Mater.* **2010**, *175* (1–3), 558–568.
5. Tame, N. W.; Dlugogorski, B. Z.; Kennedy, E. M. Formation of Dioxins and Furans during Combustion of Treated Wood. *Prog. Energy Combust. Sci.* **2007**, *33* (4), 384–408.
6. Katz, S. A.; Salem, H. Chemistry and Toxicology of Building Timbers Pressure-Treated with Chromated Copper Arsenate: A Review. *J. Appl. Toxicol.* **2005**, *25* (1), 1–7.

7. Schmidt-Sonnenschein, B. The European Biocidal Products Directive. In *Directory of Microbicides for the Protection of Materials: A Handbook*; Paulus, W., Ed. Springer Netherlands: Dordrecht, 2005; pp 65–78.
8. Reinprecht, L. Fungicides for Wood Protection - World Viewpoint and Evaluation/Testing in Slovakia. In *Fungicides*; Carisse, O., Ed. InTech: 2010; pp 95–122.
9. Christen, V.; Crettaz, P.; Fent, K. Additive and Synergistic Antiandrogenic Activities of Mixtures of Azol Fungicides and Vinclozolin. *Toxicol. Appl. Pharmacol.* **2014**, 279 (3), 455–466.
10. Bauschhaus, H. U.; Valcke, A. R. *Triazoles: Synergism between Propiconazole and Tebuconazole*; IRG/WP 95-30092; International Research Group on Wood Protection: Helsingør, Denmark, 1995.
11. Bruns, R.; Kaulen, J.; Kretschik, O.; Kugler, M.; Uhr, H. R&D in Material Protection: New Biocides. In *Directory of Microbicides for the Protection of Materials*; Paulus, W., Ed. Springer Netherlands: Dordrecht, 2005; pp 25–46.
12. Valcke, A. R. *Suitability of Propiconazole (R 49362) as a New-Generation Fungicide*; IRG/WP 3529; International Research Group on Wood Protection: Lappeenranta, Finland 1989.
13. Gründlinger, R.; Exner, O. *Tebuconazole - A New Triazole Fungicide for Wood Preservation*; IRG/WP 3629; International Research Group on Wood Protection: Rotorua, New Zealand, 1990.

14. Wüstenhöfer, B.; Wegen, H. W.; Metzner, W. *Tebuconazole, a New Wood-Preserving Fungicide*; IRG/WP/3634; International Research Group on Wood Protection: Rotorua, New Zealand, 1990.
15. Barnes, H. M. Wood: Preservative Treated. In *Encyclopedia of Materials: Science and Technology*; Elsevier: Oxford, 2001; pp 9683–9688.
16. Schiopu, N.; Tiruta-Barna, L. Wood Preservatives. In *Toxicity of Building Materials*; Woodhead Publishing: Cambridge, 2012; pp 138–165.
17. Morrell, J. J. 14 - Protection of Wood-Based Materials. In *Handbook of Environmental Degradation of Materials*; William Andrew Publishing: Oxford, 2012; pp 407–439.
18. FrontResearch. *Tebuconazole Global Market and Forecast Research*; FR-9500210; 2016; p 65.
19. Fotsing, J. A. M.; Tchagang, C. W. Experimental Determination of the Diffusion Coefficients of Wood in Isothermal Conditions. *Heat Mass Transf.* **2005**, *41* (11), 977–980.
20. Lubomír Lapčík, J.; Lapčík, L.; Kubiček, P.; Lapčíková, B.; Zbořil, R.; Nevěčná, T. Study of Penetration Kinetics of Sodium Hydroxide Aqueous Solution into Wood Samples. *BioResources* **2014**, *9* (1), 881–893.
21. Sedighi-Gilani, M.; Vontobel, P.; Lehmann, E.; Carmeliet, J.; Derome, D. Liquid Uptake in Scots Pine Sapwood and Hardwood Visualized and Quantified by Neutron Radiography. *Mater. Struct.* **2014**, *47* (6), 1083–1096.

22. Nsouandélé, J. L.; Bonoma, B.; Simo Tagne, M.; Njomo, D. Determination of the Diffusion Coefficient of Water in the Tropical Woods. *Physic. Chem. News* **2010**, *54*, 61–67.
23. Sonderegger, W.; Hering, S.; Mannes, D.; Vontobel, P.; Lehmann, E.; Niemz, P. Quantitative Determination of Bound Water Diffusion in Multilayer Boards by Means of Neutron Imaging. *Eur. J. Wood Wood Prod.* **2010**, *68* (3), 341–350.
24. Mannes, D.; Sonderegger, W.; Hering, S.; Lehmann, E.; Niemz, P. Non-Destructive Determination and Quantification of Diffusion Processes in Wood by Means of Neutron Imaging. *Holzforschung* **2009**, *63* (5), 589–596.
25. Sedighi Gilani, M.; Vontobel, P.; Lehmann, E.; Carmeliet, J.; Derome, D. Moisture Migration in Wood under Heating Measured by Thermal Neutron Radiography. *Exp. Heat Transfer* **2014**, *27* (2), 160–179.
26. Han, Y.; Park, J. H.; Chang, Y. S.; Eom, C. D.; Lee, J. J.; Yeo, H. Classification of the Conductance of Moisture through Wood Cell Components. *J. Wood Sci.* **2013**, *59* (6), 469–476.
27. De Meijer, M.; Militz, H. Moisture Transport in Coated Wood. Part 2: Influence of Coating Type, Film Thickness, Wood Species, Temperature and Moisture Gradient on Kinetics of Sorption and Dimensional Change. *Holz Roh - Werkst.* **2001**, *58* (6), 467–475.

28. Shi, S. Q. Diffusion Model Based on Fick's Second Law for the Moisture Absorption Process in Wood Fiber-Based Composites: Is it Suitable or Not? *Wood Sci. Technol.* **2007**, *41* (8), 645–658.
29. Acda, M. N.; Morrell, J. J.; Levien, K. L. Supercritical Fluid Impregnation of Selected Wood Species with Tebuconazole. *Wood Sci. Technol.* **2001**, *35* (1–2), 127–136.
30. Muin, M.; Tsunoda, K. Preservative Treatment of Wood-Based Composites with 3-Iodo-2-Propynyl Butylcarbamate Using Supercritical Carbon Dioxide Impregnation. *J. Wood Sci.* **2003**, *49* (5), 430–436.
31. Lucas, S.; González, E.; Calvo, M. P.; Palencia, C.; Alonso, E.; Cocero, M. J. Supercritical CO₂ Impregnation of Radiata Pine with Organic Fungicides. Effect of Operating Conditions and Two-Parameters Modeling. *J. Supercrit. Fluids* **2007**, *40* (3), 462–469.
32. Sedighi Moghaddam, M.; Claesson, P. M.; Wålinder, M. E. P.; Swerin, A. Wettability and Liquid Sorption of Wood Investigated by Wilhelmy Plate Method. *Wood Sci. Technol.* **2013**, *48* (1), 161–176.
33. Popova, I. E.; Beklemishev, M. K.; Frihart, C. R.; Seames, W. S.; Sundstrom, T. J.; Kozliak, E. I. Penetration of Naphthalene, n-Hexadecane, and 2,4-Dinitrotoluene into Southern Yellow Pine under Conditions Modeling Spills and Floods. *Forest Prod. J.* **2006**, *56* (6), 68–75.

34. Haloui, A.; Kouali, E.; Bouzon, J.; Vergnaud, J. M. Process of Absorption and Desorption of Methanol with a 3-Dimensional Transport through Picea Wood. *Wood Sci. Technol.* **1994**, 28 (3), 173–184.
35. Siau, J. F. Wood Structure and Chemical Composition. In: *Transport Processes in Wood*; Springer Verlag: Heidelberg, 1984, pp. 35–72.
36. Siau, J.F. *Wood: Influence of Moisture on Physical Properties*; Department of Wood Science and Forest Products: Virginia Polytechnic Institute and State University: Blacksburg, VA, 1995, pp.227.
37. Comstock, G. L. Directional Permeability of Softwoods. *Wood Fiber* **1970**, 1 (4), 283–289.
38. Volkmer, T.; Landmesser, H.; Genoud, A.; Schwarze, F. W. M. R. Penetration of 3-Iodo-2-Propynyl Butylcarbamate (IPBC) in Coniferous Wood Pre-Treated with *Physisporinus Vitreus*. *J. Coat. Technol. Res.* **2010**, 7 (6), 721–26.
39. Ahmed, S. A.; Hansson, L.; Morén, T. Distribution of Preservatives in Thermally Modified Scots Pine and Norway Spruce Sapwood. *Wood Sci. Technol.* **2012**, 47 (3), 499–513.
40. Goodell, B.; Nicholas, D. D.; Schultz, T. P. Introduction to Wood Deterioration and Preservation. In *Wood Deterioration and Preservation*; American Chemical Society: 2003; Vol. 845, pp 2–7.
41. Vasishth, P.; Nicholas, D. D.; Henry, W. P.; Schultz, T. P. Effect of Polyvinyl Alcohol on Copper Leaching from Treated Wood. *Forest Prod. J.* **2009**, 59 (10), 28–30.

42. Moghaddam, A. H.; Mulligan, C. N. Leaching of Heavy Metals from Chromated Copper Arsenate (CCA) Treated Wood after Disposal. *Waste Manag.* **2008**, *28* (3), 628–637.
43. Lupsea, M. O.; Mathies, H.; Schoknecht, U.; Tiruta-Barna, L.; Schiopu, N. Leaching from New Generation Treated Wood: A Chemical Approach. *WIT Trans. Ecol. Environ.* **2012**, *162*, 529–540.
44. Lupsea, M.; Tiruta-Barna, L.; Schiopu, N.; Schoknecht, U. Modelling Inorganic and Organic Biocide Leaching from CBA-Amine (Copper-Boron-Azole) Treated Wood Based on Characterisation Leaching Tests. *Sci. Total Environ.* **2013**, *461–462*.
45. Lupsea, M.; Mathies, H.; Schoknecht, U.; Tiruta-Barna, L.; Schiopu, N. Biocide Leaching from CBA Treated Wood - A Mechanistic Interpretation. *Sci. Total Environ.* **2013**, *444*, 522–530.
46. Tiruta-Barna, L.; Schiopu, N. Modelling Inorganic Biocide Emission from Treated Wood. *J. Hazard. Mater.* **2011**, *192*, 1476–1483.
47. Schoknecht, U.; Kalbe, U.; van Zomeren, A.; Hjelmar, O. Laboratory Leaching Tests on Treated Wood According to Different Harmonised Test Procedures. *Environ. Sci. Eur.* **2014**, *26* (1).
48. Stook, K.; Tolaymat, T.; Ward, M.; Dubey, B.; Townsend, T.; Solo-Gabriele, H.; Bitton, G. Relative Leaching and Aquatic Toxicity of Pressure-Treated Wood Products Using Batch Leaching Tests. *Environ. Sci. Technol.* **2005**, *39* (1), 155–163.

49. Schultz, T. P.; Nicholas, D. D.; Preston, A. F. A Brief Review of the Past, Present and Future of Wood Preservation. *Pest Manag. Sci.* **2007**, *63* (8), 784–788.
50. Cookson, L. J. Preservative Treatments Suitable for Hardwood Window Joinery. *Int. Biodeterior. Biodegrad.* **2010**, *64* (7), 652–658.
51. Schoknecht, U.; Wegner, R.; Horn, W.; Jann, O. Emission of Biocides from Treated Materials Test Procedures for Water and Air. *Environ. Sci. Pollut. Res.* **2003**, *10* (3), 154–161.
52. Schoknecht, U.; Mathies, H.; Wegner, R.; Melcher, E.; Seidel, B.; Kussatz, C.; Maletzki, D. *The Influence of Test Parameters on the Emission of Biocides from Preservative-Treated Wood in Leaching Tests*; UFOPLAN 203(67); Report: BAM Berlin, 2004, pp.441.
53. Schoknecht, U.; Mathies, H.; Morsing, N.; Lindegaard, B.; Sloot, H. A.; Zomeren, A.; Deroubaix, G.; Legay, S.; Tadeo, J. L.; Garcia-Valcárcel, A. I.; Gigliotti, G.; Zadra, C.; Hajšlová, J.; Tomaniová, M.; Wegner, R.; Bornkessel, C.; Fürhapper, C. *Inter-Laboratory Evaluation of Laboratory Test Methods to Estimate the Leaching from Treated Wood*; European Grant Agreement no. 04/375757/C4; Report: BAM Berlin, 2005.
54. Woo, C.S.M. Efficacy of Tebuconazole and Ddac in Shell-Treated Wood [dissertation]. University of British Columbia, Vancouver, 2010, pp. 93.

55. Jaklová Dyrtrtová, J.; Fanfrlík, J.; Norková, R.; Jakl, M.; Hobza, P. Theoretical Insight into the Stabilization of Triazole Fungicides via their Interactions with Dications. *Int. J. Mass Spectrom.* **2014**, *359* (1), 38–43.
56. Dyrtrtová, J. J.; Jakl, M.; Schröder, D.; Čadková, E.; Komárek, M. Complexation between the Fungicide Tebuconazole and Copper(II) Probed by Electrospray Ionization Mass Spectrometry. *Rapid Commun. Mass Spectrom.* **2011**, *25* (8), 1037–1042.
57. Evans, P. D.; Schmalzl, K. J.; Forsyth, C. M.; Fallon, G. D.; Schmid, S.; Bendixen, B.; Heimdal, S. Formation and Structure of Metal Complexes with the Fungicides Tebuconazole and Propiconazole. *J. Wood Chem. Technol.* **2007**, *27* (3–4), 243–256.
58. Kennedy, M. J. *Depletion of Copper-Based Preservatives from Pine Decking and Impacts on Soil-Dwelling Invertebrates*. Pre-conference proceedings of the Florida Center for Environmental Solutions, Orlando, Florida, Feb. 8–11, 2004; pp 124–145.
59. Clausen, P. A.; Kofoed-Sørensen, V. Sampling and Analysis of SVOCs and POMs in Indoor Air. In *Organic Indoor Air Pollutants*; Wiley-VCH: Weinheim, 2009; pp 19–45.
60. Horn, W.; Jann, O.; Wilke, O. Suitability of Small Environmental Chambers to Test the Emission of Biocides from Treated Materials into the Air. *Atmos. Environ.* **2003**, *37* (39–40), 5477–5483.

61. Bollmann, U. E.; Tang, C.; Eriksson, E.; Jönsson, K.; Vollertsen, J.; Bester, K. Biocides in Urban Wastewater Treatment Plant Influent at Dry and Wet Weather: Concentrations, Mass Flows and Possible Sources. *Water Res.* **2014**, *60* (0), 64–74.
62. Yu, C.; Crump, D.; Brown, V. Exposure Risk Assessment of the Emissions of Wood Preservative Chemicals in Indoor Environments. *Clean Soil Air Water* **2009**, *37* (6), 466–474.
63. Obanda, D. N.; Shupe, T. F.; Catallo, W. J. Resistance of *Trichoderma Harzianum* to the Biocide Tebuconazol - Proposed Biodegradation Pathways. *Holzforschung* **2008**, *62* (5), 613–619.
64. Obanda, D. N.; Shupe, T. F. Biotransformation of Tebuconazole by Microorganisms: Evidence of a Common Mechanism. *Wood Fiber Sci.* **2009**, *41* (2), 157–167.
65. Obanda, D. N. Biotransformation of Organic Wood Preservatives by Micro-Organisms [dissertation]. Louisiana State University, Baton Rouge, LA, 2008, p. 89.
66. White, P. M.; Potter, T. L.; Culbreath, A. K. Fungicide Dissipation and Impact on Metolachlor Aerobic Soil Degradation and Soil Microbial Dynamics. *Sci. Total Environ.* **2010**, *408* (6), 1393–1402.
67. Potter, T. L.; Strickland, T. C.; Joo, H.; Culbreath, A. K. Accelerated Soil Dissipation of Tebuconazole Following Multiple Applications to Peanut. *J. Environ. Qual.* **2005**, *34* (4), 1205–1213.

68. Woo, C.; Daniels, B.; Stirling, R.; Morris, P. Tebuconazole and Propiconazole Tolerance and Possible Degradation by Basidiomycetes: A Wood-Based Bioassay. *Int. Biodeterior. Biodegrad.* **2010**, *64* (5), 403–408.
69. Kim, I. S.; Shim, J. H.; Suh, Y. T. Laboratory Studies on Formation of Bound Residues and Degradation of Propiconazole in Soils. *Pest Manag. Sci.* **2003**, *59* (3), 324–330.
70. Satapute, P.; Kaliwal, B. Biodegradation of the Fungicide Propiconazole by *Pseudomonas Aeruginosa* PS-4 Strain Isolated from a Paddy Soil. *Ann. Microbiol.* **2016**, *66* (4), 1355–1365.
71. American Wood-Preserver's Association. *Standard Method for Determination of Propiconazole and Tebuconazole in Wood, in Waterborne Formulations and in Treating Solutions by HPLC*; Standard A28-05; AWWA: Birmingham, AL, 2006: pp. 2.
72. Kamal, N.; Galvez, R.; Buelna, G. Application of a Solid Phase Extraction-Liquid Chromatography Method to Quantify Phenolic Compounds in Woodwaste Leachate. *Water Qual. Res. J. Can.* **2014**, *49* (3), 210–222.
73. Kalogridi, E.-C.; Christophoridis, C.; Bizani, E.; Drimaropoulou, G.; Fytianos, K. Part I: Temporal and Spatial Distribution of Multiclass Pesticide Residues in Lake Waters of Northern Greece: Application of an Optimized SPE-UPLC-MS/MS Pretreatment and Analytical Method. *Environ. Sci. Pollut. Res.* **2014**, *21* (12), 7239–7251.

74. Faria, A. M.; Maldaner, L.; Santana, C. C.; Jardim, I. C. S. F.; Collins, C. H. Poly(methyltetradecylsiloxane) Immobilized onto Silica for Extraction of Multiclass Pesticides from Surface Waters. *Anal. Chim. Acta* **2007**, *582* (1), 34–40.
75. Demoliner, A.; Caldas, S. S.; Costa, F. P.; Gonçalves, F. F.; Clementin, R. M.; Milani, M. R.; Primel, E. G. Development and Validation of a Method Using SPE and LC-ESI-MS-MS for the Determination of Multiple Classes of Pesticides and Metabolites in Water Samples. *J. Braz. Chem. Soc.* **2010**, *21*, 1424–1433.
76. Zhou, Q.; Xiao, J.; Ding, Y. Sensitive Determination of Fungicides and Prometryn in Environmental Water Samples Using Multiwalled Carbon Nanotubes Solid-Phase Extraction Cartridge. *Anal. Chim. Acta* **2007**, *602* (2), 223–228.
77. Farajzadeh, M.; Khoshmaram, L.; Afshar mogaddam, M. Combination of Solid-Phase Extraction-Hollow Fiber for Ultra-Preconcentration of Some Triazole Pesticides Followed by Gas Chromatography-Flame Ionization Detection. *J. Sep. Sci.* **2012**, *35* (1), 121–127.
78. Tuzimski, T.; Rejczak, T.; PieniAŻEK, D.; Buszewicz, G.; TeresiŃski, G. Comparison of SPE/d-SPE and QuEChERS-Based Extraction Procedures in Terms of Fungicide Residue Analysis in Wine Samples by HPLC–DAD and LC-QqQ-MS. *J. AOAC Int.* **2016**, *99* (6), 1436–1443.
79. Liu, X.; Guan, W.; Hao, X.; Wu, X.; Ma, Y.; Pan, C. Pesticide Multi-Residue Analysis in Tea Using d-SPE Sample Cleanup with Graphene Mixed with Primary Secondary Amine and Graphitized Carbon Black Prior to LC–MS/MS. *Chromatographia* **2014**, *77* (1), 31–37.

80. Kerkdijk, H.; Mol, H. G. J.; van der Nagel, B. Volume Overload Cleanup: An Approach for On-Line SPE-GC, GPC-GC, and GPC-SPE-GC. *Anal. Chem.* **2007**, *79* (21), 7975–7983.
81. Deng, Z.; Hu, J.; Qin, D.; Li, H. Simultaneous Analysis of Hexaconazole, Myclobutanil, and Tebuconazole Residues in Apples and Soil by SPE Clean-Up and GC with Nitrogen–Phosphorus Detection. *Chromatographia* **2010**, *71* (7), 679–684.
82. Juan-García, A.; Picó, Y.; Font, G. Capillary Electrophoresis for Analyzing Pesticides in Fruits and Vegetables Using Solid-Phase Extraction and Stir-Bar Sorptive Extraction. *J. Chromatogr. A* **2005**, *1073* (1), 229–236.
83. Zhao, F.; She, Y.; Zhang, C.; Cao, X.; Wang, S.; Zheng, L.; Jin, M.; Shao, H.; Jin, F.; Wang, J. Selective Solid-Phase Extraction Based on Molecularly Imprinted Technology for the Simultaneous Determination of 20 Triazole Pesticides in Cucumber Samples Using High-Performance Liquid Chromatography-Tandem Mass Spectrometry. *J. Chromatogr. B* **2017**, *1064* (Supplement C), 143–150.
84. Morris, B. D.; Schriener, R. B. Development of an Automated Column Solid-Phase Extraction Cleanup of QuEChERS Extracts, Using a Zirconia-Based Sorbent, for Pesticide Residue Analyses by LC-MS/MS. *J. Agric. Food Chem.* **2015**, *63* (21), 5107–5119.
85. Mai-ling, H.; Ming, J.; Peng, W.; Su-rong, M.; Yan-fei, L.; Xiao-zhong, H.; Yun, S.; Bin, L.; Kang, D. Selective Solid-Phase Extraction of Tebuconazole in

Biological and Environmental Samples Using Molecularly Imprinted Polymers. *Anal. Bioanal. Chem.* **2007**, *387* (3), 1007–1016.

86. Schermerhorn, P. G.; Golden, P. E.; Krynitsky, A. J.; Leimkuehler, W. M. Determination of 22 Triazole Compounds Including Parent Fungicides and Metabolites in Apples, Peaches, Flour, and Water by Liquid Chromatography /Tandem Mass Spectrometry. *J. AOAC Int.* **2005**, *88* (5), 1491–1502.

87. Miyauchi, T.; Mori, M.; Ito, K. Application of Solid-Phase Extraction to Quantitatively Determine Cyproconazole and Tebuconazole in Treated Wood using Liquid Chromatography with UV Detection. *J. Chromatogr. A* **2005**, *1063* (1), 137–141.

88. Stavova, J.; Sedgeman, C. A.; Smith, Z. T.; Frink, L. A.; Hart, J. A.; Niri, V. H.; Kubatova, A. Method Development for the Determination of Wood Preservatives in Commercially Treated Wood Using Gas Chromatography-Mass Spectrometry. *Anal. Chim. Acta* **2011**, *702* (2), 205–12.

89. Hansen, M.; Poulsen, R.; Luong, X.; Sedlak, D. L.; Hayes, T. Liquid Chromatography Tandem Mass Spectrometry Method Using Solid-Phase Extraction and Bead-Beating-Assisted Matrix Solid-Phase Dispersion to Quantify the Fungicide Tebuconazole in Controlled Frog Exposure Study: Analysis of Water and Animal Tissue. *Anal. Bioanal. Chem.* **2014**, *406* (29), 7677–7685.

91. Perazzolo, C.; Morasch, B.; Kohn, T.; Magnet, A.; Thonney, D.; Chèvre, N. Occurrence and Fate of Micropollutants in the Vidy Bay of Lake Geneva,

Switzerland. Part I: Priority List for Environmental Risk Assessment of Pharmaceuticals. *Environ. Toxicol. Chem.* **2010**, *29* (8), 1649–1657.

92. Li, Y.; Dong, F.; Liu, X.; Xu, J.; Li, J.; Kong, Z.; Chen, X.; Zheng, Y. Enantioselective Determination of Triazole Fungicide Tebuconazole in Vegetables, Fruits, Soil and Water by Chiral Liquid Chromatography/Tandem Mass Spectrometry. *J. Sep. Sci.* **2012**, *35* (2), 206–215.

93. Sennert, S.; Volmer, D.; Levsen, K.; Wünsch, G. Multiresidue Analysis of Polar Pesticides in Surface and Drinking Water by On-Line Enrichment and Thermospray LC-MS. *Fresen. J. Anal. Chem.* **1995**, *351* (7), 642–649.

94. Shoemaker, J. A. Development and Multi-Laboratory Verification of US EPA Method 543 for the Analysis of Drinking Water Contaminants by Online Solid Phase Extraction-LC-MS-MS. *J. Chromatogr. Sci.* **2016**, *54* (9), 1532–1539.

95. Madureira, F. D.; da Silva Oliveira, F. A.; de Souza, W. R.; Pontelo, A. P.; de Oliveira, M. L. G.; Silva, G. A Multi-Residue Method for the Determination of 90 Pesticides in Matrices with a High Water Content by LC–MS/MS Without Clean-Up. *Food Addit. Contam. Part A Chem. Anal. Control Expo. Risk Assess.* **2012**, *29* (4), 665–678.

96. Van De Steene, J. C.; Lambert, W. E. Validation of a Solid-Phase Extraction and Liquid Chromatography–Electrospray Tandem Mass Spectrometric Method for the Determination of Nine Basic Pharmaceuticals in Wastewater and Surface Water Samples. *J. Chromatogr. A* **2008**, *1182* (2), 153–160.

97. Singer, H.; Jaus, S.; Hanke, I.; Lück, A.; Hollender, J.; Alder, A. C. Determination of Biocides and Pesticides by On-Line Solid Phase Extraction Coupled With Mass Spectrometry and their Behaviour in Wastewater and Surface Water. *Environ. Pollut.* **2010**, *158* (10), 3054–3064.
98. Pastor-Belda, M.; Garrido, I.; Campillo, N.; Viñas, P.; Hellín, P.; Flores, P.; Fenoll, J. Combination of Solvent Extractants for Dispersive Liquid-Liquid Microextraction of Fungicides from Water and Fruit Samples by Liquid Chromatography with Tandem Mass Spectrometry. *Food Chem.* **2017**, *233*, 69–76.
99. Charalampous, A. C.; Miliadis, G. E.; Koupparis, M. A. A New Multiresidue Method for the Determination of Multiclass Pesticides, Degradation Products and PCBs in Water Using LC–MS/MS and GC–MS(n) Systems. *Int. J. Environ. Anal. Chem.* **2015**, *95* (13), 1283–1298.
100. Ye, C.-I.; Liu, Q.-I.; Wang, Z.-k.; Fan, J. Dispersive Liquid-Liquid Microextraction Combined with High-Performance Liquid Chromatography-Ultraviolet Detection for the Determination of Three Triazole Derivatives in Environmental Water Samples. *Int. J. Environ. Anal. Chem.* **2012**, *92* (10), 1176–1186.
101. Wang, W.; Ma, X.; Wu, Q.; Wang, C.; Zang, X.; Wang, Z. The Use of Graphene-Based Magnetic Nanoparticles as Adsorbent for the Extraction of Triazole Fungicides from Environmental Water. *J. Sep. Sci.* **2012**, *35* (17), 2266–2272.

102. Gao, Y.; Zhou, Q.; Xie, G.; Yao, Z. Temperature-Controlled Ionic Liquid Dispersive Liquid-Phase Microextraction Combined with HPLC with Ultraviolet Detector for the Determination of Fungicides. *J. Sep. Sci.* **2012**, *35* (24), 3569–3574.
103. Rousova, J.; Kusler, K.; Liyanage, D.; Leadbetter, M.; Dongari, N.; Zhang, K. K.; Novikov, A.; Sauter, E. R.; Kubátová, A. Determination of Trans-Resveratrol and its Metabolites in Rat Serum Using Liquid Chromatography with High-Resolution Time of Flight Mass Spectrometry. *J. Chromatogr. B* **2016**, *1039*, 35–43.
104. Robles-Molina, J.; Lara-Ortega, F. J.; Gilbert-López, B.; García-Reyes, J. F.; Molina-Díaz, A. Multi-Residue Method for the Determination of over 400 Priority and Emerging Pollutants in Water and Wastewater by Solid-Phase Extraction and Liquid Chromatography-Time-of-Flight Mass Spectrometry. *J. Chromatogr. A* **2014**, *1350*, 30–43.
105. Amelin, V.; Andoralov, A. High-Performance Liquid Chromatography-Time-of-Flight Mass Spectrometry in the Identification and Determination of 111 Pesticides in Food, Feed, Water, and Soil. *J. Anal. Chem.* **2016**, *71* (1), 82–93.
106. Popova, I. E.; Kozliak, E. I. Efficient Extraction of Fuel Oil Hydrocarbons from Wood. *Sep. Sci. Technol.* **2008**, *43* (4), 778–793.
107. Wang, J. *Analytical Electrochemistry*; John Wiley & Sons: Hoboken, NJ, 2006; pp. 272.

108. Kumaran, M. K. Moisture Diffusivity of Building Materials from Water Absorption Measurements. *J. Therm. Envel. Build. Sci.* **1999**, *22*, 349–355.
109. Perez, N. Kinetics of Concentration Polarization. In *Electrochemistry and Corrosion Science*; Perez, N., Ed. Springer US: 2004; pp 121–154.
110. ANSYS FLUENT User's Guide. <http://users.ugent.be/~mvbelleg/flug-12-0.pdf> (accessed February 6, 2018).
111. Leonard, B. P.; Mokhtari, S. *ULTRA-SHARP Nonoscillatory Convection Schemes for High-Speed Steady Multidimensional Flow*; NASA-TM-102568, ICOMP-90-12; NASA Lewis Research Center: Cleveland, OH, 1990.
112. Reinprecht, L.; Kmet'ová, L. Fungal Resistance and Physical-Mechanical Properties of Beech Plywood Having Durable Veneers or Fungicides in Surfaces. *Eur. J. Wood Wood Prod.* **2014**, *72* (4), 433–443.
113. Danvind, J.; Ekevad, M. Local Water Vapor Diffusion Coefficient when Drying Norway Spruce Sapwood. *J. Wood Sci.* **2006**, *52* (3), 195–201.
114. Kositchaiyong, A.; Rosarpitak, V.; Hamada, H.; Sombatsompop, N. Anti-Fungal Performance and Mechanical-Morphological Properties of PVC and Wood/PVC Composites under UV-Weathering Aging and Soil-Burial Exposure. *Int. Biodeterior. Biodegrad.* **2014**, *91*, 128–137.
115. Lee, D. H.; Tsunoda, K.; Takahashi, M. Photostability of Organoiodine Wood Preservatives. I. Progressive Degradation and Loss in Fungal Inhibition Rate Through Photoirradiation. *Mokuzai Gakkaishi* **1991**, *37* (1), 76–81.

116. Schmidt, S. R.; Launsby, R. G. *Understanding Industrial Designed Experiments*; Air Academy Press: Colorado Springs, 1992; pp. 768.
117. Minitab Support Taguchi Designs. <http://support.minitab.com/en-us/minitab/17/topic-library/modeling-statistics/doe/taguchi-designs/taguchi-designs> (accessed February 6, 2018).
118. Styszko, K.; Bollmann, U. E.; Bester, K. Leaching of Biocides from Polymer Renders under Wet/Dry Cycles – Rates and Mechanisms. *Chemosphere* **2015**, *138*, 609–615.
119. Ho, Y.-S.; Harouna-Oumarou, H. A.; Fauduet, H.; Porte, C. Kinetics and Model Building of Leaching of Water-Soluble Compounds of Tilia Sapwood. *Sep. Purif. Technol.* **2005**, *45* (3), 169–173.
120. Kukowski, K.; Martinská, V.; Krishnamoorthy, G.; Kubátová, A.; Kozliak, E. Diffusion of Tebuconazole into Softwood under Ambient Conditions and its Distribution in Freshly Treated and Aged Wood. *Int. J. Heat Mass Transfer* **2016**, *102*, 1257–1266.
121. Scown, D. K.; Cookson, L. J.; McCarthy, K. J.; Chew, N. *Accelerated Testing of Window Joinery Made from Eucalypts*; FWPRDC Project No. PN98.702; Forest and Wood Products Research and Development Corporation: Victoria, 2004; pp. 45.
122. Kukowski, K.; Martinská, V.; Sedgeman, C. A.; Kuplic, P.; Kozliak, E. I.; Fisher, S.; Kubátová, A. Fate of Triazoles in Softwood upon Environmental Exposure. *Chemosphere* **2017**, *184*, 261–268.

123. *Woodlife 111*; Document No. 60061-103; U.S. Environmental Protection Agency: Washington, D.C., 2014; pp. 2.
124. *PROVOST 433 SC*; Document No.264-861; U.S. Environmental Protection Agency: Washington, D.C., 2008; pp. 9.
125. *TOPSIN XTR*; Document No. 73545-19; U.S. Environmental Protection Agency: Washington, D.C., 2009; pp. 10.
126. Dongari, N.; Sauter, E. R.; Tande, B. M.; Kubátová, A. Determination of Celecoxib in Human Plasma Using Liquid Chromatography with High Resolution Time of Flight-Mass Spectrometry. *J. Chromatogr. B* **2014**, 955–956, 86–92.
127. Müller, A.; Flottmann, D.; Schulz, W.; Seitz, W.; Weber, W. H. Alternative Validation of a LC-MS/MS-Multi-Method for Pesticides in Drinking Water. *Clean Soil Air Water* **2007**, 35 (4), 329–338.
128. Bezerra, M. A.; Santelli, R. E.; Oliveira, E. P.; Villar, L. S.; Escaleira, L. A. Response Surface Methodology (RSM) as a Tool for Optimization in Analytical Chemistry. *Talanta* **2008**, 76 (5), 965–977.